

# Singularization of knots and closed braids

Thomas Fiedler

December 6, 2024

*pour Séverine*

## Abstract

We construct the first combinatorial 1-cocycle with values in the  $\mathbb{Z}[x, x^{-1}]$ -module of isotopy classes of singular long knots in 3-space with a signed planar double point, and which represents a non trivial cohomology class in the topological moduli space of long knots. It can be interpreted as an invariant with values in a  $\mathbb{Z}[x, x^{-1}]$ -module generated by 3-manifolds for each element of infinite order of the mapping class group of the complement of a satellite knot in  $S^3$ .

The 1-cocycle seems to be trivial on all loops for long knots which are not satellites but it is already non trivial on the Fox-Hatcher loop of any composite knot, on the loop which consists of *dragging* a trefoil through another trefoil and on the *scan-arc* for the 2-cable of the trefoil. The *canonical resolution* of the value of the 1-cocycle for dragging a knot through another knot leads to a symmetric bilinear form on the free  $\mathbb{Z}[x, x^{-1}]$ -module of all unframed oriented knot types into itself. We conjecture that its radical contains only the trivial knot.

Evaluating e.g. the Kauffman-Vogel HOMFLYPT polynomial for singular knots on the value of the 1-cocycle applied to the associated quadratic form, leads to a couple of new 3-variable knot polynomials.

We construct also the first non trivial 1-cocycle for those closed positive 4-braids which contain a half-twist. It takes its values in a symmetric power of the  $\mathbb{Z}$ -module of isotopy classes of closed positive 4-braids with a double point.

1

---

<sup>1</sup>2000 *Mathematics Subject Classification*: 57M25 *Keywords*: singularization, 1-cocycle invariants, global tetrahedron equation, cube equations, tetrahex equation

# Contents

<b>1</b>	<b>Introduction and basic definitions</b>	<b>2</b>
<b>2</b>	<b>Main results and an application</b>	<b>24</b>
2.1	The 1-cocycle $R_x$ for long knots . . . . .	24
2.2	The 1-cocycle $R_1^{split}$ for positive closed 4-braids . . . . .	34
2.3	The Entropy conjecture for 4-braids . . . . .	40
<b>3</b>	<b>Examples</b>	<b>43</b>
3.1	Long knots . . . . .	43
3.2	Positive closed 4-braids . . . . .	61
<b>4</b>	<b>Proofs</b>	<b>69</b>
4.1	Generalities and reductions by using singularity theory . . . . .	70
4.2	Reidemeister II moves in a cusp and in a flex . . . . .	82
4.3	Simultaneous Reidemeister moves . . . . .	82
4.4	Tetrahedron equation for long knots . . . . .	87
4.5	Tetrahedron equation for closed braids and the Tetrahex equation . . . . .	108
4.6	Cube equations . . . . .	119
4.7	Moving cusps and scan-property . . . . .	129

## 1 Introduction and basic definitions

The non trivial topology of moduli spaces of non singular knots wasn't yet used to define new knot invariants. Vassiliev's theory, see [65] and [66], concentrates mostly on  $H_0$  of the moduli spaces in order to define finite type invariants. In this paper we use the  $H_1$ , i.e. we consider smooth 1-parameter families of oriented smooth knots in 3-manifolds.

*Our main achievement is a construction which associates to each oriented loop of non-singular long knots a finite combination with coefficients in a polynomial ring of singular long knots, each with exactly one signed ordinary double point. Homological loops are mapped to the same combination but with the singular long knots replaced by their isotopy classes and such that the double points stay planar.*

There are several canonical ways to associate a loop to a knot  $K$ . We call the non trivial image of a loop a *singularization* of  $K$ .

Our result is based on a surprising connection between two different discriminants, Vassiliev's discriminant of singular long knots and the discriminant of non generic projections of non-singular long knots into the plan. The main problem was to break the symmetry in the construction so that our 1-cocycle does not always represent the trivial cohomology class.

**Definition 1** *A long knot  $K$  is an oriented smooth knot in  $\mathbb{R} \times \mathbb{C}$  which coincides with the real axes in  $\mathbb{C}$  outside a compact set. A  $n$ -string link  $K$  is a  $n$ -component link where each component is parallel to a long knot outside some compact set.*

Examples of  $n$ -string links are  $n$ -cables of framed long knots and  $n$ -braids.

First of all we choose an abstract closure of the string link to an oriented circle and we choose a point at infinity in the boundary of the string link (in the case of long knots there aren't any choices). So, a string link is for us a circle with only a part of it embedded in 3-space and with a marked point in the remaining (abstract) part.

For each generic long knot (or string link) we have a finite number of *vertical chords*, i.e. chords connecting points with the same  $\mathbb{R}$ -coordinate. These points correspond to the crossings for the natural projection of the knot into  $\mathbb{C} \times 0$ .

**Definition 2** *Let  $K$  be an isotopy class of a long knot, i.e. a long knot up to smooth isotopy of long knots which is the identity outside a compact set.*

*An embedded chord diagram for  $K$  is a trivalent graph obtained from a diagram for  $K$  together with exactly one vertical chord. The chord is oriented from the undercross to the overcross and it is signed by the usual writhe of the corresponding ordinary crossing. An isotopy of an embedded chord diagram is a smooth isotopy of the trivalent graph and such that the vertical chord stays vertical all the time.*

In particular, each embedded chord diagram decomposes in a canonical way into a knot part and into the chord. If we contract the vertical chord and we drop the sign then we obtain a *singular knot* in the usual sense (see e.g. [46]). However, our notion of isotopy is a refinement of the usual notion of isotopy for singular knots, namely we do *not* allow the move which corresponds to reversing the orientation of a vertical chord. We illustrate the forbidden move in Fig. 1. We call an ordinary double point *planar* if the projection of the plan spanned by the tangent vectors at the double point to  $\mathbb{C}$  is surjective.

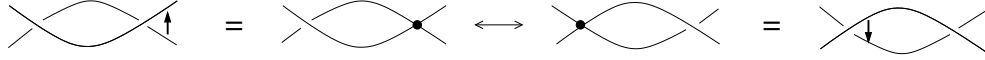


Figure 1: Forbidden move

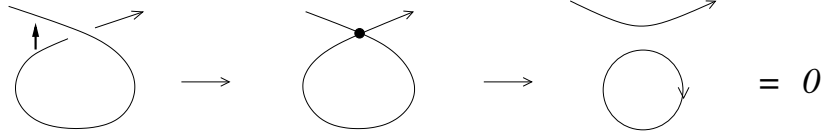


Figure 2: Smoothing link and embedded 1T-relation

**Definition 3** *An isotopy of a long knot with an ordinary planar double point is called planar if the double point stays an ordinary planar double point within the whole isotopy.*

Notice that in the planar isotopy branches of the knot are allowed to move over or under the double point.

To each embedded chord diagram corresponds an underlying abstract chord diagram in the following way: the knot is an oriented circle with a marked point, which corresponds to the point at infinity, and an oriented signed arrow which connect points on the circle and which correspond to the oriented signed vertical chord (with the direction from the under-cross to the over-cross). This is usually called a *Gauss diagram of K* if all crossings of K are considered (see [56], [19]). So, the underlying abstract chord diagram is a sub-diagram of a Gauss diagram. We will shortly call it the *underlying Gauss diagram*.

Contracting the chord and smoothing the double point with respect to the orientation leads to an oriented link with one more component, which we call the *smoothing link*. We show an example in Fig. 2.

Let K be an isotopy class of a long knot (or n-string link) and let  $\mathbb{Z}[x, x^{-1}]$  be the ring of integer Laurent polynomials.

**Definition 4**  $\mathbb{D}_K^1$  is the free  $\mathbb{Z}[x, x^{-1}]$ -module generated by all planar isotopy classes of embedded chord diagrams for K with the underlying Gauss diagrams shown in Fig. 3 modulo the following embedded 1T-relation: an embedded chord diagram is 0 in  $\mathbb{D}_K^1$  if and only if the corresponding smoothing link is a split link which contains a trivial knot (long or compact) as a component (e.g. as in Fig. 2).

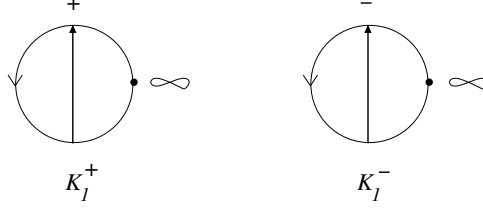


Figure 3: Underlying Gauss diagrams for  $K_1$

We denote by  $\mathbb{D}_K^1 = \mathbb{D}_K^+ \oplus \mathbb{D}_K^-$  the natural splitting of  $\mathbb{D}_K^1$  with respect to the sign of the double points.

Let us denote by  $\mathbb{D}$  the  $\mathbb{Z}[x, x^{-1}]$ -module freely generated by all oriented unframed long knot types.

Let  $M_K$  be the *topological moduli space* of the long knot or string link  $K$ , i.e. the space of all long knots or string links smoothly isotopic to  $K$  (seen as one dimensional  $C^\infty$ -submanifolds of  $\mathbb{R} \times \mathbb{C}$  and which are standard near infinity). Notice that each generator of  $\mathbb{D}_K^1$  is a singular knot which is a first generic degeneration of the knot  $K$ , i.e. it is in a codimension 1 stratum which is adjacent to the codimension 0 stratum  $M_K$  in Vassiliev's stratification of  $C^\infty$ -maps from  $\mathbb{R}^1$  to  $\mathbb{R}^3$  standard near infinity.

Instead of a 0-cocycle with values in some algebra of abstract chord diagrams (the *Kontsevich integral*, see [50] et [3]) we construct now a 1-cocycle, called  $R_x$  ("R" stands for Reidemeister), with values in  $\mathbb{D}_K^1$ . Instead of integrating a differential form we introduce a *discrete combinatorial integration*: in a generic 1-parameter family of diagrams only a finite number of Reidemeister moves appear and we associate an element of  $\mathbb{D}_K^1$  to each (co-oriented) Reidemeister move of type III and of type II (see e.g. [12] for the definition of Reidemeister moves). Instead of showing that a differential form is closed we show in a combinatorial way (and by using some global singularity theory for projections of knots into the plan) that the sum of the contributions of the Reidemeister moves does not change when non generic diagrams (as e.g. quadruple crossings or crossings of a branch with an auto-tangency) occur in a generic deformation of the 1-parameter family.

The value of  $R_x$  on a loop in the topological moduli space  $M_K$  is an invariant of the homology class of the loop. In order to obtain an isotopy invariant of  $K$  itself we need canonical choices of loops in  $M_K$ .

There are two canonical loops associated to each long knot and which are homologically non trivial for non trivial knots: Gramain's loop, denoted by

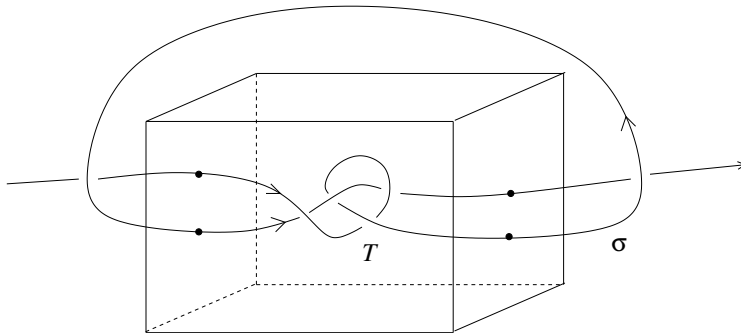


Figure 4: A partial closure of a tangle to a long knot

$rot(K)$ , and the Fox-Hatcher loop, denoted by  $hat(K)$ . *Gramain's loop* is induced by the rotation of the 3-space around the long axes of the long knot (see [35]). *Fox-Hatcher's loop* is defined as follows: one puts a pearl (i.e. a small 3-ball  $B$ ) on the closure of the long framed knot  $K$  in the 3-sphere. The part of  $K$  in  $S^3 \setminus B$  is a long knot. Pushing  $B$  once along the knot with respecting the framing induces the Fox-Hatcher loop in  $M_K$  (see [38] and also [26]). The homology class of  $rot(K)$  does not depend on the framing of  $K$  and changing the framing of  $K$  adds multiples of  $rot(K)$  to  $hat(K)$ . Notice that the Fox-Hatcher loop has a canonical orientation induced by the orientation of the long knot. The same loops are still well defined and non trivial for those  $n$ -string links which are  $n$ -cables of a non trivial framed long knot.

The complement in  $\mathbb{R}^3$  of a general  $n$ -string link  $T$  for  $n > 1$  does not contain any incompressible torus and its topological moduli space is contractible. In this case we consider the string link  $T$  as a tangle in a cube  $I^3$  and we chose a partial closure  $\sigma$  of  $T$  outside the cube as shown e.g. in Fig. 4. We consider now the resulting tangle  $T \cup \sigma$  of one component again as a long knot in 3-space and we can apply the Fox-Hatcher loop to it.  $R_x$  of this loop is an isotopy invariant of the string link  $T$  (but which depends of course of the chosen closure  $\sigma$ ).

Gramain's and the Fox-Hatcher loop have nice geometric realizations. Gramain's loop can be represented by pushing the knot through a curl as shown in Fig. 5 (see [62]). The Fox-Hatcher loop corresponds to the following loop: we go on  $K$  from  $\infty$  to the first crossing. If we arrive at an under-cross then we move the branch of the over-cross over the rest of the knot up to the end of  $K$ . If we arrive at an over-cross then we move the branch of the under-cross under the rest of the knot up to its end. We continue the process up to



$R_x$  does not depend on the choice of the point at infinity on  $K$  since  $R_x$  is a 1-cocycle already for unframed knots and two long knots are isotopic if and only if the corresponding closed knots in  $S^3$  are isotopic. It looks to us that in reality  $R_x$  is a 1-cocycle for  $M_{K \subset S^3}$  (which would prove one direction of the conjecture), but we have no proof of this fact.

Let  $K \subset S^3$  be a satellite and let  $N(K)$  be an open tubular neighborhood of  $K$ . Then there is an incompressible and not boundary parallel torus  $T^2$  in  $S^3 \setminus N(K)$ . We know from Johannson that each "3-dimensional Dehn twist" of  $T^2 \times I$  in the direction of an essential simple closed curve in  $T^2$  defines an orientation preserving diffeomorphism, say  $\phi$ , of infinite order in the mapping class group  $MCG(S^3 \setminus N(K), rel\partial)$ , see [40] p. 190 (thanks to Francesco Costantino for indicating the reference). This diffeomorphism  $\phi$  is the identity on  $\partial\bar{N}(K)$  and its natural extension to a diffeomorphism of  $S^3$  is isotopic to the identity. This isotopy defines an ambient isotopy of  $K$  to itself. By acting with  $SO(4)$  on  $S^3$  we can assume that one point in  $K$  and a frame of  $S^3$  at this point stay fixed in the ambient isotopy. Consequently, it defines an oriented loop in  $M_K$ .

*$R_x$  evaluated on this loop is an invariant of  $[\phi] \in MCG(S^3 \setminus N(K), rel\partial)$  (i.e. isotopy classes of orientation preserving diffeomorphisms which are the identity on the boundary), called  $R_x(\phi)$ .*

Indeed, the only ambiguity comes from the action of  $SO(4)$  on  $S^3$  to keep a framed point fixed and of the action of  $\pi_1(Diff^+(S^3))$  from relating  $\phi$  to the identity. We know from Hatcher [37] that  $Diff^+(S^3)$  deformation retracts onto  $SO(4)$  and hence its fundamental group is isomorphic to  $\mathbb{Z}/2\mathbb{Z}$ . The non trivial loop in  $\pi_1(SO(4)) \cong \pi_1(SO(3)) \cong \mathbb{Z}/2\mathbb{Z}$  corresponds to the rotation of  $\mathbb{R}^3$  around the long axis. But this rotation induces just Gramain's loop in  $M_K$  and we know already that  $R_x$  vanishes on it.

Conversely, each smooth isotopy of  $K \subset S^3$  to itself, which preserves the orientation of  $K$  and which fixes one point on  $K$ , induces an element  $[\phi] \in MCG(S^3 \setminus N(K), rel\partial)$  by the isotopy extension theorem.

$R_x(\phi)$  takes its values in  $\mathbb{D}_K^1$ . By taking out tubular neighborhoods in  $S^3$  of the singular knots in  $\mathbb{D}_K^1$ , the value of the 1-cocycle  $R_x(\phi)$  becomes a combination with coefficients in  $\mathbb{Z}[x, x^{-1}]$  of oriented 3-manifolds, each with a boundary which is a surface of genus 2. We call them *adjacent 3-manifolds* of  $S^3 \setminus N(K)$ . *They are invariants of the element  $[\phi] \in MCG(S^3 \setminus N(K), rel\partial)$ .*

In this paper we develop the combinatorial theory for the invariant  $R_x(\phi)$ : we show that it exists, that it can be calculated and that it is not always trivial, see the examples below. But in analogy with Witten's partition



function via Feynmann integrals and the Reshetikhin-Turaev invariants for links in 3-manifolds it seems to us that for a better understanding of our combinatorial invariants it is of crucial importance to find a differential-geometric interpretation (coming from some mathematical physics) for them (see [68] and [59]).

**Question 1** *Let  $\phi$  be a diffeomorphism of infinite order in the mapping class group  $MCG(S^3 \setminus N(K), \text{rel} \partial)$  and let  $T(\phi)$  be its mapping torus. Does there exist a partition function  $Z_\phi$  with values in  $\mathbb{D}_K^1$  (or at least with values in quantum invariants evaluated on  $\mathbb{D}_K^1$ ) on the 4-manifold  $T(\phi)$  which comes from some function (which uses the projection  $\text{pr}$ ) on it with a physical meaning and such that  $Z_\phi = R_x(\phi)$  (or at least a quantum invariant evaluated on  $R_x(\phi)$ )?*

*Otherwise, let us consider the loop space  $\Omega M_K$ . It is known that  $\Omega M_K$  is homeomorphic to the mapping class group (with its discrete topology) of the knot exterior cartesian product with a contractible space (thanks to Ryan Budney for pointing this out). In fact, it is known that each  $M_K$  is a  $K(\pi, 1)$  which is homotopy equivalent to a finite dimensional CW-complex, see [39].  $R_x$  can be seen as a continuous map from  $\Omega M_K$  to  $\mathbb{D}_K^1$  and hence it is constant on each component of  $\Omega M_K$ . Let us replace  $\mathbb{D}_K^1$  by the  $\mathbb{R}[x, x^{-1}]$ -module freely generated by all embedded chord diagrams (without taking the quotient by isotopy). Does there exist a natural differentiable map from  $\Omega M_K$  to this module and such that its critical values coincide with  $R_x$  up to normalization?*

The study of 3-manifolds so far has mainly concentrated on hyperbolic manifolds and on homology spheres. They have both finite MCG and hence diffeomorphisms of infinite order simply didn't appear.

The simplest satellite is just the connected sum of two non trivial knots. We have calculated that  $R_x(\text{hat}(4_1 \# 4_1)) \neq 0$ . Its precise value is given in Fig. 6, where as usual in the figures vertical chords are contracted. Notice that the embedded 1T-relation does not annihilate  $R_x$  because non of the knots in the smoothing link is the trivial knot and note also that the value in  $\mathbb{D}_K^1$  would vanish in this example without the signs of the double points. (It comes from the symmetry of  $4_1$  that the Fox-Hatcher loop is in this case the double covering of our loop.)

In fact, it could be proven that for arbitrary non trivial prime knots  $K_1$  and  $K_2$  we have  $R_x(\text{hat}(K_1 \# K_2)) \neq 0$  with the precise value given in Fig. 7,

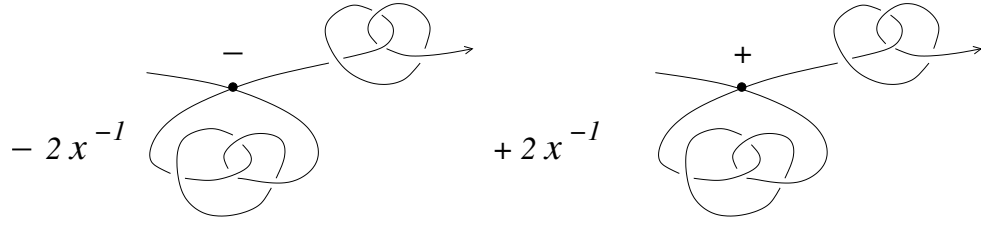


Figure 6:  $R_x(\text{hat}(4_1 \sharp 4_1))$

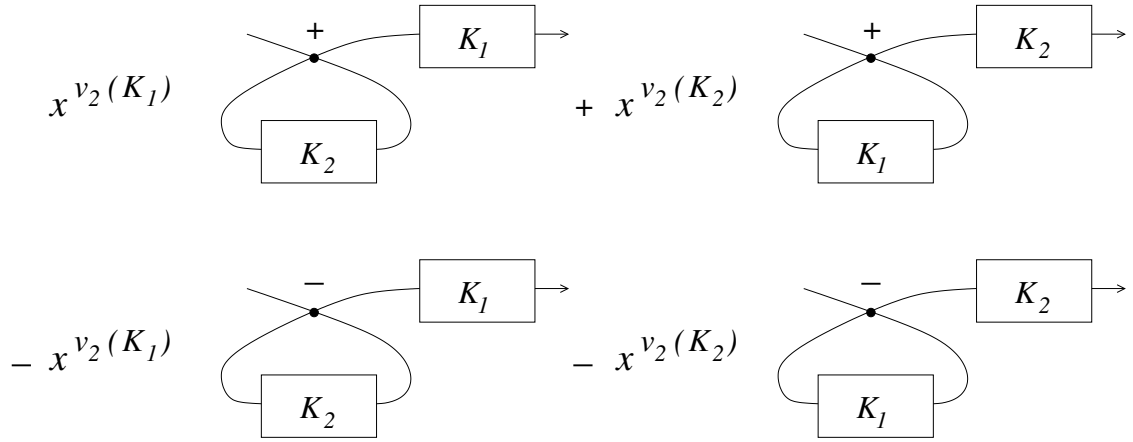


Figure 7:  $R_x(\text{hat}(K_1 \sharp K_2))$

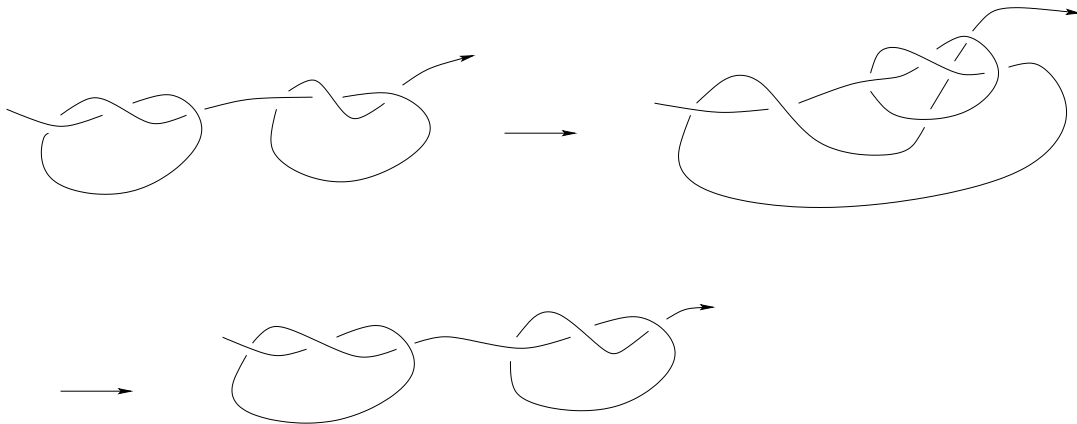


Figure 8: dragging a trefoil through another trefoil

where  $v_2(\cdot)$  is the Vassiliev invariant of degree 2. But we left the proof to the reader.

However, the value of  $R_x((\text{hat}(K_1 \sharp K_2)))$  is not very interesting, because it does not lead to any new knot types. If we replace a positive double point by a positive crossing or a negative double point by a negative crossing then we get back of course our original knot.

**Definition 5** *Let  $\gamma$  be an oriented loop in  $M_K$ . Then the canonical resolution of  $R_x(\gamma) \in \mathbb{D}_K^1$  is obtained by replacing each positive double point by a negative crossing and each negative double point by a positive crossing. We denote the result in  $\mathbb{D}$  by  $\mathbb{D}R_x(\gamma)$ .*

So, in the canonical resolution we push the knot  $K$  through walls in the boundary of its moduli space. One sees immediately that all knots in  $\mathbb{D}R_x((\text{hat}(K_1 \sharp K_2)))$  are again just the original knot  $K_1 \sharp K_2$ .

But instead of the Fox-Hatcher loop for  $K_1 \sharp K_2$  we can consider another loop, namely we can drag  $K_1$  through  $K_2$  and then again  $K_2$  through  $K_1$  in the same direction. The result is an oriented loop in  $M_{K=K_1 \sharp K_2}$  which we denote by  $\text{drag}(K_1, K_2)$ . We show an example in Fig. 8. (If  $K_1 = K_2$  then we can stop of course already after the first dragging and  $\text{drag}(K_1, K_2)$  is just twice this loop.)

We have calculated that already  $R_x(\text{drag}(3_1^+, 3_1^+)) \neq 0$ . Its precise value is given in Fig. 9 and one easily sees that its canonical resolution

$$\mathbb{D}R_x(\text{drag}(3_1^+, 3_1^+)) = 2(+8_{21}^+ - 3_1^+) \in \mathbb{D}.$$

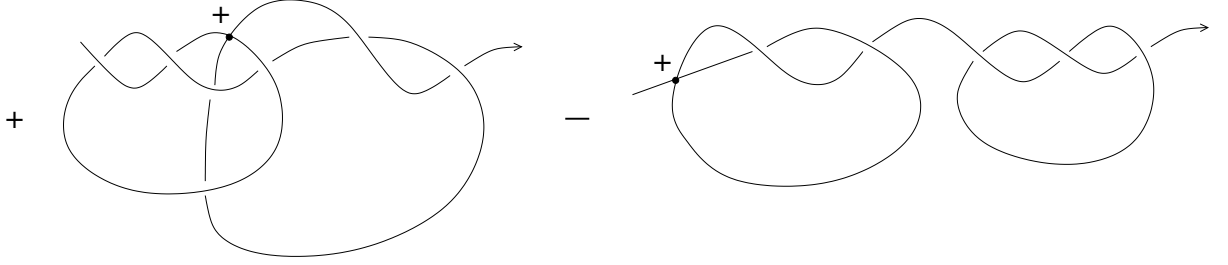


Figure 9:  $R_x(\text{drag}(3_1^+, 3_1^+))$

(Here  $8_{21}^+$  is the knot  $8_{21}$  which has a diagram with 8 crossings and total writhe +4.) It follows that each invariant of  $8_{21}^+$  is a new invariant of the positive trefoil! For example, the simplicial volume of the right hand side, which is equal to twice the hyperbolic volume of the complement of  $8_{21}$ , is an invariant of the positive trefoil. Moreover, we can iterate the construction and consider  $2\mathbb{D}R_x(\text{drag}(8_{21}^+, 8_{21}^+)) - 2\mathbb{D}R_x(\text{drag}(3_1^+, 3_1^+)) \in \mathbb{D}$  and we get still new invariants of the positive trefoil.

Because of its fundamental importance we give the calculation of

$R_x(\text{drag}(3_1^+, 3_1^+))$  in all details in Section 3.

More generally,  $R_x(\text{drag}(K_1, K_2))$  defines in the natural way a *bilinear form*

$$B_{\mathbb{D}^1} : \mathbb{D} \times \mathbb{D} \rightarrow \mathbb{D}^1$$

Indeed, changing the framing of  $K_1$  or  $K_2$  would just add multiples of Gramain loops, but  $R_x$  vanishes on Gramain's loop. Using the canonical resolution,  $B_{\mathbb{D}^1}$  induces a bilinear form with values in  $\mathbb{D}$ . It follows directly from its definition and from the fact that  $R_x$  does not depend on the choice of the point at infinity that the form  $B_{\mathbb{D}^1}$  is *symmetric* (and *even*, in the sense that all coefficients on the diagonal are divisible by 2 in  $\mathbb{Z}[x, x^{-1}]$ ). The trivial knot is evidently in the radical of  $B_{\mathbb{D}^1}$ . Let  $\mathbb{D}_0$  be the  $\mathbb{Z}[x, x^{-1}]$ -module freely generated by all oriented unframed non trivial knot types.

**Conjecture 2** *The even symmetric bilinear form*

$$B_{\mathbb{D}^1} : \mathbb{D}_0 \times \mathbb{D}_0 \rightarrow \mathbb{D}$$

*is non degenerate.*

Moreover, we can iterate  $B_{\mathbb{D}^1}$  and we can extract numerical knot invariants by combining it e.g. with the usual knot invariants. If Conjecture 2

would be true then this would be certainly a big step towards a calculable complete knot invariant. It could even be that *each* non trivial knot invariant becomes a complete knot invariant. But for each given knot invariant, e.g. the first non trivial Vassiliev invariant  $v_2$  as the simplest one, an effective upper bound for the complexity of the diagrams with which a given diagram has to be paired as well as an effective upper bound for the number of needed iterations would be still missing.

*However, it seems to us that a combinatorial proof of the Conjectures 1 and 2 is out of reach and that a proof of them will necessarily use a positive answer to Question 1.*

Another easy way to create satellites is *cabling*. If the long oriented knot is framed, i.e. a trivialization (standard at infinity) of its normal bundle is chosen, then we can replace the knot  $K$  by  $n$  parallel oriented copies with respect to this framing. The result is a  $n$ -string link which is called the non-twisted  $n$ -cable  $Cab_n(K)$  if the framing was zero. Evidently, the loop  $drag(Cab_n(K_1), Cab_n(K_2))$  is still well defined.

Unfortunately I am not able to write any computer program. So, all our examples are calculated by hand. Calculating by hand  $R_x$  for the simplest loop for 2-cables is already too extensive for us. Luckily,  $R_x$  has a very important property which allows to extract by hand an invariant for the 2-cable of the trefoil. Let  $T$  be a string link. We fix an arbitrary abstract closure  $\sigma$  of  $T$  to an oriented circle and we fix a *point at infinity* in  $\partial T$ . Let  $R$  be any combinatorial 1-cocycle in the topological moduli space  $M_T$  (i.e. we sum up contributions from Reidemeister moves) which takes its values in a module generated by singular string links.

**Definition 6** *A 1-cocycle  $R$  has the scan-property if the contribution of each Reidemeister move  $t$  doesn't change when a branch of  $T$  has moved under the Reidemeister move  $t$  to the other side of it.*

Let us add a small positive curl to an arbitrary component of  $T$  near to the boundary  $\partial T$  (at infinity) of  $T$ .

**Definition 7** *The scan-arc  $scan(T)$  in  $M_T$  is the regular isotopy which makes the small curl big under the rest of  $T$  up to being near to infinity, compare Fig. 10.*

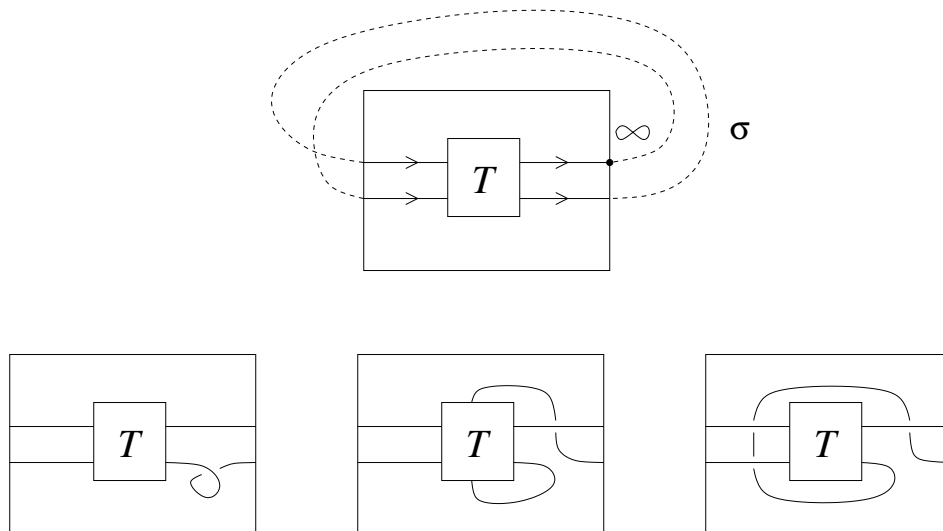


Figure 10: scan-arc for a tangle (or string link)  $T$

The 1-cocycle  $R$  can be *graded* by considering only those singular string links with the double point as intersection of two given components of the string link.

*The value  $R_x(scan(T))$  of the graded 1-cocycle on the scan-arc with values in  $\mathbb{D}_T^1$  does not depend on the chosen regular diagram of  $T$  (but it depends on the chosen closure, on the chosen component for the curl and of the choice of  $\infty$  in  $\partial T$ ). Consequently,  $R_x(scan(T))$  is an isotopy invariant of the the string link  $T$ .*

This means that the evaluation of our 1-cocycle on some canonical arc (instead of a loop) is already an invariant. This is a consequence of the scan-property. Notice that the scan-property is a priori a property of the cocycle and not of the corresponding cohomology class. (There are "dual" 1-cocycles which have the scan-property for small curls which become big over everything instead of under everything. We don't know whether they represent the same cohomology class.)

Let us come back to the case of long knots. We prove that  $R_x(scan(K)) = 0$  for each long knot  $K$ .

But let us consider the string link  $Cab_2(K)$  for a long knot  $K$ . We color by red the component of the string link which contains the moving arc in the scanning and we chose the point at infinity as shown in Fig. 11. We are only interested in the part of  $R_x$  for which the double points are intersections of

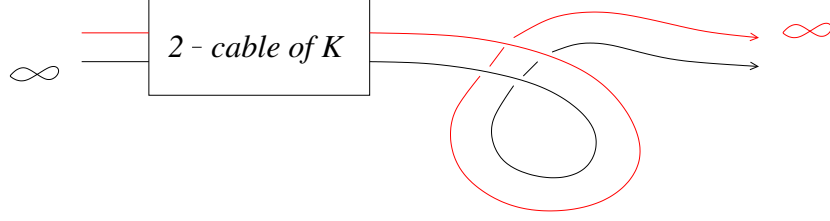


Figure 11: red-red scanning of a 2-cable

the red component with itself, lets call it  $R_{x,red-red}$ .

We have calculated that already  $R_{x,red-red}(scan(Cab_2(3_1^+))) \neq 0$ . Its precise value is given in Fig. 12. (It turns out that  $R_x(scan(Cab_2(3_1^+))) = 0$  for the other choice of the point at infinity independent of the grading if we move only the red arc.)

*Notice that as for  $R_x(drag(3_1^+, 3_1^+))$  the canonical resolution of*

*$R_{x,red-red}(scan(Cab_2(3_1^+)))$  contains long knots or string links which are no longer satellites of torus knots, but for which the closure is a hyperbolic knot!*

**Remark 1** *The link of an irreducible singularity of a complex algebraic plan curve is an iterated torus knot. The JSJ-decomposition of its complement in the 3-sphere contains only Seifert fibered pieces but it has lots of diffeomorphisms of infinite order (if the singularity is not simple). As we have seen in the examples for drag and scan the complement of the canonical resolution of the value of  $R_x$  can contain nevertheless hyperbolic pieces. This makes a potential connection between classical singularity theory and hyperbolic geometry.*

Let *flip* denote a rotation in 3-space around a vertical axis in the plan (i.e. it interchanges the two ends of a long knot) followed by an abstract orientation reversing. It is easy to see that a long knot  $K$  is isotopic to the long knot  $flip(K)$  if and only if the closure of  $K$  is an invertible knot in the 3-sphere (see e.g. [19], [17]). Most of the ingredients in our construction are not invariant under *flip* and hence at least a priori the 1-cocycle  $R_x$  is not invariant under *flip* too. It would be very interesting to find out (with a computer program) whether  $R_x(scan(Cab_2(K)))$  can already detect the non-invertibility of a knot  $K$ .

Simply cabling a framed knot defines evidently another map from the space of all knots to itself. However, quantum knot invariants (see [41]

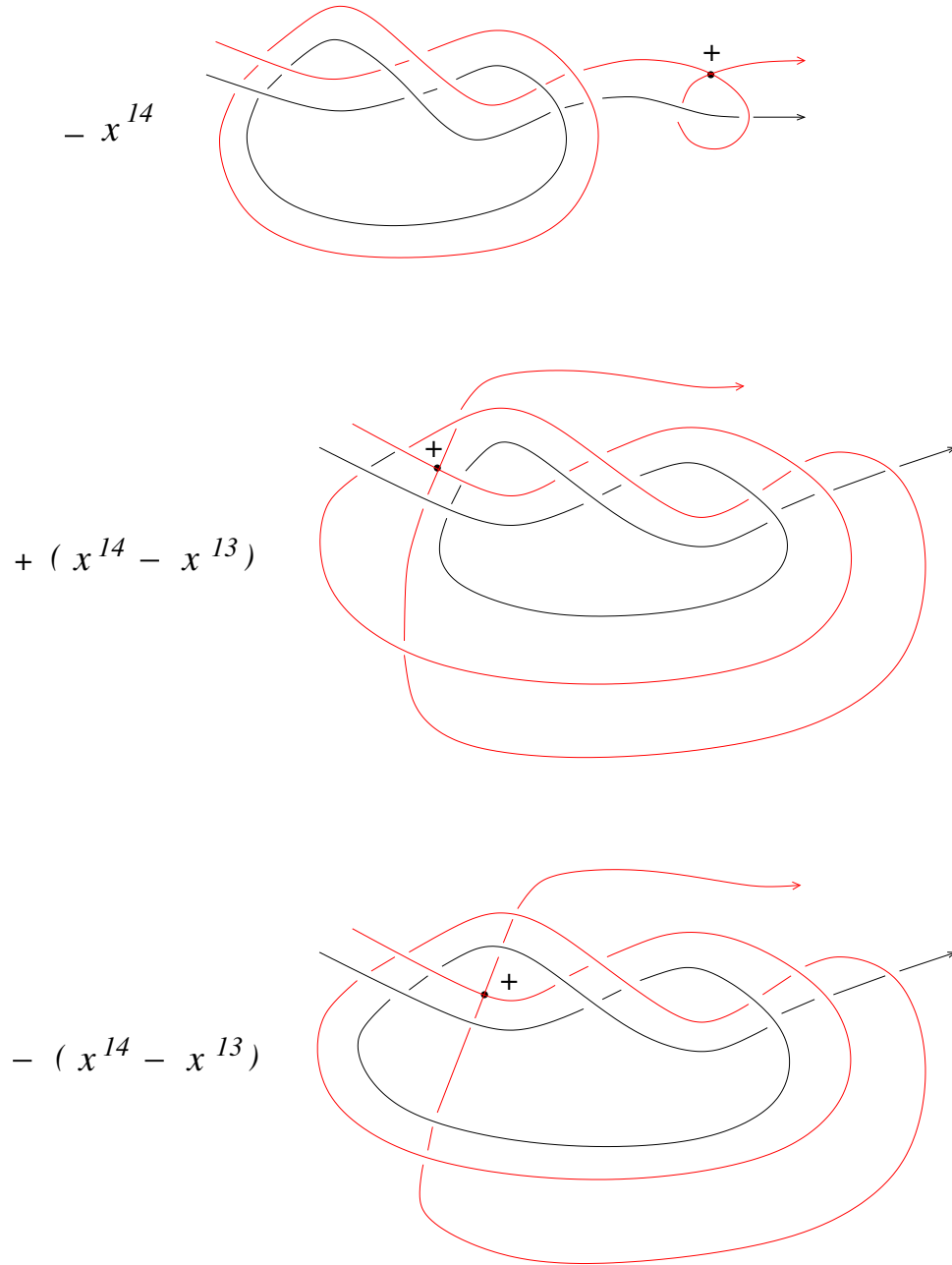


Figure 12:  $R_{x,red-red}(scan(Cab_2(3_1^+)))$



and [63]) are dominated by finite type invariants (see e.g. [3]) but the latter behave functorial under cabling and twisted cabling (see e.g. [6]). Hence this map does not lead to new knot invariants in contrast to  $B_{\mathbb{D}^1}$  and  $R_x(\text{scan}(\text{Cab}_2(K)))$ .

In order to obtain numerical knot invariants from  $R_x$  we can use e.g. quantum polynomials for singular links. We replace each singular knot in  $R_x$  (or even of its restriction to  $\mathbb{D}_K^+$  or to  $\mathbb{D}_K^-$ ) by a quantum invariant for singular links, e.g. the HOMFLYPT polynomial  $P$  for singular links defined by Kauffman-Vogel (see [46]). We recall its skein relations in Fig. 13. It is an invariant of regular isotopy for singular links and it becomes an isotopy invariant after normalization with  $v^{-w(K)}$ , where  $w(K)$  is the usual writhe of the diagram of the singular knot  $K$ . The double points come with a sign in our case. There is an evident refinement of the Kauffman-Vogel invariant by replacing  $A$  and  $B$  by  $A^+$  respectively  $B^+$  for a positive double point and by  $A^-$  respectively  $B^-$  for a negative double point. Indeed, at most one double point enters into a skein relation and hence Kauffman-Vogel's proof extends word for word. But the former relation  $A - B = z$  splits now into two relations  $A^+ - B^+ = z$  and  $A^- - B^- = z$ .

We denote by  $PR_x$  the resulting quantum invariant of  $K$ . We could consider it as an ordered couple of 3-variable polynomials (in  $x, z, v$ ). Changing the orientation of a loop changes the sign of the polynomials. Hence these polynomials can distinguish the homology class of a loop from its inverse in the first homology group of the topological moduli space of knots, in contrast to the usual knot polynomials.

(Notice that instead of the HOMFLYPT invariant for singular links we could also use the refined Kauffman polynomial for singular links [46] and the Alexander or Jones polynomial for singular links via state sum models [21].)

**Remark 2** *An easy calculation shows that for the substitution  $A = vz/(v - v^{-1})$  and  $B = v^{-1}z/(v - v^{-1})$  into  $PR_x$  the embedded 1T-relation disappears for each string link, i.e. the contribution to the invariant of the corresponding singular string link from the embedded 1T-relation is 0.*

*Notice that we could also eliminate the embedded 1T-relation by associating some contribution to the RI-moves (compare [23]), but it becomes unnecessarily complicated.*

Let  $\gamma$  be an oriented loop in  $M_K$  and which represents a non trivial class in

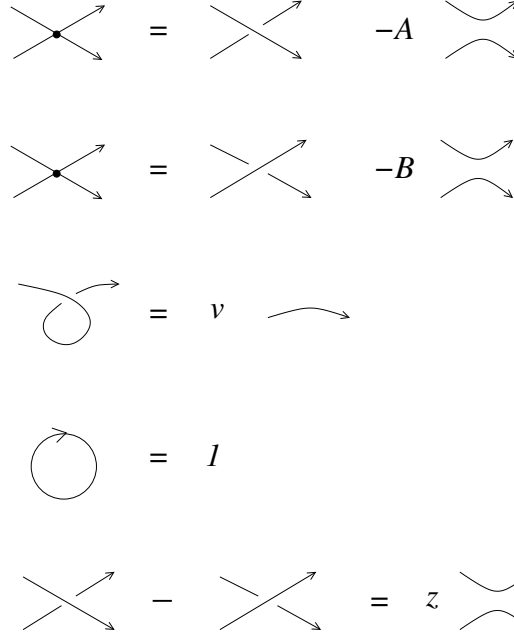


Figure 13: Kauffman-Vogel skein relations for HOMFLYPT of singular links

$H_1(M_K; \mathbb{Q})$ . We call  $R_x(\gamma(K))$  and all derived quantum invariants *1-cocycle invariants* for  $K$ .

**Remark 3**  $R_x(\gamma(K))$  is not an invariant of finite type even for long knots. Indeed, switching a crossing of  $K$  leads in general to a new knot  $K'$ .  $R_x(\gamma(K))$  takes its values in  $\mathbb{D}_K^1$  and  $R_x(\gamma(K'))$  in  $\mathbb{D}_{K'}^1$  (we need a natural identification here of the loops  $\gamma$  which are in different components of the space, e.g. rot or hat or drag). But the intersection of these two modules is 0 if  $K$  is not isotopic to  $K'$ . Indeed, even if a singular knot is in the intersection of  $\mathbb{D}_K^1$  with  $\mathbb{D}_{K'}^1$ , the double points have necessarily different signs because the singular knot is the degeneration of knots which are in adjacent components of the space of all knots. Hence no non-trivial combination of the invariants could sum up to 0.

It is clear that this is still true for  $PR_x(\gamma(K))$  because of the  $\mathbb{Z}/2\mathbb{Z}$  -grading by the sign of the double point and the fact that there is no skein relation for the new variable  $x$ . But for a formal proof one would have to calculate a series of concrete example.

In the case of classical knots we have made heavy use in the construction

of  $R_x$  of the existence of a projection into the plan as well as of the point at infinity on the knot. What about the more general case of knots in 3-manifolds?

Our philosophy, which is at the origin of this paper, is that for *classifying a topological object one has to use the topology of its topological moduli space*. For most knots in 3-manifolds the topological moduli space is just a contractible space. In particular, we need to define our 1-cocycles only for knots. Links have to be treated as a knot in the 3-manifold which is the complement of the remaining components of the link. We believe that if the moduli space is contractible then finite type invariants are enough to separate knots. A good example is Bar Natan's result, which says that finite type invariants separate all braids, see [4] (it is well known that the moduli space of braids is contractible). Another indication is the result of Duzhin and Karev [17] that finite type invariants can detect already the orientation of some 2-component links. It is still not known whether finite type invariants can detect the orientation of a knot. But a 2-component link of two non trivial knots and which is not a split link can be seen as a knot in a 3-manifold with contractible moduli space.

Let  $M^3$  be an irreducible closed oriented 3-manifold and let  $K \subset M^3$  be a knot which is not contained in a 3-ball. The moduli space of  $K$  is not contractible (and has infinite first integer homology group) if  $K$  is a satellite. Then there is a solid torus  $V$  in  $M^3$  which contains  $K$  and such that  $\partial V$  is an incompressible not boundary parallel torus in  $M^3 \setminus N(K)$ . The satellite construction implies that there is a canonical identification of  $V$  with the standard solid torus in  $\mathbb{C} \times \mathbb{R}$ .

Let  $V$  be now the standard solid torus in  $\mathbb{C} \times \mathbb{R}$  which intersects  $\mathbb{C} \times 0$  in an annulus around the origin. There are two 1-parameter families of diffeomorphisms of the solid torus: one is induced by the rotation of the 3-space around the axes  $0 \times \mathbb{R}$  and it is called  $hat(V)$ . The other is induced by the rotation of  $V$  around its core  $\{|z| = 1\} \times 0$  and it is called  $rot(V)$ . For a knot  $K \subset V$  this induces two loops, called  $hat(K)$  and  $rot(K)$  respectively.

We have again a projection (into the annulus this time) but there is no longer a marked point at infinity on  $K$ , which was extremely useful for the construction of  $R_x$ . However, we can attach now an integer to each crossing  $q$  of  $K$ . This integer corresponds to the homology class in  $H_1(V; \mathbb{Z}) \cong \mathbb{Z}$  represented by the loop (denoted by  $K_q^+$ ) in the Gauss diagram of  $K$  which consists of the arrow corresponding to the crossing  $q$  together with the part of  $K$  which goes from the head of the arrow to its foot. We call this integer

the *homological marking* of  $q$ .

In this paper we will not treat the general case  $K \subset V$ , which is extremely complicated. Instead we will concentrate on the very particular case that  $K$  is a closed 4-braid in the solid torus, but which leads already to a non trivial solution of a new and very interesting equation.

A knot  $K \subset V$  is called a *closed geometric braid*, or usually simply called closed braid, if its projection into  $\mathbb{C}^* \times 0$  is positively transverse to the fibers of the function  $arg(z) : \mathbb{C}^* \rightarrow S^1$ . A generic closed braid is denoted by  $\hat{\beta}$ , where  $\beta$  is a braid word in the standard generators and their inverses of the braid group  $B_n$  and  $\hat{\beta}$  denotes as usual the standard closure of the braid in the solid torus. It is well known that closed braids are isotopic as knots in  $V$  if and only if they are isotopic as closed braids in  $V$ , see e.g. [54]. The topological moduli space of all closed braids isotopic to  $\hat{\beta}$  in  $V$  is denoted by  $M_{\hat{\beta}}$ .

Hatcher has proven a result for closed braids which is analog to his result for long knots:  $rot(\hat{\beta})$  and  $hat(\hat{\beta})$  represent linearly dependent homology classes in  $H_1(M_{\hat{\beta}}; \mathbb{Q})$  if and only if  $\hat{\beta}$  is isotopic to a torus knot in  $\partial V$  (personal communication, see also Section 2.3). On the other hand, it is well known that a braid  $\beta$ , which closes to a knot, is *periodic* if and only if  $\hat{\beta}$  is isotopic to a torus knot in  $\partial V$  (see e.g. [8]).

Let  $\mathbb{D}_{\hat{\beta}}^1$  be the  $\mathbb{Z}$ -module freely generated by all isotopy classes of closed  $n$ -braids  $\hat{\beta}$  with exactly one ordinary positive double point and which comes from a crossing with homological marking 1.

Using Garside's theory, see [31], and *Orevkov's observation*, see Section 2.2, we show that in the case of closed positive braids which contain a half-twist  $\Delta$  we don't need to solve the cube equations (see below) and we can construct already 1-cocycles with values in modules of singular closed braids for braids which represent elements in the positive braid monoid  $B_n^+$  (see Section 2).

First we define a 1-cocycle  $R_{xy}$  for closed positive  $n$ -braids, with  $n > 3$ , which are knots very much along the same lines as we have defined  $R_x$  in the case of long knots in 3-space.

We see immediately that  $R_{xy}(hat(\hat{\beta})) = 0$  for all closed  $n$ -braids because  $hat(\hat{\beta})$  is just an isotopy of diagrams without any Reidemeister moves at all. Hence  $rot(\hat{\beta})$  is the only interesting loop. It corresponds to pushing a full twist  $\Delta^2 = (\sigma_1 \sigma_2 \dots \sigma_{n-1})^n$  through the closed braid (we use the standard notations from e.g. [7]), or equivalently pushing  $\Delta$  twice through the closed

braid. It follows now from Hatcher's result that  $R_{xy}(\text{rot}(\hat{\beta})) = 0$  for each positive periodic  $n$ -braid which contains a half-twist and which closes to a knot.

We have tested it for the pseudo-Anosov 4-braid  $\beta = \sigma_3\sigma_2^{-1}\sigma_1^{-1}\Delta^2 = \sigma_3^2\sigma_1\sigma_2\sigma_1\Delta$  and it turns out that  $R_{xy}(\text{rot}(\hat{\beta})) = 0$  too.

**Question 2** *Is  $[R_{xy}] = 0$  for all closed positive  $n$ -braids which contain a half-twist and which are knots?*

Our 1-cocycles so far are based on solutions of the *positive global tetrahedron equation* (corresponding to the RIII-moves in a meridian for a positive quadruple crossing in the space of all knot diagrams, see Section 4) and they can be extended to solutions of the cube equations (corresponding to the RII- and RIII-moves in the meridians of all selftangencies with in addition a transverse branch to the selftangency in the projection). The positive quadruple crossing can be represented by a positive 4-braid. The six ordinary crossings from a quadruple crossing form naturally the edges of a tetrahedron and the RIII-moves correspond to the vertices of the tetrahedron. By going along the meridian of the stratum of codimension 2 in  $M_{\hat{\beta}}$ , which corresponds to a positive quadruple crossing, we see also six commutations of braid generators in 4-braids. They correspond twice to the three couples of dual edges of the tetrahedron. These commutations form naturally a hexagon and give rise to the *hexagon equation*, which says that the sum of the contributions of the commutations in the meridian is 0.

**Definition 8** *The positive global tetrahex equation says that all contributions of RIII-moves and commutation relations sum up together to 0 when we go once along the meridian of the positive quadruple crossing, no matter how the four local branches are connected globally to a knot (see Section 4.5).*

*We have found a solution with values in  $\mathbb{D}_{\beta}^1$ , called  $R_1$ , of the positive global tetrahex equation for  $n = 4$  and which does not split into a solution of the positive global tetrahedron equation and a solution of the hexagon equation!*

Surprisingly,  $R_1$  can not be extended to a solution of the cube equations. (Notice, that there are no commutation relations in the cube equations because they can be represented by sequences of 3-braids.)

*This shows that at least the positive global tetrahex equation and the cube equations are independent equations in the space of all knot diagrams! (But*

we don't know whether the positive global tetrahedron equation and the cube equations are already independent. This question generalizes the question whether each solution of the positive Yang-Baxter equation can be extended to a knot invariant.)

However, unfortunately  $R_1(\text{rot}(\hat{\beta})) = 0$  too for the pseudo-Anosov braid  $\beta = \sigma_3\sigma_2^{-1}\sigma_1^{-1}\Delta^2 = \sigma_3^2\sigma_1\sigma_2\sigma_1\Delta \in B_4^+$ . It is the sum of 38 singular closed braids (compare Section 3.2). Therefore we refine  $R_1$  by introducing a "local system": we give names  $x(i)$  to the crossings with homological marking 1, which are all preserved in the isotopy through positive closed braids. Assume that  $\hat{\beta}$  has exactly  $k$  crossings of homological marking 1. The restriction of  $R_1(\text{rot}(\hat{\beta}))$  for each  $i \in \{1, \dots, k\}$  to only those double points with the name  $x(i)$  splits  $R_1(\text{rot}(\hat{\beta}))$  into an unordered set of  $k$  linear combinations of singular closed braids. Hence the corresponding 1-cocycle  $R_1^{\text{split}}(\text{rot}(\hat{\beta}))$  takes its values in the symmetric product of  $k$  copies of  $\mathbb{D}_\beta^1$ .

Let us denote a double point which comes from a standard generator  $\sigma_i$  by  $t_i$ . Then in the above example  $k = 4$  and  $R_1^{\text{split}}(\text{rot}(\hat{\beta}))$  becomes an unordered set of four combinations of closed singular 4-braids (their sum  $R_1$  is 0, as mentioned above).

$$R_1^{\text{split}}(\text{rot}(\hat{\beta})) = \{+\hat{t}_1\sigma_2\sigma_1\sigma_3\sigma_2\sigma_1\sigma_3\sigma_3\sigma_1\sigma_2\sigma_1, 0, -\hat{t}_1\sigma_3\sigma_2\sigma_1\sigma_3\sigma_3\sigma_1\sigma_2\sigma_1\sigma_1\sigma_2, -\hat{t}_1\sigma_2\sigma_1\sigma_3\sigma_2\sigma_1\sigma_3\sigma_3\sigma_1\sigma_2\sigma_1 + \hat{t}_1\sigma_3\sigma_2\sigma_1\sigma_3\sigma_3\sigma_1\sigma_2\sigma_1\sigma_1\sigma_2\}.$$

$R_1^{\text{split}}(\text{rot}(\hat{\beta}))$  is an isotopy invariant of  $\hat{\beta} \subset V$ . This is the first non trivial singularization of closed braids. The same refinement gives also a non trivial 1-cocycle  $R_{xy}^{\text{split}}(\text{rot}(\hat{\beta}))$ .

The loop  $\text{hat}(\hat{\beta})$  doesn't contain any commutation relations neither and it follows again from Hatcher's result that  $R_1^{\text{split}}(\text{rot}(\hat{\beta})) = 0$  for each positive periodic  $n$ -braid which contains a half-twist and which closes to a knot. It is well known that the entropy and the simplicial volume vanish for periodic braids. This suggests that there could be a relation between  $R_1^{\text{split}}(\text{rot}(\hat{\beta}))$  and the entropy and the hyperbolic volume of a pseudo-Anosov braid  $\beta$ . In Section 2.3 we make a first try of such a conjectural connection with the entropy of 4-braids  $\beta$ .

Let us mention that our 1-cocycles allow sometimes to answer in the negative a very difficult question: *given two loops in  $M_K$  by sequences of Reidemeister moves of diagrams, are the two loops homologous in  $M_K$ ?* For example,  $R_x$  shows that the loops  $\text{drag}(3_1^+, 3_1^+)$ ,  $\text{rot}(3_1^+ \# 3_1^+)$  and  $\text{hat}(3_1^+ \# 3_1^+)$

are pairwise not homologous.  $R_1^{split}$  shows that for  $\beta = \sigma_3\sigma_2\sigma_1^{-1}\Delta^2 \in B_4$  the loops  $hat(\hat{\beta})$  and  $rot(\hat{\beta})$  are not homologous.

Notice also that our invariants can not be extended to virtual knots in contrast to the usual quantum knot invariants, because the loops would contain lots of forbidden moves for virtual knots, see e.g. [45].

The relation between the topology and the geometry of knots was discovered by W. Thurston, see e.g. [61]. Relations of quantum topology with the geometry of knots as the Volume Conjecture and the Slope Conjecture, are studied e.g. in [42], [55], [32], [33], [34], [28], [29], [30], [51]. Far reaching generalizations of the volume conjecture are contained in [27] and in [15].

Finally, let us mention that the topology of knot spaces was much studied in [38], [39], [9], [10], [11], [67]. It seems that the Teiblum-Turchin 1-cocycle  $v_3^1$  and its lift to  $\mathbb{R}$  by Sakai are the only other known 1-cocycles for long knots which represent a non trivial cohomology class. The Teiblum-Turchin 1-cocycle is an integer valued 1-cocycle of degree 3 in the sense of Vassiliev's theory. Its reduction mod 2 has a combinatorial description and can be calculated (see [65], [66] and [62]). Sakai has defined a  $\mathbb{R}$  valued version of the Teiblum-Tourchine 1-cocycle via configuration space integrals (see [60]). Moreover, he has shown that the value of his 1-cocycle on  $rot(K)$  is equal to the Vassiliev invariant  $v_2(K)$ . Mortier has defined another formula for an integer valued 1-cocycle for long knots which extends  $v_3^1 \bmod 2$ , and which is conjectured to coincide with  $v_3^1$  (see [52] and [53] for a generalization).

Integer valued finite type 1-cocycles of all degrees for closed braids were constructed in the unpublished paper [20]. They are already sufficient to detect that e.g. the braids  $\sigma_1\sigma_2^{-1} \in B_3$  and  $\sigma_1\sigma_2\sigma_3^{-1} \in B_4$  are not periodic, because they distinguish the loops  $rot(\hat{\beta})$  and  $hat(\hat{\beta})$  in  $H_1(M_{\hat{\beta}}; \mathbb{Q})$ .

**Remark 4** (*History*)

*The construction of the 1-cocycle  $R_x$  for long knots has taken many years and it has therefore already its own history. It has started with the 1-cocycles  $S$  in [22],  $\bar{R}^{(1)}$  in [23] and  $R_1$  (for long knots) in [24]. They are related in the following way:  $R_1 = dR_x/dx(x = 1)$ .  $\bar{R}^{(1)}$  is obtained from  $R_1$  by smoothing all double points with respect to the orientation and evaluating the HOMFLYPT polynomial on the resulting links and by adding some finite type correction term.  $S$  is obtained from  $\bar{R}^{(1)}$  by setting the weights  $W_2 = 1$  and  $W_1 = 0$  and by forgetting the correction term of  $\bar{R}^{(1)}$ .*

*$S$  represents the trivial cohomology class, as was pointed out by Karen Chu.  $\bar{R}^{(1)}$  reduces to multiples of the HOMFLYPT polynomial for all the*

above mentioned examples and in [23] we have missed the main point: replacing the smoothing of a crossing by its singularization. One sees immediately from  $R_x$  that  $R_1(\text{drag}(3_1^+, 3_1^+)) = 0$  but already  $R_1(\text{scan}(\text{Cab}_2(3_1^+))) \neq 0$  and its canonical resolution leads to interesting prime knots (but we haven't considered this example in [24]). It was also pointed out by Dror Bar-Natan that the 1-cocycle  $R_2$  from [24] is always trivial.

### Acknowledgments

I have started this work in 2006. Over the years I have profited from the help of many people, in particular: Christian Blanchet, Ryan Budney, Karen Chu, Alan Hatcher, Vitaliy Kurlin, Gregor Masbaum, Arnaud Mortier, Hugh Morton, Hitoshi Murakami, Stepan Orevkov, Victor Turchin. I wish to thank all of them and especially Dror Bar-Natan for pointing out an error in the previous version of this paper. Finally, let me mention that without Séverine, who has created all the figures, this paper wouldn't exist.

## 2 Main results and an application

We split our main result into two theorems corresponding to the non trivial 1-cocycle for long knots and to the non trivial 1-cocycle which uses also commutation relations for positive closed 4-braids which contain a half-twist. Each of our 1-cocycles determines of course "dual" 1-cocycles by applying the obvious symmetries as e.g. replacing all our constructions by their mirror images or by their images under flips.

### 2.1 The 1-cocycle $R_x$ for long knots

To each Reidemeister move of type III corresponds a diagram with a *triple crossing*  $p$ : three branches of the knot (the highest, middle and lowest with respect to the projection  $pr : \mathbb{C} \times \mathbb{R} \rightarrow \mathbb{C}$ ) have a common point in the projection into the plane. A small perturbation of the triple crossing leads to an ordinary diagram with three crossings near  $pr(p)$ .

**Definition 9** *We call the crossing between the highest and the lowest branch of the triple crossing  $p$  the distinguished crossing of  $p$  and we denote it by  $d$ . The crossing between the highest branch and the middle branch is denoted by  $hm$  and that of the middle branch with the lowest is denoted by  $ml$ . Smoothing a crossing  $q$  with respect to the orientation splits the closure of  $K$  into two*



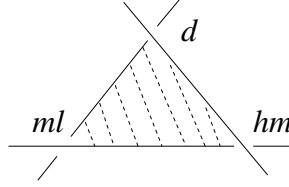


Figure 14: The names of the crossings in a R III move

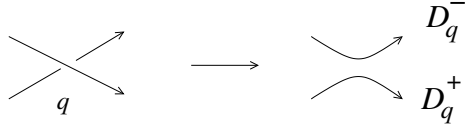


Figure 15: Two ordered knot diagrams associated to a crossing  $q$

oriented and ordered circles. We call  $D_q^+$  the component which goes from the under-cross to the over-cross at  $q$  and by  $D_q^-$  the remaining component (compare Fig. 15).

In a Reidemeister move of type II both new crossings are considered as distinguished and we often identify them.

A *Gauss diagram* of  $K$  is an oriented circle with oriented chords and a marked point. There exists an orientation preserving diffeomorphism from the oriented line to oriented the knot  $K$  such that each chord connects a pair of points which are mapped onto a crossing of  $pr(K)$  and infinity is mapped to the marked point. The chords are oriented from the preimage of the under crossing to the pre-image of the over crossing (here we use the orientation of the  $\mathbb{R}$ -factor). The circle of a Gauss diagram in the plan is always equipped with the counter-clockwise orientation.

A *Gauss diagram formula* of degree  $k$  is an expression assigned to a knot diagram which is of the following form:

$$\sum_{\text{configurations}} \text{function}(\text{ writhes of the crossings})$$

where the sum is taken over all possible choices of  $k$  (unordered) different crossings in the knot diagram such that the chords arising from these crossings in the knot diagram of  $K$  build a given sub-diagram with given marking. The marked sub-diagrams are called *configurations*. If the function is (as usual) the product of the writhes of the crossings in the configuration,

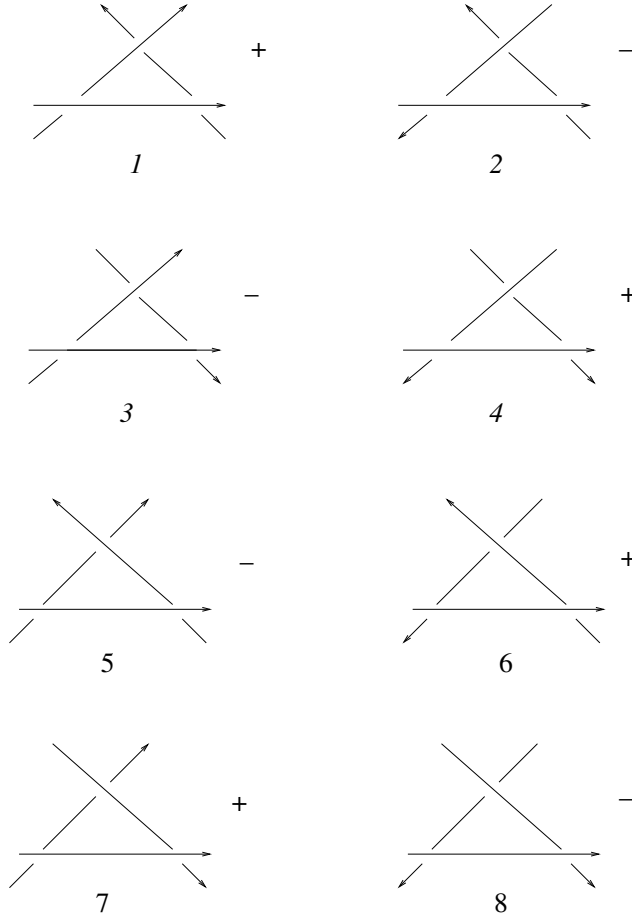


Figure 16: Local types of a triple crossing

then we will denote the sum shortly by the configuration itself. There are exactly eight local types of Reidemeister III moves and four local types of Reidemeister II moves. We show them in Fig. 16 and Fig. 17. (We attach numbers once for all to the local types of Reidemeister III moves for shorter writing.) The sign in the figures denotes the local side of the diagram with respect to the discriminant of diagrams with a triple crossing or respectively with an auto-tangency in the projection (see Section 4.1).

**Definition 10** *The sign of a Reidemeister move  $p$ , denoted by  $\text{sign}(p)$ , is equal to  $+1$  if the move is from the negative side to the positive side and  $-1$  otherwise.*

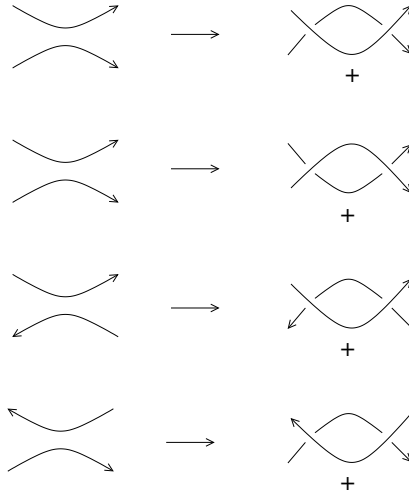


Figure 17: Local types of Reidemeister II moves

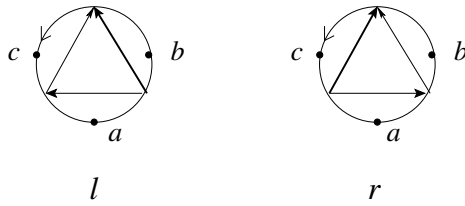


Figure 18: The six global types of triple crossings

For example, a positive Reidemeister III move of type 1 corresponds to an application of a local braid relation  $\sigma_1\sigma_2\sigma_1 \rightarrow \sigma_2\sigma_1\sigma_2$ .

Let us consider the *Gauss diagram of a triple crossing*  $p$ , but without taking into account the writhe of the crossings. In the oriented circle  $K$  we connect the preimages of the triple point  $pr(p)$  by arrows which go from the under-cross to the over-cross and we obtain a triangle. The distinguished crossing  $d$  is always drawn by a thicker arrow.

There are exactly six different *global types* of triple crossings with a point at infinity. We give names to them and show them in Fig. 18. (Here "r" indicates that the crossing between the middle and the lowest branch goes to the right and "l" indicates that it goes to the left.)

**Definition 11** *An ordinary crossing  $q$  in a diagram  $K$  is of type 1 if  $\infty \in D_q^+$  and is of type 0 otherwise.*

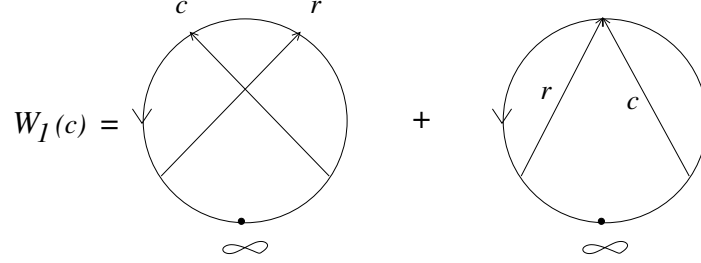


Figure 19: The linear weight  $W_1(c)$  for  $c$  of type 1

Let  $K(p)$  be a generic diagram with a triple crossing or a self-tangency  $p$  and let  $d$  be the distinguished crossing for  $p$ . In the case of a self-tangency we consider both new crossings as the distinguished crossings. The 48 types of triple crossings correspond of course to 48 different Gauss diagrams.

**Definition 12** *Let  $c$  be a crossing of type 1. Then the linear weight  $W_1(c)$  is defined as the sum of the writhes of the crossings  $r$  in  $K(p)$  which form one of the configurations shown in Fig. 19. The crossings  $r$ , which are of type 0 are called  $r$ -crossings of  $c$ .*

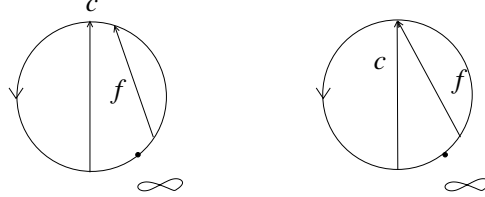
Notice that we do not multiply  $W_1(c)$  by the writhe  $w(c)$ . The weight  $W_1(c)$  will appear only for the crossing  $c = hm$  and only for the global types  $r_a$  and  $l_c$  of triple crossings.

**Definition 13** *Let  $c$  be a crossing of type 0. Then the quadratic weight  $W_2(c)$  is defined by the Gauss diagram formula shown in Fig. 20. The crossings  $f$ , which are of type 1, are called  $f$ -crossings of  $c$ .*

In other words, the "foot" of  $f$  in the Gauss diagram is in the sub arc of the circle which goes from  $\infty$  to the head of  $c$  and the head of  $f$  is in the sub arc which goes from the foot of  $f$  to  $\infty$ . Not all crossings of type 1 are  $f$ -crossings. We illustrate this in Fig. 21. (The letter "f" stands for "foot" or "Fuß" and not for "fiedler".) Notice that we make essential use here of the fact that no crossing can ever move over the point at infinity.

The second (degenerate) configuration in Fig. 20 can of course not appear for a self-tangency  $p$ . The above weights  $W_1(c)$  and  $W_2(c)$  will appear for positive triple crossings, i.e. of local type 1. There is a constant correction by  $+1$  or  $-1$  for certain local types but only for the global type  $r_a$ .

$$W_2(c) = \sum_c w(f) W_I(f) + \sum w(f) W_I(f)$$



$$+ \sum_c w(f) W_I(f) + \sum w(f) W_I(f)$$

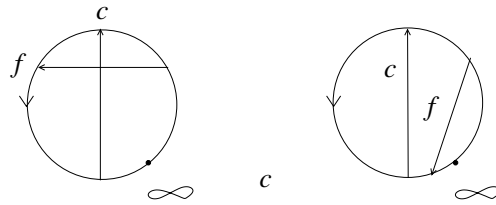


Figure 20: The quadratic weight  $W_2(c)$  for  $c$  of type 0

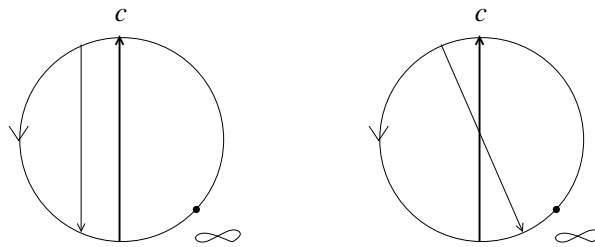


Figure 21: Crossings of type 1 that are not  $f$ -crossings

We are now ready to define the *contributions*  $R_x(p)$  of a Reidemeister move  $p$ . They depend on the local and of the global type of  $p$ . The local type is given by the number from Fig. 16 and the global type by the notation from Fig. 18. Each term in the contribution is an element in  $\mathbb{D}_K^1$ . The local type is always given by the braid on the negative side of the discriminant, compare Fig. 16.

**Definition 14** *The contributions  $R_x(p)$  are defined as follows:*

*local type 1:*  $\sigma_1\sigma_2\sigma_1$

*global types  $r_a, r_b, l_b$ :*  $w(d)x^{W_2(d)}(\sigma_2t_1^+\sigma_2 - \sigma_1t_2^+\sigma_1)$

*global types  $r_a, l_c$ :*  $w(hm)(x^{W_2(ml)+w(hm)W_1(hm)} - x^{W_2(ml)})t_1^+\sigma_2\sigma_1$

*local type 3:*  $\sigma_1\sigma_2^{-1}\sigma_1^{-1}$

*global types  $r_a, r_b, l_b$ :*  $w(d)x^{W_2(d)}(t_2^-\sigma_1^{-1}\sigma_2 - \sigma_1\sigma_2^{-1}t_1^-)$

*global types  $r_a, l_c$ :*  $w(hm)(x^{W_2(ml)+w(hm)W_1(hm)} - x^{W_2(ml)})\sigma_1t_2^-\sigma_1^{-1}$

*local type 4:*  $\sigma_1^{-1}\sigma_2^{-1}\sigma_1$

*global types  $r_b, l_b$ :*  $w(d)x^{W_2(d)}(\sigma_2\sigma_1^{-1}t_2^{-1} - t_1^-\sigma_2^{-1}\sigma_1)$

*global type  $r_a$ :*  $w(d)x^{W_2(d)-1}(\sigma_2\sigma_1^{-1}t_2^{-1} - t_1^-\sigma_2^{-1}\sigma_1)$

$+w(hm)(x^{W_2(ml)+w(hm)W_1(hm)-1} - x^{W_2(ml)})\sigma_1^{-1}\sigma_2^{-1}t_1^+$

*global type  $l_c$ :*  $w(hm)(x^{W_2(ml)+w(hm)W_1(hm)} - x^{W_2(ml)})\sigma_1^{-1}\sigma_2^{-1}t_1^+$

*local type 5:*  $\sigma_2\sigma_1\sigma_2^{-1}$

*global types  $r_b, l_b$ :*  $w(d)x^{W_2(d)}(\sigma_1^{-1}\sigma_2t_1^+ - t_2^+\sigma_1\sigma_2^{-1})$

*global type  $r_a$ :*  $w(d)x^{W_2(d)-1}(\sigma_1^{-1}\sigma_2t_1^+ - t_2^+\sigma_1\sigma_2^{-1})$

$+w(hm)(x^{W_2(ml)+w(hm)W_1(hm)-1} - x^{W_2(ml)})t_1^-\sigma_2\sigma_1$

*global type  $l_c$ :*  $w(hm)(x^{W_2(ml)+w(hm)W_1(hm)} - x^{W_2(ml)})t_1^-\sigma_2\sigma_1$

*local type 7:*  $\sigma_2^{-1}\sigma_1\sigma_2$

*global types  $r_a, r_b, l_b$ :*  $w(d)x^{W_2(d)}(t_1^+\sigma_2\sigma_1^{-1} - \sigma_2^{-1}\sigma_1t_2^+)$

*global types  $r_a, l_c$ :*  $w(hm)(x^{W_2(ml)+w(hm)W_1(hm)} - x^{W_2(ml)})\sigma_1t_2^+\sigma_1^{-1}$

*local type 8:*  $\sigma_2^{-1}\sigma_1^{-1}\sigma_2^{-1}$

*global types  $r_a, r_b, l_b$ :*  $w(d)x^{W_2(d)}(\sigma_1^{-1}t_2^-\sigma_1^{-1} - \sigma_2^{-1}t_1^-\sigma_2^{-1})$

*global types  $r_a, l_c$ :*  $w(hm)(x^{W_2(ml)+w(hm)W_1(hm)} - x^{W_2(ml)})\sigma_1^{-1}\sigma_2^{-1}t_1^-$

$$\begin{aligned}
r_b, l_b &: w(d)x^{W_2(d)} \left( \begin{array}{c} \text{Diagram 1} \\ \text{Diagram 2} \end{array} - \begin{array}{c} \text{Diagram 3} \\ \text{Diagram 4} \end{array} \right) \\
r_a &: w(d)x^{W_2(d)+1} \left( \begin{array}{c} \text{Diagram 1} \\ \text{Diagram 2} \end{array} - \begin{array}{c} \text{Diagram 3} \\ \text{Diagram 4} \end{array} \right) \\
l_c &: w(hm) \left( x^{W_2(ml) + w(hm)W_1(hm)} - x^{W_2(ml)} \right) \begin{array}{c} \text{Diagram 5} \\ \text{Diagram 6} \end{array} \\
r_a &: w(hm) \left( x^{W_2(ml) + w(hm)W_1(hm)+1} - x^{W_2(ml)} \right) \begin{array}{c} \text{Diagram 5} \\ \text{Diagram 6} \end{array}
\end{aligned}$$

Figure 22: Contributions  $R_x(p)$  for the local type 2

The contributions of the two triple crossings which can not be represented as braids are shown in Fig. 22 and Fig. 23. The contributions of the self-tangencies are shown in 24. The sign of each double point is equal to the sign of the underlying crossing which can be found in Fig. 16. All other Reidemeister moves contribute 0 (i.e.  $R$  III moves of global type  $l_a$  and  $r_c$ ,  $R$  II moves with  $d$  of global type 1 and all  $R$  I moves).

Notice that the two singular knots, which are associated to the distinguished crossing  $d$ , are even globally not isotopic (they can be distinguished by the linking number of the smoothing link). If the double point of the contribution corresponds to the crossing  $ml$  then the singular knot on the positive side of the triple crossing is even locally isotopic to the singular knot on the negative side of the triple crossing.

We could give Definition 14 in a more compact (but less practical) form: the contributions with  $d$  singular are always of the form (besides for the constant correction term in  $r_a$ ) the singular knot on the positive side of the discriminant minus the singular knot on the negative side of the discriminant and both with the coefficient  $w(d)x^{W_2(d)}$ . If the double point of the contribution corresponds to the crossing  $ml$  then the singular knot enters always (besides for the constant correction term in  $r_a$ ) with the co-

$$\begin{aligned}
r_b, l_b : & \quad w(d)x^{W_2(d)} \left( \begin{array}{c} \diagup \quad \diagdown \\ \diagdown \quad \diagup \end{array} \begin{array}{c} - \\ - \end{array} - \begin{array}{c} \diagup \quad \diagdown \\ \diagdown \quad \diagup \end{array} \begin{array}{c} - \\ - \end{array} \right) \\
r_a : & \quad w(d)x^{W_2(d)+1} \left( \begin{array}{c} \diagup \quad \diagdown \\ \diagdown \quad \diagup \end{array} \begin{array}{c} - \\ - \end{array} - \begin{array}{c} \diagup \quad \diagdown \\ \diagdown \quad \diagup \end{array} \begin{array}{c} - \\ - \end{array} \right) \\
l_c : & \quad w(hm) \left( x^{W_2(ml) + w(hm)W_1(hm)} - x^{W_2(ml)} \right) \begin{array}{c} \diagup \quad \diagdown \\ \diagdown \quad \diagup \end{array} \begin{array}{c} - \\ + \end{array} \\
r_a : & \quad w(hm) \left( x^{W_2(ml) + w(hm)W_1(hm)+1} - x^{W_2(ml)} \right) \begin{array}{c} \diagup \quad \diagdown \\ \diagdown \quad \diagup \end{array} \begin{array}{c} - \\ + \end{array}
\end{aligned}$$

Figure 23: Contributions  $R_x(p)$  for the local type 6

$$\begin{aligned}
& \begin{array}{c} \diagup \quad \diagdown \\ \diagdown \quad \diagup \end{array} \\
& \begin{array}{c} \bullet \\ \uparrow \\ \text{circle} \\ \downarrow \\ \bullet \end{array} \quad d \quad x^{W_2(d)} \left( \begin{array}{c} \diagup \quad \diagdown \\ \diagdown \quad \diagup \end{array} \begin{array}{c} + \\ - \end{array} - \begin{array}{c} \diagup \quad \diagdown \\ \diagdown \quad \diagup \end{array} \begin{array}{c} - \\ + \end{array} \right) \\
& \begin{array}{c} \diagup \quad \diagdown \\ \diagdown \quad \diagup \end{array} \\
& \begin{array}{c} \bullet \\ \uparrow \\ \text{circle} \\ \downarrow \\ \bullet \end{array} \quad d \quad x^{W_2(d)} \left( \begin{array}{c} \diagup \quad \diagdown \\ \diagdown \quad \diagup \end{array} \begin{array}{c} + \\ - \end{array} - \begin{array}{c} \diagup \quad \diagdown \\ \diagdown \quad \diagup \end{array} \begin{array}{c} - \\ + \end{array} \right)
\end{aligned}$$

Figure 24: Contributions  $R_x(p)$  for self-tangencies independent of their local type



efficient  $w(hm)(x^{W_2(ml)+w(hm)W_1(hm)} - x^{W_2(ml)})$ . The correction term in  $r_a$  for both  $W_2(d)$  and  $W_2(ml) + w(hm)W_1(hm)$  is equal to  $-1$  if and only if  $w(d) = -w(ml)$  and the R III move can be represented by braids. The correction term in  $r_a$  for both  $W_2(d)$  and  $W_2(ml) + w(hm)W_1(hm)$  is equal to  $+1$  if and only if  $w(d) = -w(ml)$  and the R III move can not be represented by braids. The contributions of the Reidemeister II moves do not depend on the local type of the move and enter with the coefficient  $w(d)x^{W_2(d)}$ .

It is very important to notice that the contributions of a R III move do not depend only of the types (0 or 1) and the writhe of the three crossings of the move but they depend strongly on the global and local type of the move: for example,  $r_a$  contributes in two different ways but  $l_a$  does never contribute at all.

The boundary  $\partial K$  of a string link  $K$  is an ordered set in the marked circle (which depends of course of the chosen abstract closure  $\sigma$  of the string link).

**Definition 15** *Let  $q$  be the underlying crossing of a double point. The grading of a double point is the intersection of  $D_q^+$  (compare Definition 9) with the boundary  $\partial K$ .*

**Definition 16** *Let  $\gamma$  be an oriented generic arc in  $M_K$  (for the precise definition of "generic" we need the stratification of  $M_K$ , see Section 4.1). The 1-cochain  $R_x(\gamma)$  is defined as*

$$\sum_p \text{sign}(p) R_x(p)$$

where the sum is taken over all Reidemeister moves  $p$  in  $\gamma$  with the same fixed chosen grading for all double points.

(It follows immediately from our definitions that the gradings of all double points in  $R_x(\gamma)$  are the empty set in the particular case of long knots and we can ignore them. In the case of string links with exactly two components the grading is determined by the choice of the marked point at infinity and we can ignore it too.)

We are now ready to formulate the first part of our main result.

**Theorem 1** *Let  $K$  be an oriented string link. Then the graded 1-cochain  $R_x(\gamma)$  with values in  $\mathbb{D}_K^1$  is a 1-cocycle. Moreover,  $R_x$  has the scan-property,*

i.e.  $R_x(scan(K))$  is an isotopy invariant of  $K$ . If  $K$  is a long knot such that its closure in  $S^3$  is a satellite then  $R_x$  gives rise to a not always trivial cohomology class  $[R_x] \in H^1(M_K; \mathbb{D}_K^1)$ .

(Remember that the only relation in  $\mathbb{D}_K^1$  is the embedded 1T-relation, compare the Introduction.)

The theorem applied to the loops  $drag(K, K)$ ,  $drag(Cab_n(K), Cab_n(K))$  and to  $scan(Cab_n(K))$  for  $n > 1$  gives the first *singularization* of knots and of  $n$ -cables of framed long knots.

## 2.2 The 1-cocycle $R_1^{split}$ for positive closed 4-braids

Let  $V$  be the standard solid torus in  $\mathbb{C} \times \mathbb{R}$  which intersects  $\mathbb{C} \times 0$  in an annulus around the origin. We identify  $H_1(V; \mathbb{Z})$  with  $\mathbb{Z}$  by sending the oriented closed 1-braid to  $+1$ . Let  $\beta$  be a  $n$ -braid which closes to a knot and let  $q$  be a crossing of  $\beta$ . We assume  $n > 3$ .

**Definition 17** *The homological marking of  $q$  in  $\{1, 2, \dots, n-1\}$  is the homology class represented by  $D_q^+$ . We write it as a number on the left side of the corresponding arrow.*

Remember that we consider (geometric) braids as tangles and not as isotopy classes of tangles (or elements in the braid group). So, a generic braid is for us a word in the standard generators and their inverses of the braid group.

If a braid  $\beta$  is in *Garsides normal form*, see [31], then it is in particular of the form  $\beta^+(\Delta^2)^k$ , where  $\beta^+$  is a positive braid,  $k$  is an integer and  $\beta^+$  is not divisible by  $\Delta^2$ .

Let  $\beta^+(\Delta^2)^k$  and  $\beta'^+(\Delta^2)^k$  be two  $n$ -braids in Garsides normal form. *Garsides solution of the conjugacy problem* says that the isotopy classes of the braids are conjugate in  $B_n$  if and only if  $\beta^+$  and  $\beta'^+$  can be related by a sequence of the following operations (see [31]):

- 1) isotopy amongst positive braids
- 2) cyclic permutation
- 3) conjugacy with permutation braids  $s\beta^+s^{-1}$  followed by a simplification to a positive braid (where the *permutation braids*  $s$  are exactly the left and right divisors in the braid monoid  $B_n^+$  of Garsides braid  $\Delta$ , i.e. there exist positive  $n$ -braids  $s'$  and  $s''$  such that  $ss'$  is isotopic to  $s''s$  which is isotopic to  $\Delta$ ).

Stepan Orevkov has made the following important observation (personal communication).

**Observation 1** (*Orevkov*)

*Assume that the closure  $\hat{\beta}^+$  contains a half-twist  $\Delta$ , i.e.  $\beta^+$  is equivalent to  $\beta''^+\Delta$  for some positive braid  $\beta''^+$  by operations 1 and 2 only. Then we can skip the operation 3 in Garsides solution of the conjugacy problem.*

*Proof.* Indeed, assume that we have to perform the operation 3:

$$\beta^+ \rightarrow s\beta^+s^{-1} = \beta'^+.$$

From our hypothesis  $\beta^+ = \beta''^+\Delta$  by using operations 1 and 2.  $\beta''^+\Delta = \beta''^+s''s \rightarrow s\beta''^+s''ss^{-1} = s\beta''^+s'' = \beta'^+$ . But by using only operations 2 we can bring the last braid to  $\beta''^+s''s = \beta''^+\Delta = \beta^+$ . Consequently, we have replaced the operation 3 by a sequence of only operations of type 1 and 2.

□

Orevkov's observation implies that if two positive closed braids which contain a half-twist are isotopic in the solid torus then there is such an isotopy which stays within positive closed braids (because negative crossings occur only in operation 3). The loop  $rot(\beta''^+\Delta)$  can be represented by pushing twice  $\Delta$  through  $\beta''^+$ . It follows easily now (by considering braids as diffeomorphisms of the punctured disc and  $rot$  as the rotation from 0 to  $2\pi$  of the disc around its center) that if  $\beta''^+\Delta$  is isotopic to  $\hat{\beta}'^+\Delta$  then the loops  $rot(\beta''^+\Delta)$  and  $rot(\hat{\beta}'^+\Delta)$  are homotopic through positive closed braids (i.e. all generic crossings are positive).

Adding full-twists to a braid does not change its geometry and its geometric invariants (as hyperbolic volume or entropy for pseudo-Anosov braids) and a full twist (which generates the center of the braid group) in a closed braid can be easily detected. Using Orevkov's observation we can therefore restrain ourself to the heart of the matter: constructing 1-cocycles for positive closed braids in  $M_{\hat{\beta}^+\Delta}$ .

**Definition 18** *Let  $c$  be a crossing of homological marking 1. Then the linear weight  $W_1(c)$  is defined as the sum of the writhes of the crossings  $q$  in  $\hat{\beta}(p)$  which form the configuration shown in Fig. 25. The linear weight  $W_{n-2}(c)$  is defined as the sum of the writhes of the crossings  $q$  in  $\hat{\beta}(p)$  which form the configuration shown in Fig. 26.*

It follows directly from our definitions that a Reidemeister III move with a distinguished crossing  $d$  with marking 1 is necessarily of global type  $r$  and that the crossings  $hm$  and  $ml$  have each a marking strictly greater than 1.

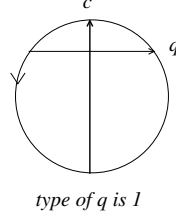


Figure 25: linear weight  $W_1(c)$  for closed braids

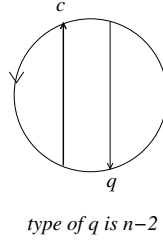


Figure 26: linear weight  $W_{n-2}(c)$  for closed braids

**Definition 19** Let us encode the global types of  $R$  III moves for closed  $n$ -braids by the homological markings in the order:  $r(d, hm, ml)$  and  $l(d, hm, ml)$ .

Let  $\mathbb{Z}[x, x^{-1}, y, y^{-1}]$  be the ring of integer Laurent polynomials of two variables and let  $\hat{\beta}_{xy}^1$  be the  $\mathbb{Z}[x, x^{-1}, y, y^{-1}]$ -module freely generated by all isotopy classes of closed  $n$ -braids  $\hat{\beta} = \hat{\beta}^+ \Delta$  with exactly one ordinary double point which comes from a crossing with homological marking 1.

(The signs of all double points are positive and we can skip them.) We consider Reidemeister III moves as moves on local 3-braids. Notice that only the local type 1 occurs.

**Definition 20** The contributions  $R_{xy}(p)$  in  $\hat{\beta}_{xy}^1$  are defined as follows:

*R III of local type 1:*

$$r(1, ., .): x^{W_1(d)} y^{W_{n-2}(d)} (\sigma_2 t_1 \sigma_2 - \sigma_1 t_2 \sigma_1)$$

$$l(n-1, n-2, 1): x^{W_1(ml)} (y^{W_{n-2}(ml)+1} - y^{W_{n-2}(ml)}) t_1 \sigma_2 \sigma_1$$

$$l(n-1, 1, n-2): x^{W_1(hm)} (y^{W_{n-2}(hm)+1} - y^{W_{n-2}(hm)}) \sigma_1 \sigma_2 t_1$$

$$l(2, 1, 1): y^{W_{n-2}(ml)} (x^{W_1(ml)} - x^{W_1(ml)+1}) t_1 \sigma_2 \sigma_1$$

All other Reidemeister III moves contribute 0.

The homological markings of  $hm$  and  $ml$  are allowed to be arbitrary in the case of  $d$  with marking 1 (but they satisfy of course an evident linear

relation). The Reidemeister III move  $l(2, 1, 1)$  is the only move of global type  $l$  and with a distinguished crossing with marking 2. This comes from the obvious fact that each of the three arcs in the circle, which are determined by the vertices of the triangle, represents a positive homology class in the solid torus. Notice that in all cases only crossings with marking 1 could become singular.

**Definition 21** *Let  $\gamma$  be an oriented generic arc in  $M_{\hat{\beta}}$ . The 1-cochain  $R_{xy}(\gamma)$  is defined as*

$$\sum_p \text{sign}(p) R_{xy}(p)$$

where the sum is taken over all Reidemeister III moves  $p$  in  $\gamma$ .

**Proposition 1** *The 1-cochain  $R_{xy}(\gamma)$  with values in  $\hat{\beta}_{xy}^1$  is a 1-cocycle.*

Unfortunately, we do not know whether or not it represents always the trivial cohomology class. Therefore we define another 1-cocycle in a much more sophisticated way, but which turns out to be non trivial already in the simplest example.

Let us restrain now to positive closed 4-braids, which contain a half-twist and which are knots.

In an generic arc in  $M_{\hat{\beta}=\hat{\beta}+\Delta}$  occur only Reidemeister moves of type III, which are of local type 1, but there occur also commutation relations, corresponding to passing through a closed braid in which two crossings have the same coordinate  $\arg(z)$ .

**Definition 22** *The sign of the commutation relation  $\sigma_3\sigma_1 \rightarrow \sigma_1\sigma_3$  is +1 and -1 in the opposite direction.*

We are now ready to define the contributions  $R_1(p)$  of these moves in  $\mathbb{D}_{\beta}^1$  (compare the Introduction).

**Definition 23** *The contributions  $R_1(p)$  of R III moves are:*

$$\begin{aligned} r(1, 3, 2): & +\sigma_1 t_2 \sigma_1 \\ r(1, 2, 3): & -\sigma_2 t_1 \sigma_2 \\ l(2, 1, 1): & +\sigma_1 \sigma_2 t_1 - t_1 \sigma_2 \sigma_1 \end{aligned}$$

$$l(3, 1, 2): -\sigma_1\sigma_2t_1$$

$$l(3, 2, 1): +t_1\sigma_2\sigma_1$$

The contributions  $R_1(p)$  of commutation relations are:

$$\sigma_3 \text{ of marking 1 and } \sigma_1 \text{ of marking 3: } +t_3\sigma_1$$

$$\sigma_3 \text{ of marking 3 and } \sigma_1 \text{ of marking 1: } -t_1\sigma_3$$

$$\sigma_3 \text{ of marking 1 and } \sigma_1 \text{ of marking 1: } +t_1\sigma_3 - t_3\sigma_1$$

All other  $R$  III moves and commutation relations contribute 0.

Notice that in contrast to  $R_{xy}$  the moves  $r(1, 3, 2)$  and  $r(1, 2, 3)$  do not contribute in the same way and that we don't need any weights in  $R_1$ . Again, only crossings with marking 1 could become singular (this explains the index "1" in  $R_1$ ).

**Definition 24** Let  $\gamma$  be an oriented generic arc in  $M_{\hat{\beta}+\Delta}$ . The 1-cochain  $R_1(\gamma)$  is defined as

$$\sum_p \text{sign}(p) R_1(p)$$

where the sum is taken over all  $R$  III moves and commutation relations  $p$  in  $\gamma$ .

**Proposition 2** The 1-cochain  $R_1(\gamma)$  with values in  $\mathbb{D}_\beta^1$  is a 1-cocycle.

Unfortunately, we do not know again whether or not it represents always the trivial cohomology class. Therefore we refine it by a "local system", which was first introduced in [20]. We chose a base point  $\hat{\beta}$  in  $M_{\hat{\beta}+\Delta}$ . Let  $\{x(1), \dots, x(k)\}$  be the crossings of marking 1 in  $\hat{\beta}$ . Let  $\gamma$  be a loop based in  $\hat{\beta}$  in  $M_{\hat{\beta}+\Delta}$ . The loop  $\gamma$  induces a permutation  $m_\gamma$  of  $\{x(1), \dots, x(k)\}$  because there are no Reidemeister moves of type II and of type I in the loop and hence all crossings survive in an isotopy. This permutation is called the *monodromy*  $m_\gamma(x(i))$  and it preserves of course the homological marking. It is not very difficult to see that  $m_{rot}$  is always a cycle of length  $k$  in the symmetric group (compare [20]), and of course  $m_{hat} = id$ .

**Definition 25** The 1-cochains  $R_{x(i)}(\gamma)$  for  $i \in \{1, \dots, k\}$  are defined as

$$\sum_p \text{sign}(p) R_{x(i)}(p)$$

where the sum is taken over all those  $R$  III moves and commutation relations  $p$  in  $\gamma$  for which the crossing which becomes singular is exactly  $x(i)$ .

Let  $Sym_k(\mathbb{D}_\beta^1)$  denote the symmetric product of  $k$  copies of  $\mathbb{D}_\beta^1$ . We are now ready to formulate the second part of our main result.

**Theorem 2** *Let  $\beta^+\Delta$  be a 4-braid which closes to a knot. Then the unordered set  $\{R_{x(1)}(\gamma), \dots, R_{x(k)}(\gamma)\}$  represents a not always trivial cohomology class, called  $[R_1^{split}] \in H^1(M_{\hat{\beta}^+\Delta}; Sym_k(\mathbb{D}_\beta^1))$ .*

The 1-cocycle  $R_1^{split}$  applied to the loop  $rot(\hat{\beta}^+\Delta)$  gives the first *singularization* of positive closed 4-braids in the solid torus (where we don't have any longer a point at infinity on the knot).

For a pseudo-Anosov 4-braid  $\beta = \beta^+\Delta$  the group  $H_1(M_{\hat{\beta}^+\Delta}; \mathbb{Z}) \cong \pi_1(M_{\hat{\beta}^+\Delta}; \hat{\beta}) \cong \mathbb{Z} \times \mathbb{Z}$  is generated by the loops *rot* and *hat*. It follows that  $R_1^{split}$  is already a well defined homomorphism of  $H_1(M_{\hat{\beta}^+\Delta}; \mathbb{Z}) \rightarrow (\mathbb{D}_\beta^1)^k / \langle m_{rot} \rangle$ , where  $k$  is the number of crossings of homological marking 1.

**Remark 5** *It is clear that our solution  $R_1$  of the global tetrahex equation could be generalized for  $n > 4$  (but the number of equations in the global tetrahex equation increases rapidly with  $n$ ). However, for  $n > 4$  a new stratum of codimension 2 with respect to the projection into  $(\mathbb{C}^*, \arg)$  appears in  $M_{\hat{\beta}^+\Delta}$ : a triple crossing and an ordinary crossing with the same coordinate  $\arg(z)$ . For  $n > 5$  another new stratum of codimension 2 appears: three ordinary crossings with the same coordinate  $\arg(z)$  (see Section 4 for the stratification with respect to the projection into the plan of topological moduli spaces of knots). A 1-cocycle has to stay invariant for homotopies of loops which pass through these strata of codimension 2. It is a challenging open problem to construct non trivial 1-cocycles (with values in modules generated by singular closed braids and which generalize  $R_1^{split}$ ) for  $n > 4$ .*

**Remark 6** *We can consider the thickened torus as  $T^2 \times I = V \setminus C$ . Here  $V$  is the solid torus and  $C$  is its core, the closed 1-braid. We consider closed braids  $\hat{\beta}$  which are knots in  $V \setminus C$ . Orevkov's observation is still valid if the closed positive 5-braid  $\hat{\beta} \cup C$  contains  $\Delta \in B_5$ . The loops *rot* and *hat* are still well defined and keep the closed 1-braid  $C$  invariant and we don't care about the crossings between  $\hat{\beta}$  and  $C$  in the moves and in the weights. It follows that the 1-cocycles  $R_{xy}$  and  $R_1^{split}$  are still well defined for a class of closed braids in the thickened torus.*

Notice that even in the case of knots in the thickened torus  $K \subset T^2 \times I = V \setminus C$  it is essential to use the projection of  $K \cup C$  into the annulus rather than the natural projection of  $K$  into  $T^2$ , because for the latter there aren't any moves in the loops of knots in  $T^2 \times I$  induced by the loops in  $\text{Diff}_+(T^2 \times I)$ .

The last step in the constructive part of knot theory could be to construct such non trivial 1-cocycles even for essential knots (i.e. not contained in a 3-ball) in the solid torus  $V$  and which are no longer closed braids.

## 2.3 The Entropy conjecture for 4-braids

Let us start by recalling Hatcher's result.

**Proposition 3** *The loops  $\text{rot}(\hat{\beta})$  and  $\text{hat}(\hat{\beta})$  represent linearly dependent homology classes in  $H_1(M_{\hat{\beta}}; \mathbb{Q})$  if and only if  $\hat{\beta}$  is isotopic to a torus knot in  $\partial V$ .*

*Proof (Hatcher).* The rotations give an action of  $\mathbb{Z} \times \mathbb{Z}$ , and one can look at the induced action on the fundamental group of the knot complement, with respect to a base point in the boundary torus  $\partial V$  of the solid torus. Call this fundamental group  $G$ . The action of  $\mathbb{Z} \times \mathbb{Z}$  on  $G$  is conjugation by elements of the  $\mathbb{Z} \times \mathbb{Z}$  subgroup of  $G$  represented by loops in the boundary torus. The action will be faithful (zero kernel) if the center of  $G$  is trivial. The only (irreducible) 3-manifolds whose fundamental groups have a nontrivial center are Seifert fibered manifolds defined by a circle action. The only such manifolds that embed in  $\mathbb{R}^3$  and have two boundary components (as here) are the obvious ones that correspond to cable knots, that is, the complement of a knot in a solid torus that is isotopic to a nontrivial loop in the boundary torus.  $\square$

The Nielsen-Thurston classification says that a braid which is not periodic (i.e. some power of it is isotopic to a power of the full twist) neither composite (i.e. there is a not boundary parallel incompressible torus in the complement of its closure in  $V$ ) is of pseudo-Anosov type (see e.g. [18]). The *entropy*  $h(\beta)$  of a pseudo-Anosov braid is known to be equal to  $\log(\lambda_\beta)$ , where  $\lambda_\beta > 1$  is the *stretching factor* of one of the two transverse invariant measured foliations associated to  $\beta$  (see [18]). The foliation is called *transverse orientable* if no arc transverse to the foliation intersects a leaf positively and negatively (or equivalently, if the invariant foliations have odd order singularities at all punctures and all interior singularities are of even order, see e.g. [2], [49]).



We consider now the unordered set of quantum invariants  $\{PR_{x(1)}(rot(\hat{\beta}^+\Delta)), \dots, PR_{x(k)}(rot(\hat{\beta}^+\Delta))\}$  in the HOMFLYPT skein module of the solid torus (for the definition of skein modules see [58], [64]), which is obtained from  $\{R_{x(1)}(rot(\hat{\beta}^+\Delta)), \dots, R_{x(k)}(rot(\hat{\beta}^+\Delta))\}$  by applying the Kauffman-Vogel skein relations (here we do not need to normalize because Reidemeister I moves do not appear in an isotopy of closed braids). Setting  $v = t$  and substituting  $z = t^{1/2} - t^{-1/2}$  we obtain an unordered set of elements  $\{\Delta R_{x(1)}(rot(\hat{\beta}^+\Delta)), \dots, \Delta R_{x(k)}(rot(\hat{\beta}^+\Delta))\}$  in the Alexander skein module of the solid torus. Using skein relations we express each element in  $\{\Delta R_{x(1)}(rot(\hat{\beta}^+\Delta)), \dots, \Delta R_{x(k)}(rot(\hat{\beta}^+\Delta))\}$  in the standard basis of the Alexander skein module, namely the isotopy classes in  $V$  of all those closed positive permutation braids which stay permutation braids under cyclic permutations. Each closed permutation braid  $\hat{\sigma}$  is now replaced by its 2-variable Alexander polynomial  $\Delta_{\hat{\sigma} \cup L}(u, t) = \det(uId - B_{\sigma}^r(t))$ . Here  $L = (0 \times \mathbb{R}) \cup \infty \subset S^3$  is the braid axes and  $B_{\sigma}^r(t)$  is the reduced Burau matrix for  $\sigma$ . (The variable  $u$  corresponds to the meridian of  $L$  and the variable  $t$  corresponds to the meridian of  $\hat{\sigma}$ .) We make the substitutions  $A - B = z = t^{1/2} - t^{-1/2}$  (compare the definition of the HOMFLYPT polynomial for singular links by Kauffman-Vogel) and  $A = vz/(v - v^{-1}) = t/(t^{1/2} + t^{-1/2})$ , which annihilates the embedded 1T-relation (compare Remark 2 in the Introduction). We obtain this way an unordered set  $\{\Delta R_{x(1)}(u, t), \dots, \Delta R_{x(k)}(u, t)\}$  of Laurent polynomials in  $t^{1/2}$  which are polynomials in  $u$  of degree 3.

**Definition 26** For each  $\Delta R_{x(i)}(u, t)$  let  $\lambda_{x(i)} \in \mathbb{C}$  be the zero in  $u$  of  $\Delta R_{x(i)}(u, t)$  with the greatest absolute value for  $t$  on the unit circle. If  $\Delta R_{x(i)}(u, t)$  is identical 0 then we set  $\lambda_{x(i)} = 1$ .

One easily sees (by using skein relations and a basis of the skein module consisting of closed permutation braids) that each  $\Delta R_{x(i)}(u, -1)$  contains  $u - 1$  as a factor. Consequently, we have always  $|\lambda_{x(i)}| \geq 1$ .

**Definition 27** We chose a base point  $\hat{\beta}$  in  $M_{\hat{\beta}^+\Delta}$ . Let  $\{x(1), \dots, x(k)\}$  be the crossings of marking 1 in  $\hat{\beta}$  and let  $rot(\hat{\beta})$  be the oriented loop defined above. A crossing  $x(i)$  is called periodic if  $|\lambda_{x(i)}| = 1$  and it is called hyperbolic if  $|\lambda_{x(i)}| > 1$ .

Evidently, the type of a crossing, periodic or hyperbolic, does not depend on the choice of a base point and depends only on the homology class of the loop.

**Definition 28** The 1-cocycle spectral radius  $\lambda_{R(\beta)}$  is defined as

$$\lambda_{R(\beta)} = 1/k_{hyp} \sum_{x(i)} |\lambda_{x(i)}|$$

where the sum is over all hyperbolic crossings  $x(i)$  and  $k_{hyp} \leq k$  denotes the number of hyperbolic crossings.

Let us now formulate the (optimistic) *Entropy conjecture*.

**Conjecture 3** Let  $\beta = \beta^+ \Delta$  be a positive pseudo-Anosov 4-braid which contains a half-twist and which closes to a knot. Then

$$\lim_{m \rightarrow \infty} \lambda_{R(\beta^+ \Delta^{2m+1})} = \lambda_\beta.$$

We have calculated (see Section 3.2) that for the simplest positive pseudo-Anosov 4-braid which contains a half-twist  $\beta = \sigma_3 \sigma_2^{-1} \sigma_1^{-1} \Delta^2 = \sigma_3^2 \sigma_1 \sigma_2 \sigma_1 \Delta$  we have already for  $m = 0$

$$\lambda_\beta / \lambda_{R(\beta)} = 1.0060\dots$$

Could this be a simple coincidence? A computer program would be very helpful.

The origin of the conjecture needs some explanations. Following Artin, a  $n$ -braid can be considered as an automorphism of the free group  $F_n$  (in fact, the fundamental group of the  $n$ -punctured disc with the base point on the boundary of the disc). One fixes a system of generators  $x$  of  $F_n$  and one defines the *growth rate* of  $\beta$  by

$$GR(\beta) = \sup_{x \in F_n} \lim_{k \rightarrow \infty} |\beta^k(x)|^{1/k}$$

where  $|\cdot|$  denotes the reduced word length with respect to the generators  $x$  and their inverses. It is well known that  $GR(\beta) = \lambda_\beta$  for a pseudo-Anosov braid  $\beta$  (for all this see [18], [2], [49], [47]). Multiplying by full-twists does not change the geometric invariants of the braid, which are also invariant under conjugation. Moreover, it is known that the invariant measured foliation is transverse orientable if and only if there do not occur accidental reductions of the word length  $|\beta^k(x)|$  and hence  $GR(\beta) = \sup_{x \in F_n} |\beta(x)|$ . In this case it is known that  $\lambda_\beta$  is the greatest real zero of  $\Delta_{\hat{\beta} \cup L}(u, t = -1) = \det(u \text{Id} - B_\beta^r(-1))$  (see [48], [47], [2]). In general we have *Kolev's inequality* [48] which says that  $\lambda_\beta$  is not smaller than the greatest absolute value of a zero in  $u$  of  $\Delta_{\hat{\beta} \cup L}(u, t)$  for  $t$  on the unit circle.

It is known that for the pseudo-Anosov 4-braid  $\beta = \sigma_3\sigma_2^{-1}\sigma_1^{-1}$  the measured invariant foliation is not transverse orientable and in fact  $\Delta_{\hat{\beta}\cup L}(u, -1) = (u - 1)^3$ . The stretching factor  $\lambda_\beta \approx 2.2966$  is the greatest real zero of  $u^4 - 2u^3 - 2u + 1$  (obtained from the action of  $\beta$  on the corresponding train track, see e.g. [49], [47]) and Kolev's inequality gives only  $\lambda_\beta > 2.17$ .

In the definition of  $\lambda_{R(\beta)}$  we replace the quantity which appears in Kolev's inequality, namely the greatest absolute value of a zero in  $u$  of  $\Delta_{\hat{\beta}\cup L}(u, t)$  for  $t$  on the unit circle (the spectral radius of the Burau matrix on the unit circle), by a certain average of these quantities over all the invariant combinations of braids which appear in the value of  $R_1^{split}(rot(\hat{\beta}))$ .

Finally, is there perhaps a relation between the hyperbolic volume of the mapping torus of  $\beta$  (seen as a diffeomorphism of the punctured disc), i.e.  $S^3 \setminus (\hat{\beta} \cup L)$ , and  $R_1^{split}(rot(\hat{\beta}))$ ? (For an ideal triangulation of the mapping torus for the above braid see [1].)

### 3 Examples

We give some examples in much detail in the hope that it will make it easier for the reader to become familiar with the new invariants.

#### 3.1 Long knots

Let us start by showing that the loop  $rot(K)$  is not really interesting for us (this is not too surprising because the loop is just induced by a rotation of the whole 3-space which doesn't depend on the knot at all).

**Proposition 4** *Let  $K$  be a long knot. Then  $R_x(rot(K)) = 0$ .*

*Proof.* We can assume that  $K$  is a closed braid with just one strand which is opened to go to infinity. Let us represent  $rot(K)$  by pushing  $K$  through a curl with positive writhe and positive Whitney index as shown in Fig. 27. In the first half of the loop we move for each Reidemeister move from the overcross of the distinguished crossing  $d$  to  $\infty$  and in the second half we move from  $\infty$  to the undercross of  $d$ . It follows that all distinguished crossings  $d$  are of type 1. Consequently, only Reidemeister III moves of global type  $l_c$  could contribute non trivially to  $R_x(rot(K))$  (compare Definition 14). Each positive crossing in  $K$  contributes in the first half of the loop by a R III move

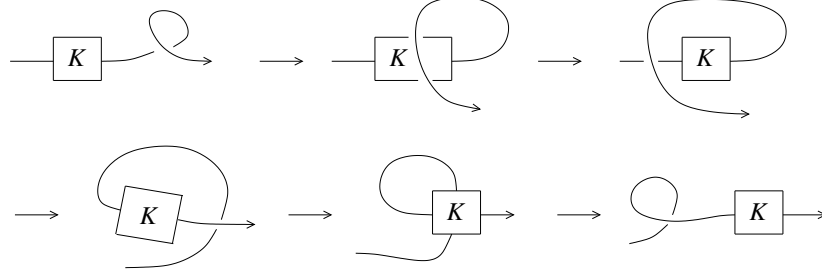


Figure 27: A representative of Gramain's loop for which  $R_x$  is identical 0

of local type 1 and of global type  $l_c$ . However, the arc from the overcross of  $d$  to  $\infty$  goes over everything in the first half of the loop and hence there are no r-crossings for  $hm$  at all. It follows that  $W_1(hm) = 0$  and consequently,  $x^{W_2(ml)+W_1(hm)} - x^{W_2(ml)} = 0$  (compare Definition 14). Each negative crossing of  $K$  contributes in the first half of the loop by a R III move of global type  $r_c$  and consequently, its contribution is 0. In the second half of the loop we move always directly from  $\infty$  to the undercross of  $d$ . It follows that all Reidemeister III moves are of global type  $r_c$  or  $l_a$  and do not contribute at all.  $\square$

**Remark 7** *It is amazing that not only the value of  $R_x$  on the homology class represented by  $\text{rot}(K)$  vanishes but that this class can be represented by such loops for which the 1-cocycle itself vanishes, i.e.  $R_x$  is identical 0 on each arc in the loop. This suggests that in a future differential geometric approach the functional on the mapping torus for these loops should be constant (compare the Introduction).*

As a warm-up for the reader we calculate now  $R_x(\text{rot}(3_1^+))$  by pushing the knot through a curl with positive writhe but negative Whitney index. The loop is shown in Fig. 28 (where as usual we attach numbers to the moves). The relevant signs, types and weights are shown in Fig. 29 and  $R_x(\text{rot}(3_1^+))$  is calculated in Fig. 30. We see that the 1-cocycle is not identical 0 here and that its value on the loop vanishes only because of the embedded 1T-relation.

**Remark 8** *The embedded 1T-relation is forced from the moving cusps, compare Section 4.7. In [23] (which doesn't contain any singularization) we have considered instead of the embedded 1T-relation some correction term  $V^{(1)}$ ,*

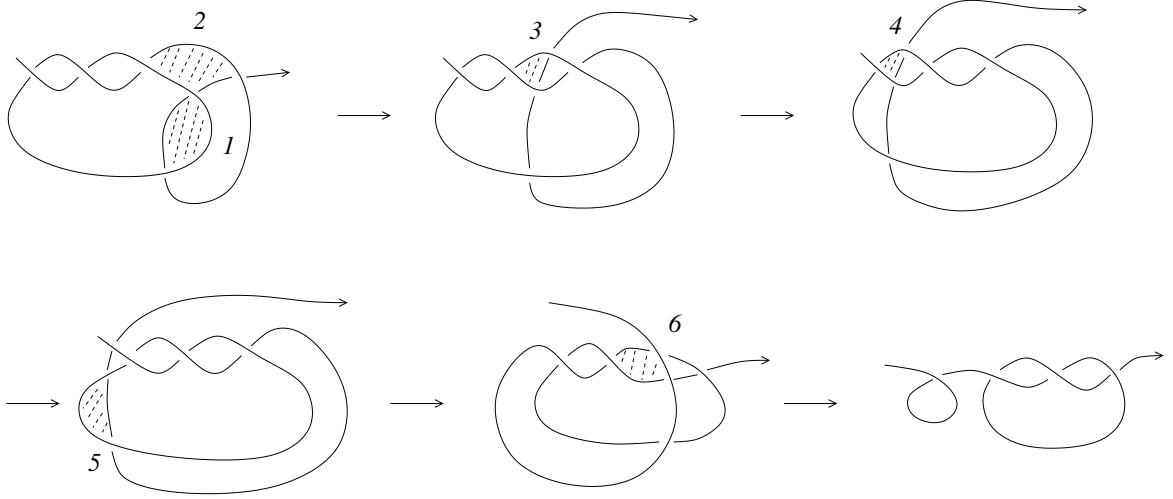


Figure 28: Another representative of Gramain's loop for the trefoil

which is of relative finite type (for the definition compare [23]). So, it seems that the Teiblum-Turchin 1-cocycle on  $\text{rot}(K)$  corresponds just to this correction term and in  $PR_1 = dPR_x/dx(x = 1)$  we quotient out in fact finite type 1-cocycles in Vassiliev's sens (which are multiplied by the HOMFLYPT polynomial).

**Proposition 5** *Let  $K$  be any long knot. Then  $R_x(\text{scan}(K)) = 0$ .*

*Proof.* We represent  $\text{rot}(K)$  by pushing  $K$  through a curl with positive writhe but negative Whitney index as in the example for  $3_1^+$ . Then  $\text{scan}(K)$  is just the first half of the loop. But in the second half of the loop no Reidemeister move at all contributes to  $R_x$  (as in the example for  $3_1^+$ ). The proposition follows now from the previous proposition together with the fact that  $R_x$  is a 1-cocycle.  $\square$

We have calculated that  $R_x(\text{hat}(4_1)) = 0$  and  $R_x(\text{hat}(5_2^+)) = 0$ , but we will not give the details.

In Fig. 31 we show the loop  $\text{hat}(4_1 \# 4_1)$ , where the dot corresponds to another copy of the knot  $4_1$ .

The calculation of  $R_x(\text{hat}(4_1 \# 4_1))$  is very long (exactly 100 Reidemeister moves to consider). Notice that not all f-crossings intersect the distinguished crossing  $d$  (compare Definition 13). Therefore the small summand  $4_1$  could contribute to the weight  $W_2(p)$  of a Reidemeister move  $p$  of the big knot

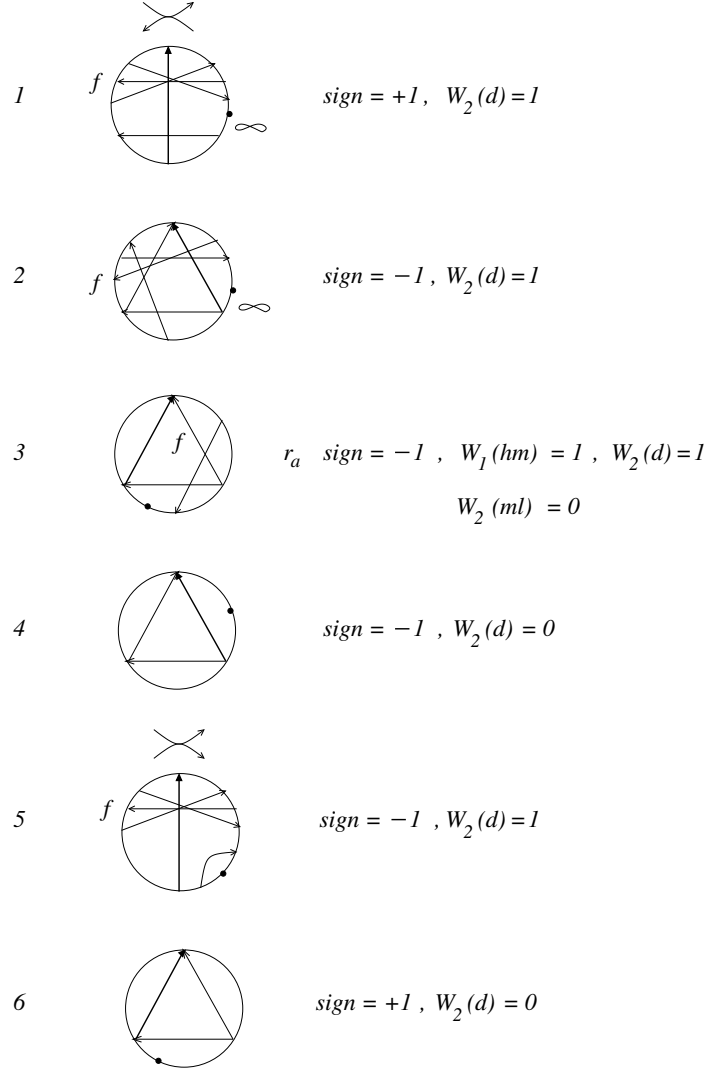


Figure 29: Gauss diagrams and weights of the moves which could a priori contribute to  $R_x(rot(3_1^+))$

$$\begin{aligned}
R_x(\text{rot}(3_1^+)) &= + x ( \text{diagram}_1 - \text{diagram}_2 ) \\
&- x ( \text{diagram}_3 - \text{diagram}_4 ) \\
&- x ( \text{diagram}_5 - \text{diagram}_6 ) \\
&-(x-1) \text{diagram}_7 \\
&- ( \text{diagram}_8 - \text{diagram}_9 ) \\
&- x ( \text{diagram}_{10} - \text{diagram}_{11} ) \\
&= -x \text{diagram}_{12} + \text{diagram}_{13} = 0
\end{aligned}$$

Figure 30: calculation of  $R_x(\text{rot}(3_1^+))$

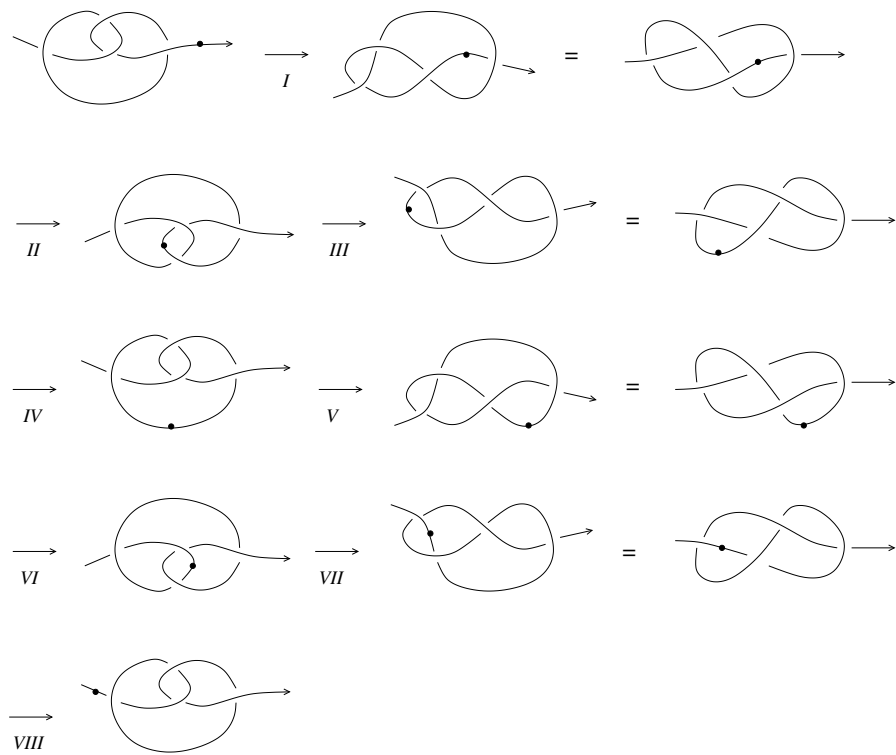


Figure 31: The loop  $\hat{4}_1 \# 4_1$



$4_1$ . Consequently, the place of the small summand  $4_1$  in the diagram of the big knot  $4_1$  is important. There were 18 Reidemeister moves (of type III and II) in  $\hat{hat}(4_1)$ , corresponding to the pieces of the loop I up to IV. There are 36 Reidemeister moves in  $\hat{hat}(4_1 \# 4_1)$ , corresponding to I up to VIII which have all a knot  $4_1$  as a summand. But pushing the strands over or under this summand leads to another 64 Reidemeister moves of type III and II. There are lots of cancellations (we use here often the obvious fact that the composition of a singular long knot with a non-singular long knot is commutative). The only two contributions which do not cancel out come from sliding branches under respectively over a small summand  $4_1$ . These contributions are not annihilated by the embedded 1T-relation because all knots in the smoothing links are the knot  $4_1$ . We indicate the place in the isotopy together with the relevant Reidemeister III move in Fig. 32. We left the verification of the details to the reader. Notice that the loop  $\hat{hat}(K_1 \# K_2)$  for  $K_1 = K_2$  is twice the loop which we have calculated.

We describe now in detail our main example, namely the calculation of  $R_x(\text{drag}(3_1^+, 3_1^+))$ . There are exactly 30 Reidemeister moves in  $\text{drag}(3_1^+, 3_1^+)$ . We number these moves in Fig. 33 - Fig. 38, where we give also the signs and the global types of the moves. Notice that all R III moves are of local type 1. In Fig. 39 and Fig. 40 we calculate the weights  $W_1$  and  $W_2$  for the 16 moves which have the right global type in order to contribute non trivially to  $R_x$  (where we write shortly  $W_2$  for  $W_2(d)$  and  $W_1$  for  $W_1(hm)$  and the f-crossings for  $d$  are drawn as dotted arrows). The calculation of  $R_x(\text{drag}(3_1^+, 3_1^+))$  is given in Fig. 41 and Fig. 42. For the convenience of the reader we indicate by numbers which contributions cancel out together (we haven't drawn the only two contributions with negative double point and which cancel out together). We see that here exactly the singular knots with coefficients in  $x$  of degree 0 remain (and hence  $dR_x/dx(1) = R_1(\text{drag}(3_1^+, 3_1^+)) = 0$ ). The canonical resolution gives the knots  $8_{21}^+$ , see Fig. 43, and  $3_1^+$ . (Thanks to Sebastian Baader for indicating the nice picture of  $8_{21}^+$ , where "+" stands for  $w(K) = 4$ .)

A computer program would be very helpful to calculate more examples. Notice that in the loop  $R_x(\text{drag}(K_1, K_2))$  we can represent  $K_1$  and  $K_2$  almost as closed braids (just one strand is opened). Hence triple crossings of the difficult local types 2 and 6 do not occur.

However, the easiest interesting non trivial example is  $R_x$  for scanning a 2-cable of a long knot. As already mentioned, we can assume that  $K$  is a closed braid with just one strand which is opened to go to infinity. Each

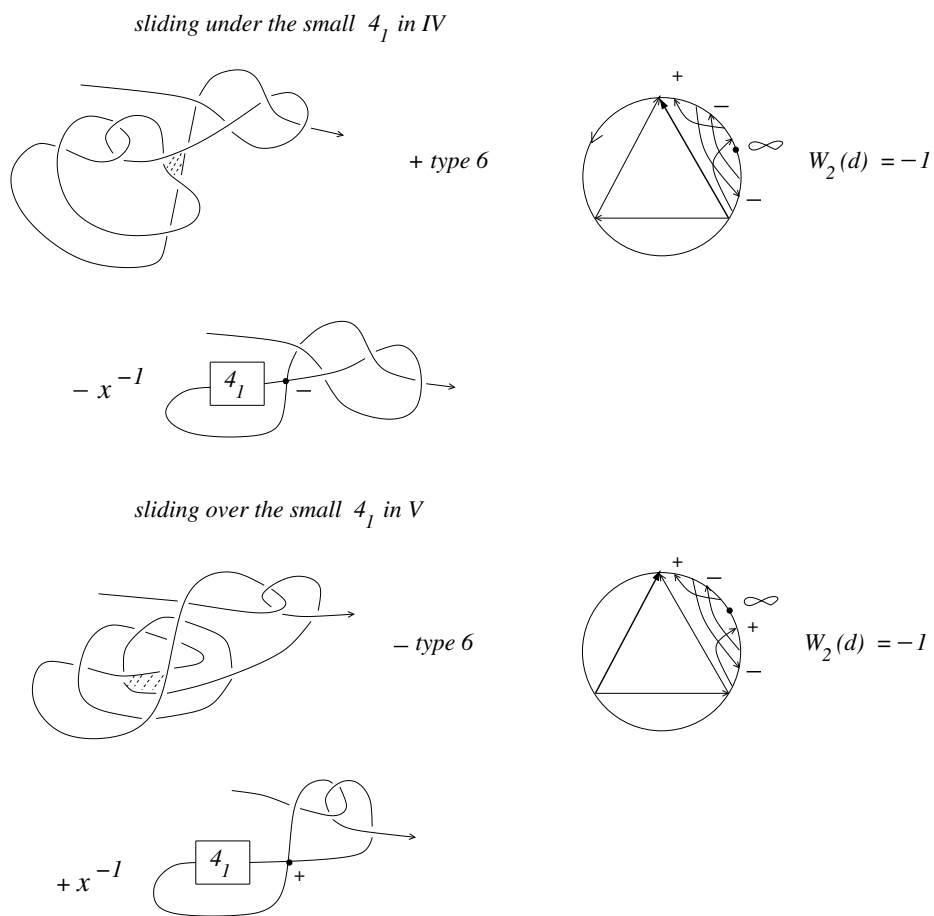


Figure 32: Calculation of  $R_x(\text{hat}(4_1 \sharp 4_1))$

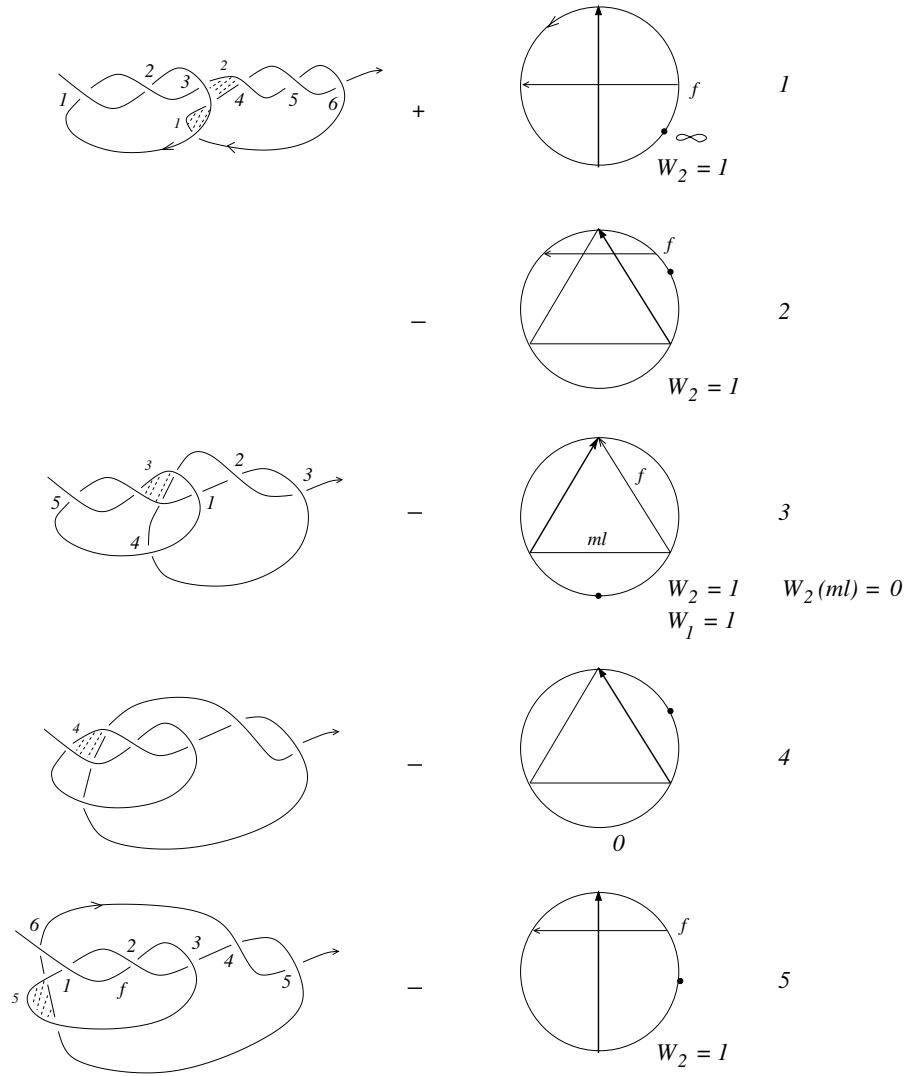
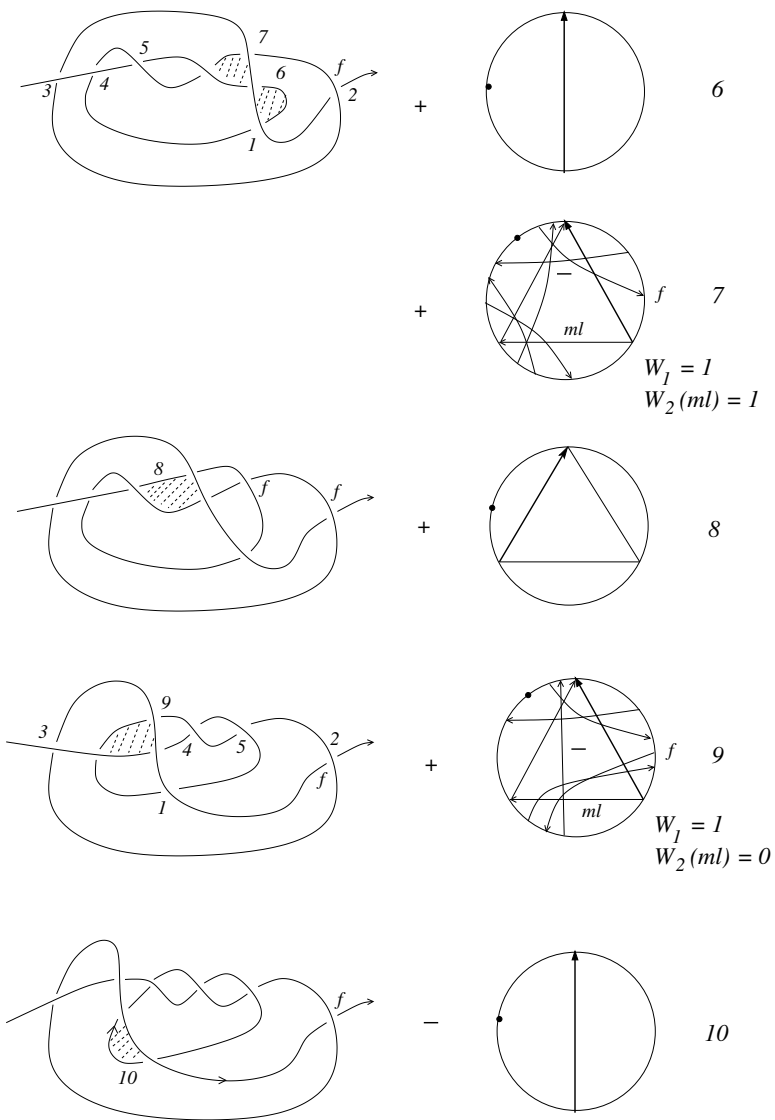


Figure 33: Dragging the trefoil through the trefoil I



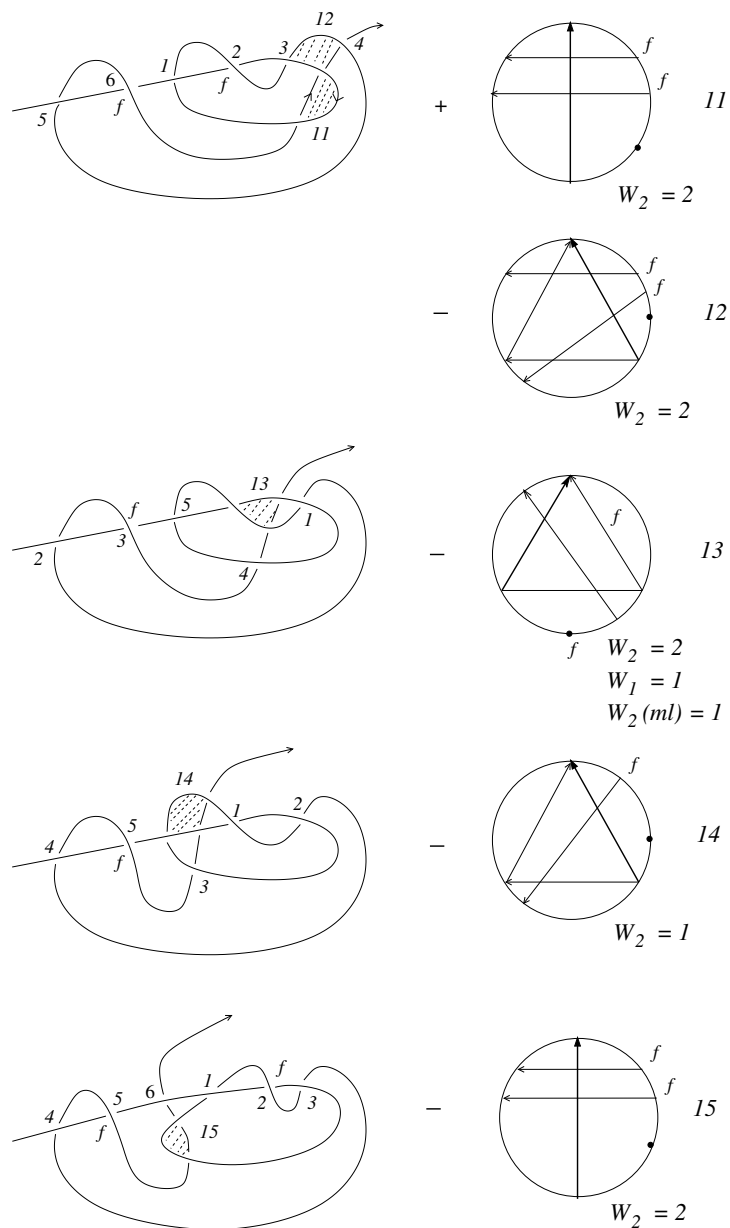


Figure 35: Dragging the trefoil through the trefoil III

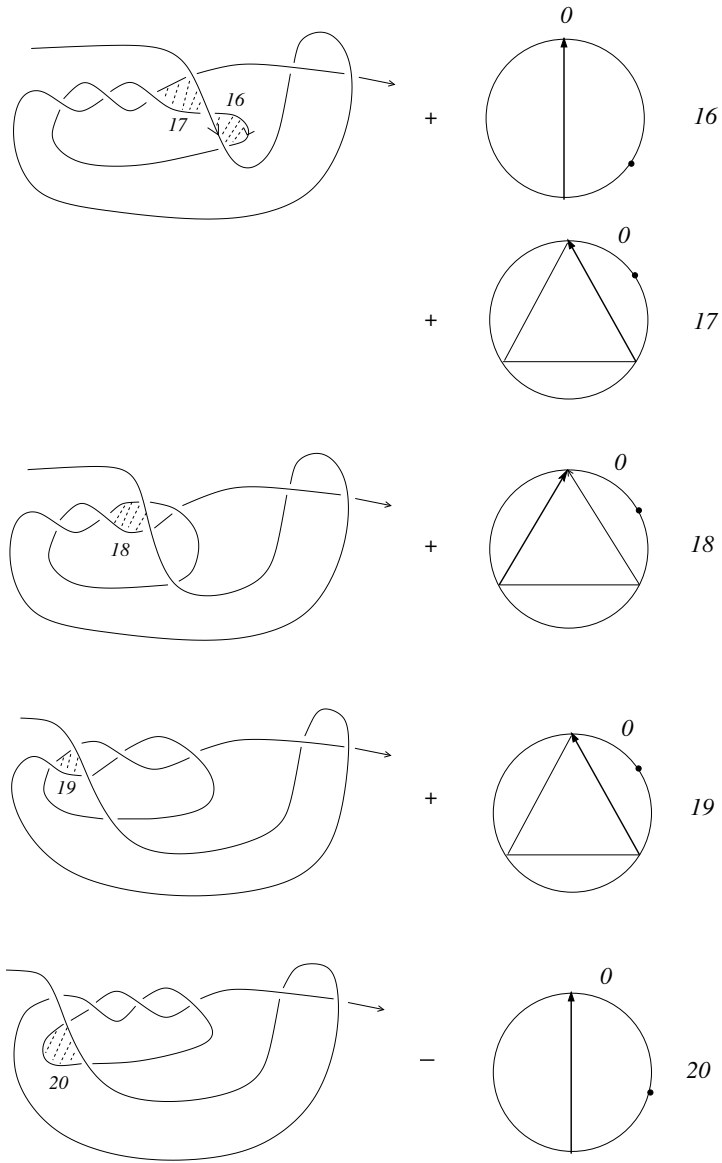


Figure 36: Dragging the trefoil through the trefoil IV

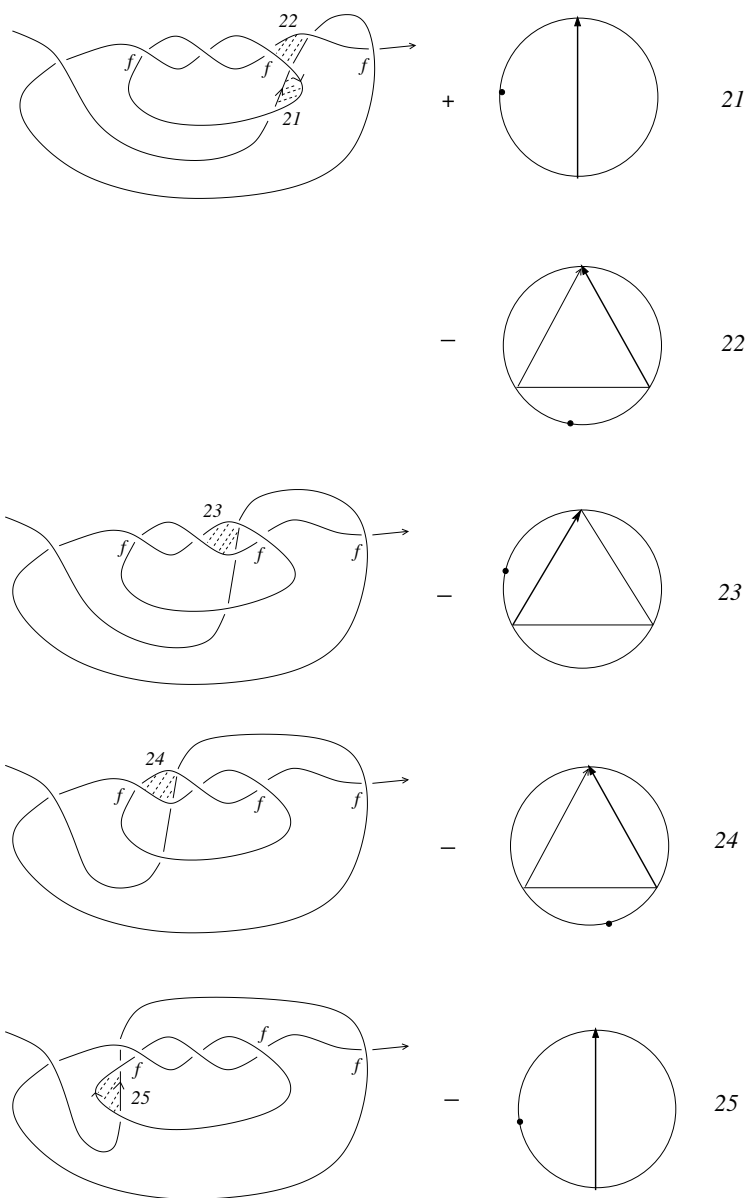


Figure 37: Dragging the trefoil through the trefoil V

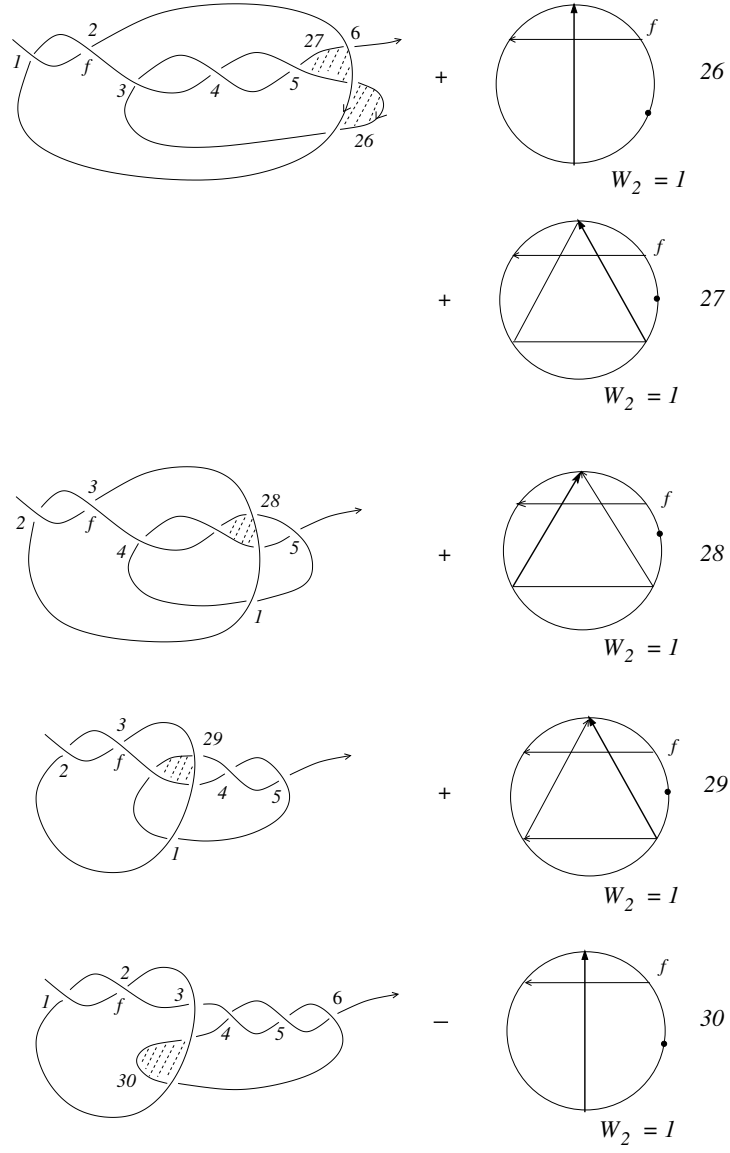


Figure 38: Dragging the trefoil through the trefoil VI



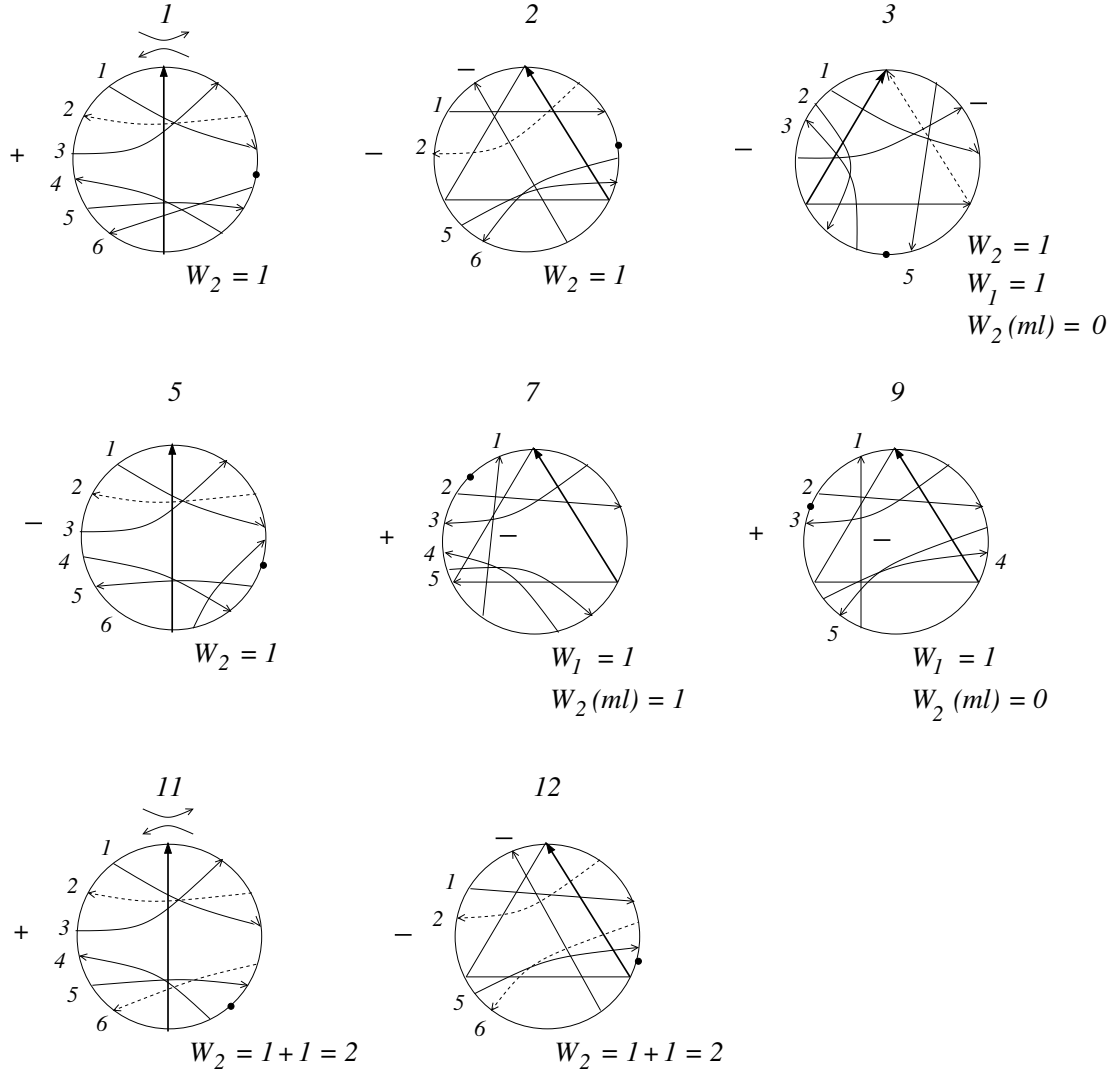


Figure 39: The weights for dragging the trefoil I

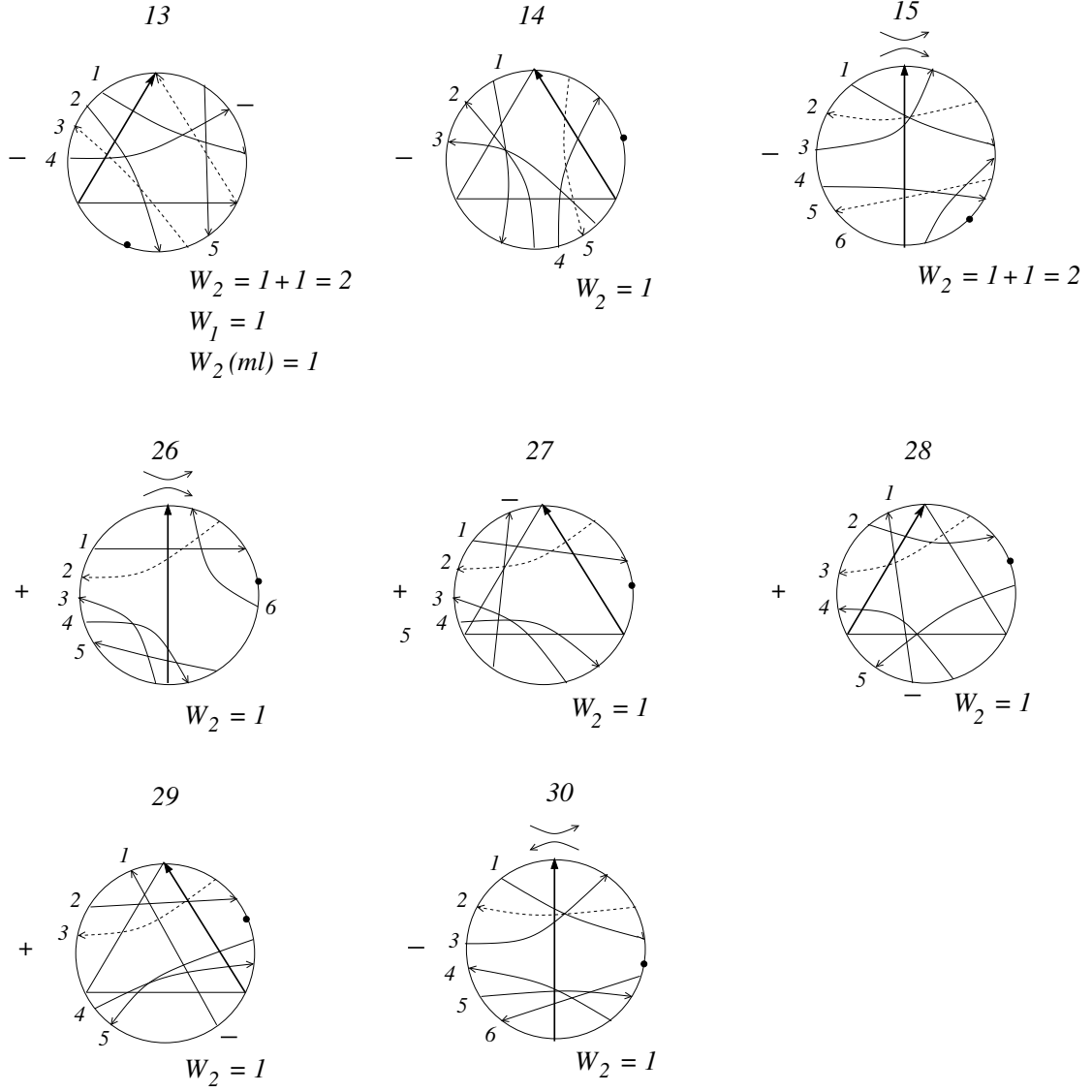


Figure 40: The weights for dragging the trefoil II

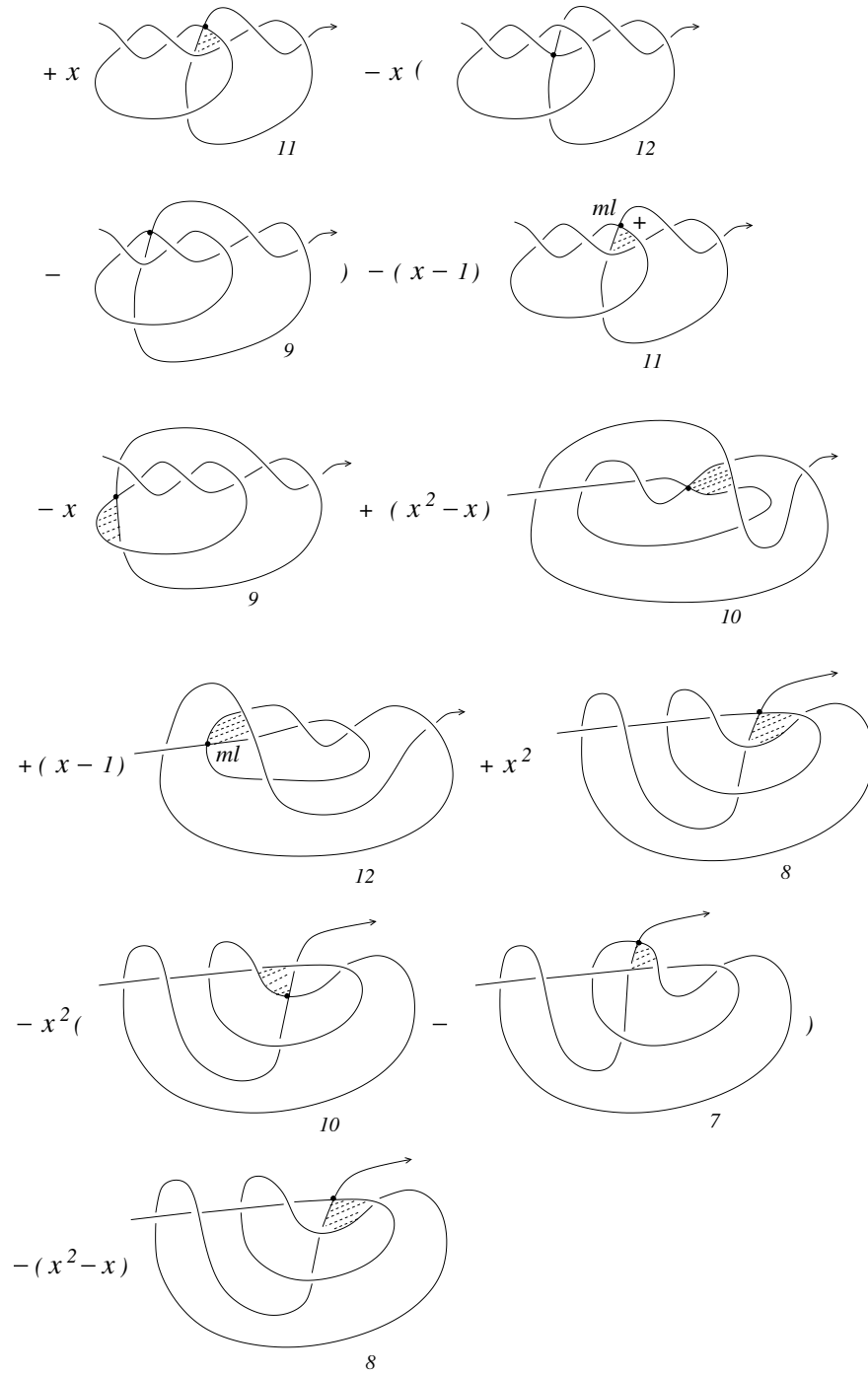


Figure 41: Calculation of  $R_x$  for dragging the trefoil I

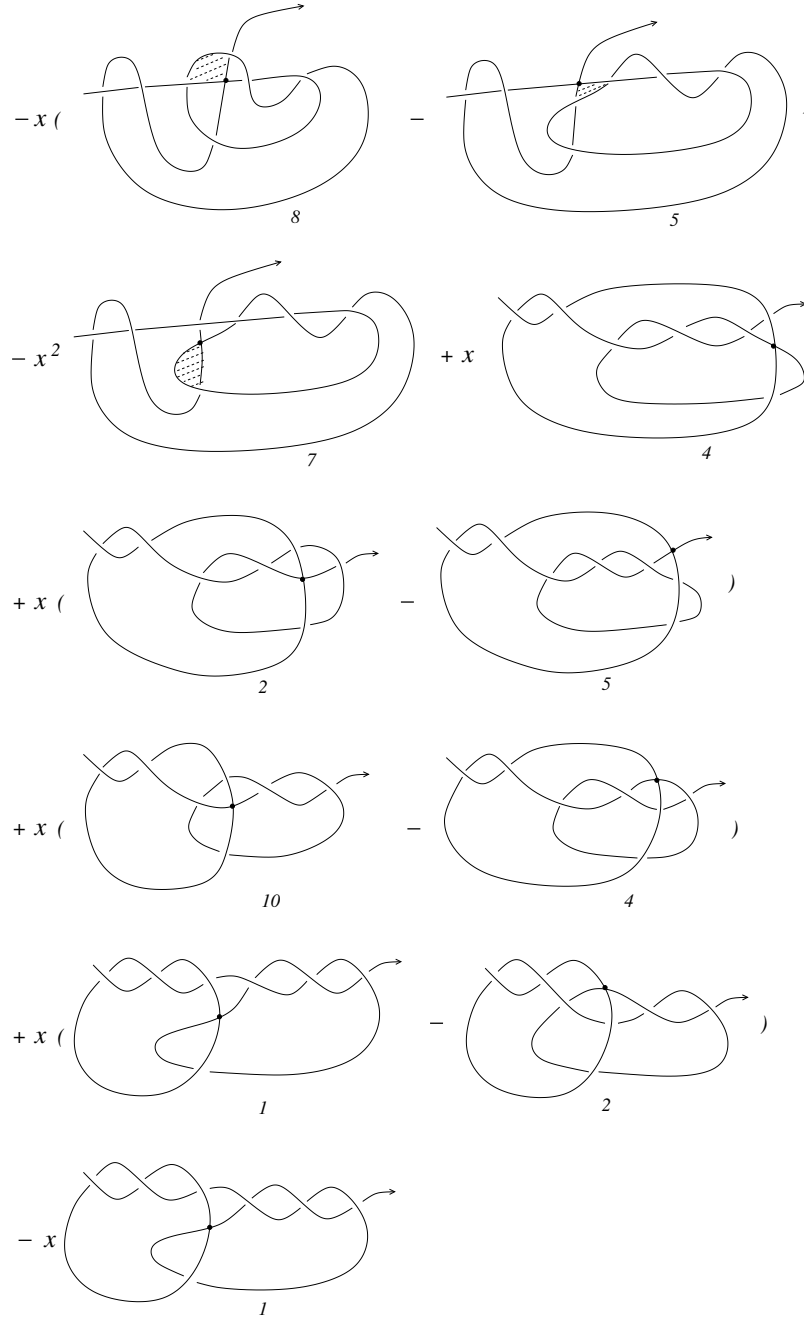


Figure 42: Calculation of  $R_x$  for dragging the trefoil II

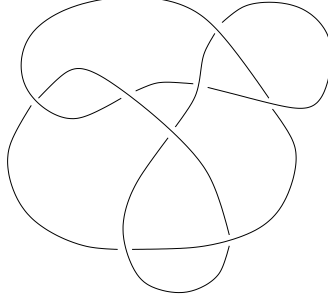


Figure 43: Nice picture of the knot  $8_{21}^+$

crossing of  $K$  gives rise to exactly four R III moves in  $scan(Cab_2(K))$ . One easily sees that such a move is of local type 1 if the crossing of  $K$  is positive and it is of local type 7 if the crossing is negative. The arc  $scan(Cab_2(3_1^+))$  contains exactly 16 Reidemeister moves. Because only the crossings  $d$  or  $ml$  can become singular (compare Theorem 1) and we are only interested in double points of the red component with itself, it turns out that only 11 moves could contribute non trivially to  $R_{x,red-red}(scan(Cab_2(3_1^+)))$ . We give these moves together with the signs and the global types in Fig. 44. It turns out that  $W_2(d) = 14$  in all cases but one (but we left the verification to the reader). Notice that the sum of the writhe of the crossings red-black is just 14. There is only exactly one R III move which could contribute with  $ml$  singular and which is of type red-red. We give its Gauss diagram in order to calculate  $W_2(ml)$  and  $W_1(hm)$  in Fig. 45. The calculation of  $R_{x,red-red}(scan(Cab_2(3_1^+)))$  is contained in Fig. 46 and Fig. 47 and leads to the result given in the Introduction. For the convenience of the reader we give numbers to the contributions which do not cancel out, compare Fig. 12. One easily sees that the string links in the canonical resolution  $\mathbb{D}R_{x,red-red}(scan(Cab_2(3_1^+)))$  are no longer satellites.

We have calculated that  $R_{x,red-red}(scan(Cab_2(3_1^+))) = 0$  for the other choice of the point at infinity, but we left the verification to the reader.

### 3.2 Positive closed 4-braids

We use the standard notations for braid groups, but for shorter writing we denote  $\sigma_i$  by  $i$ . We give names to the crossings of homological marking 1. A double point which comes from a crossing  $\sigma_i$  with name  $a$  is simply denoted by  $a_i$  in  $R_1^{split}$ .

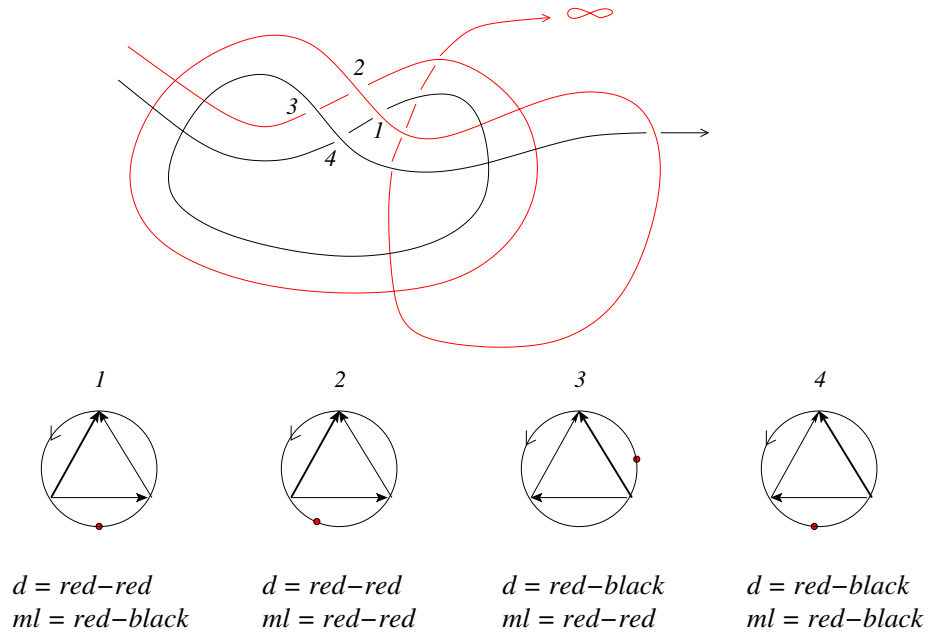
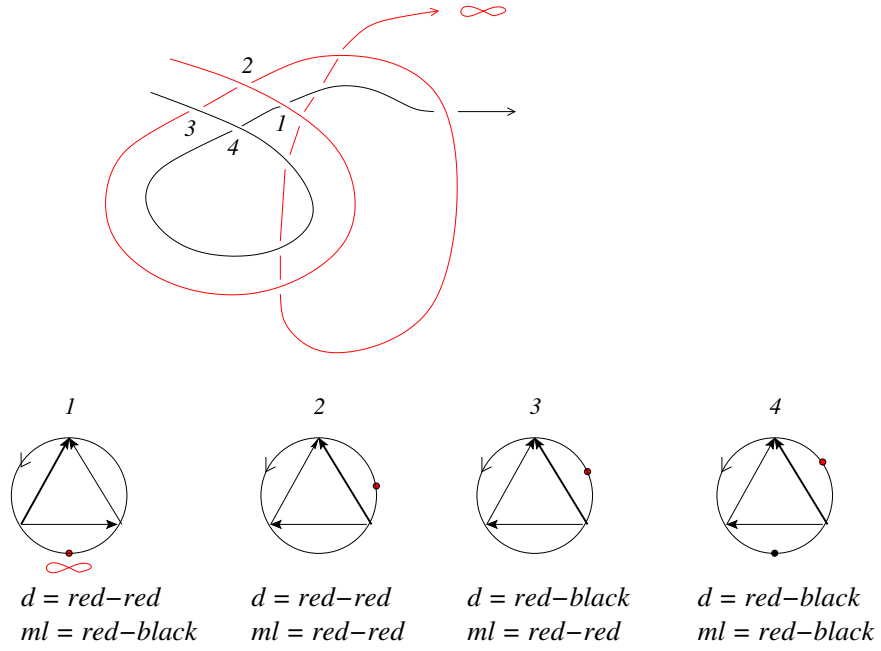


Figure 44: The global types of the moves in scanning the 2-cable of  $3_1^+$

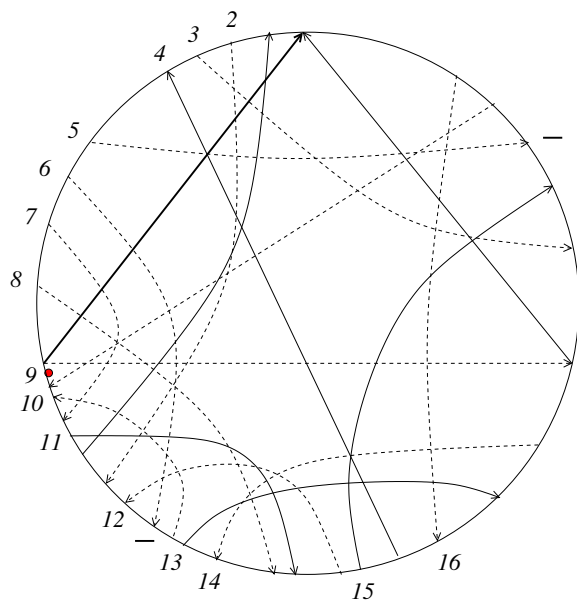


Figure 45: The only contribution with  $ml$  singular in  $R_{x,red-red}(scan(Cab_2(3_1^+)))$

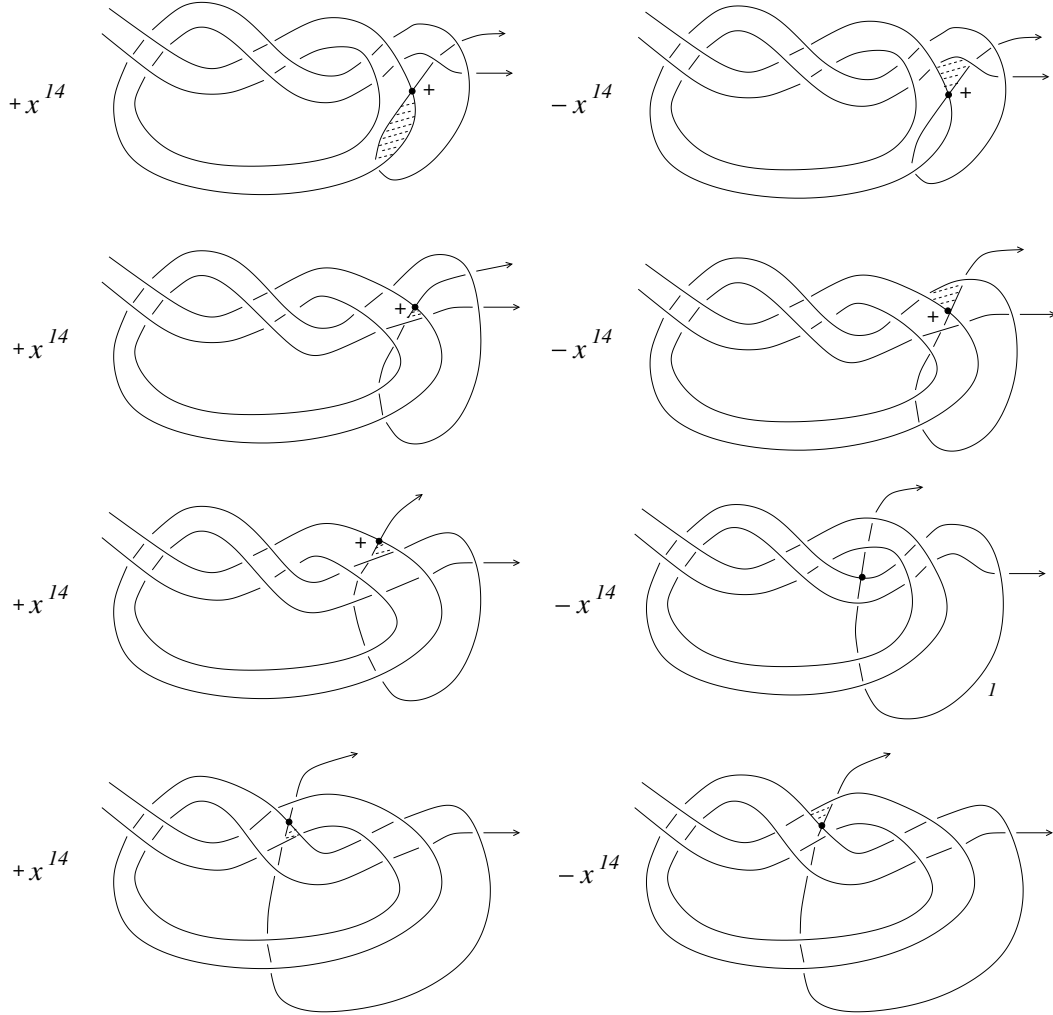


Figure 46: Calculation of  $R_{x,red-red}(scan(Cab_2(3_1^+)))$



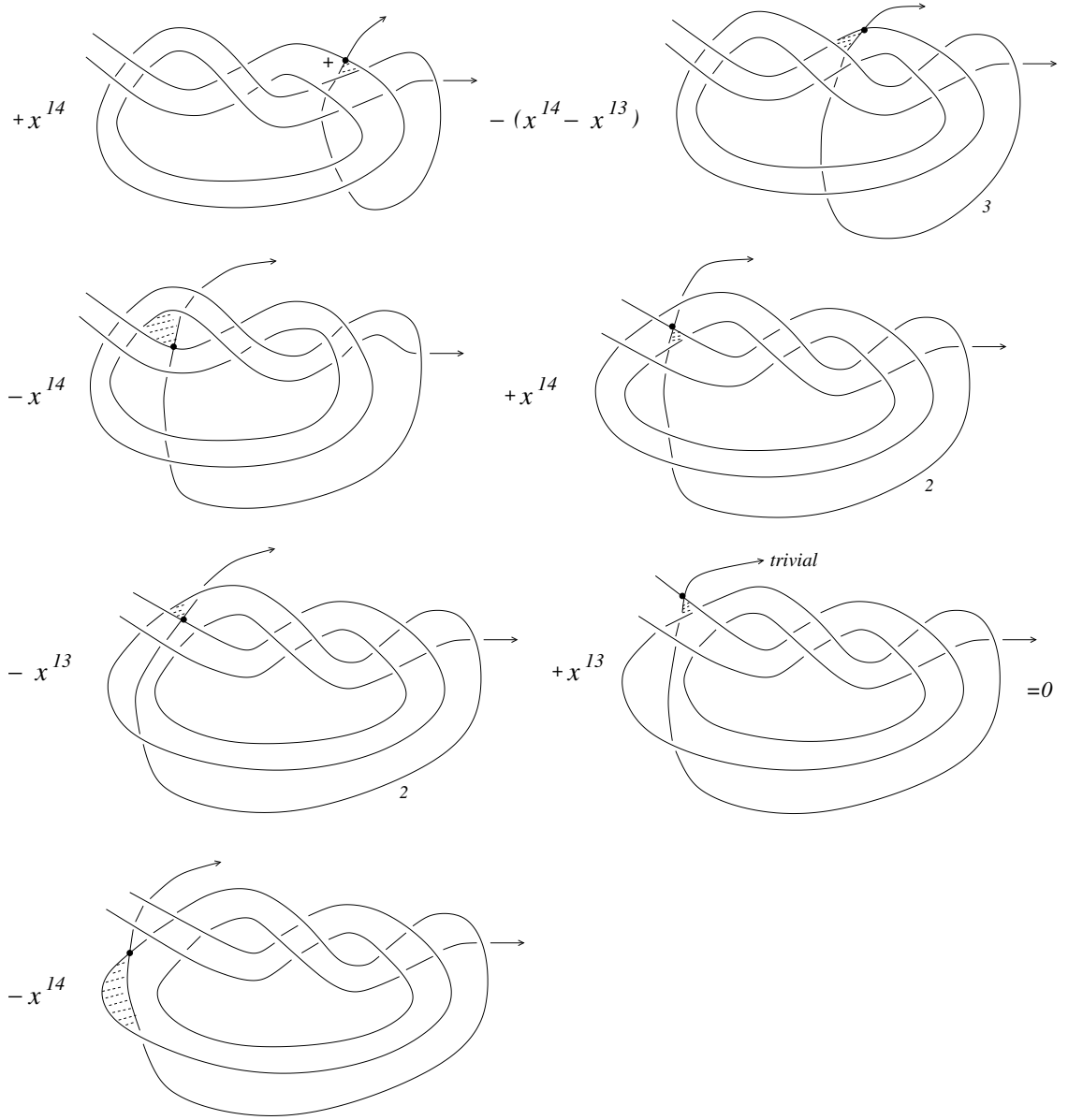


Figure 47: Continuation of the calculation of  $R_{x,red-red}(scan(Cab_2(3_1^+)))$

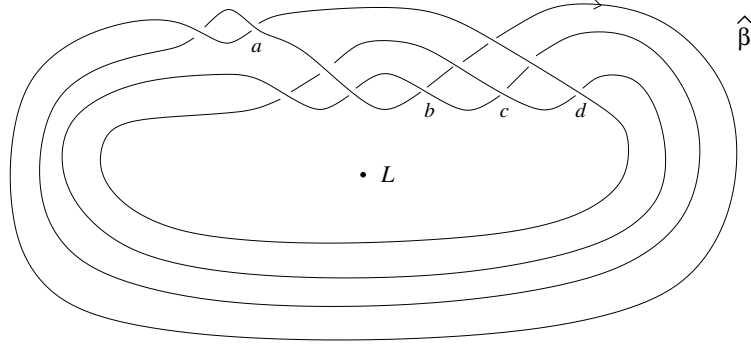


Figure 48: The closed pseudo-Anosov 4-braid  $\hat{\beta}$  with its named crossings of homological marking 1

We consider a loop representing  $rot(\hat{\beta})$  for  $\beta = \sigma_3^2 \sigma_1 \sigma_2 \sigma_1 \Delta \in B_4^+$ . Each of the 34 arrows which corresponds to a Reidemeister move or a commutation relation is numbered. There are two arrows which correspond to cyclic permutations. (Remember that the braid words correspond to closed braids and hence they are well defined up to cyclic permutations, which do not contribute to the cocycles.) For the convenience of the reader we indicate the place of the move by round brackets. There are exactly four crossings of homological marking 1 (to establish this, one has to draw  $\hat{\beta}$ , see Fig. 48) and we write their names  $a, b, c, d$  as an index.

$$\begin{aligned}
 rot(\hat{\beta}) = & \\
 & 33_a 1211_b 2(31_c) 21_d \rightarrow_{*1} \quad 33_a 121(1_b 21_c) 321_d \rightarrow_{*2} \quad 33_a 1212_c 1(2_b 32) 1_d \rightarrow_{*3} \\
 & 33_a 1212_c 132(3_b 1_d) \rightarrow_{*4} \quad 33_a 1(212_c) 1321_d 3_b \rightarrow_{*5} \quad 33_a 11_c 21(13) 21_d) 3_b \rightarrow_{*6} \\
 & 33_a 11_c 213(121_d) 3_b \rightarrow_{*7} \quad 33_a 1(1_c 21) 32_d 123_b \rightarrow_{*8} \quad 33_a 121(2_c 32_d) 123_b \rightarrow_{*9} \\
 & 33_a 12(13_d) 23_c 123_b \rightarrow_{*10} \quad 33_a 123_d 12(3_c 1) 23_b \rightarrow_{*11} \quad 3(3_a 1) 23_d 1213_c 23_b \rightarrow_{*12} \\
 & 31(3_a 23_d) 1213_c 23_b \rightarrow_{*13} \quad 312_d 3(2_a 12) 13_c 23_b \rightarrow_{*14} \quad (31) 2_d 3121_a 13_c 23_b \rightarrow_{*15} \\
 & 1(32_d 3) 121_a 13_c 23_b \rightarrow_{*16} \quad 123_d(212) 1_a 13_c 23_b \rightarrow_{*17} \quad (123_d 121) 1_a 13_c 23_b \rightarrow_{*18} \\
 & 1_a 13_c 2(3_b 1) 23_d 121 \rightarrow_{*18} \quad 1_a 13_c 21(3_b 23_d) 121 \rightarrow_{*19} \quad 1_a 13_c 212_d 3(2_b 12) 1 \rightarrow_{*20} \\
 & 1_a 13_c(212_d) 3121_b 1 \rightarrow_{*21} \quad 1_a 13_c 1_d 2(13) 121_b 1 \rightarrow_{*22} \quad 1_a 13_c 1_d 231(121_b) 1 \rightarrow_{*23} \\
 & 1_a 1(3_c 1_d) 2312_b 121 \rightarrow_{*24} \quad 1_a 11_d(3_c 23) 12_b 121 \rightarrow_{*25} \quad 1_a 11_d 23(2_c 12_b) 121 \rightarrow_{*26} \\
 & 1_a 11_d 2(31_b) 21_c 121 \rightarrow_{*27} \quad 1_a 1(1_d 21_b) 321_c 121 \rightarrow_{*28} \quad 1_a 12_b 1(2_d 32) 1_c 121 \rightarrow_{*29} \\
 & 1_a 12_b 132(3_d 1_c) 121 \rightarrow_{*30} \quad 1_a(12_b 1) 321_c 3_d 121 \rightarrow_{*31} \quad 1_a 21_b(232) 1_c 3_d 121 \rightarrow_{*32} \\
 & 1_a 2(1_b 3) 231_c 3_d 121 \rightarrow_{*33} \quad 1_a 231_b 2(31_c) 3_d 121 \rightarrow_{*34} \quad (1_a 231_b 21_c) 33_d 121 \rightarrow_{*34} \\
 & 33_d 1211_a 231_b 21_c
 \end{aligned}$$

We see that the monodromy  $m_{rot} : a \rightarrow d \rightarrow c \rightarrow b \rightarrow a$  is a 4-cycle.

One easily sees that the couple of homological markings in commutation relations for closed 4-braids which are knots is always of the form:  $\{1, 1\}$ ,  $\{1, 3\}$ ,  $\{3, 3\}$  or  $\{2, 2\}$ . Therefore, the signs and the global types of the fourteen commutation relations can be read off directly from the above sequence. All twenty R III moves are of local type 1. The global types of the moves are given below (to establish this, one has to draw the Gauss diagram in each case):

$$\begin{aligned}
&*2 : +l(2, 1, 1), *3 : +l(3, 2, 1), *5 : -l(3, 2, 1), *7 : +l(3, 1, 2), \\
&*8 : +l(3, 2, 1), *9 : +l(2, 1, 1), *13 : -l(2, 1, 1), *14 : -l(3, 1, 2), \\
&*16 : -r(1, 2, 3), *17 : -r(2, 3, 3), *19 : -l(2, 1, 1), *20 : -l(3, 1, 2) \\
&*21 : -l(3, 2, 1), *23 : +l(3, 1, 2), *25 : -r(1, 3, 2), *26 : -l(2, 1, 1) \\
&*28 : +l(2, 1, 1), *29 : +l(3, 2, 1), *31 : +r(1, 2, 3), *32 : +r(2, 3, 3)
\end{aligned}$$

One easily calculates now by using Definition 23:

R III moves which contribute:

$$\begin{aligned}
&*2 : +12c_1 32133121 - b_1 2132133121 \\
&*3 : +b_2 3213312121 \\
&*5 : -c_1 2113213331 \\
&*7 : -12d_1 33311231 \\
&*8 : +c_1 2132123331 \\
&*9 : +23d_2 12333121 - c_2 3212333121 \\
&*13 : -23a_2 12132331 + d_2 3212132331 \\
&*14 : +12a_1 13233123 \\
&*16 : -2d_3 212113231 \\
&*19 : -23b_2 12111321 + d_2 3212111321 \\
&*20 : +12b_1 11132123 \\
&*21 : -d_1 2131211113 \\
&*23 : -12b_1 11131231 \\
&*25 : +23c_2 12121111 \\
&*26 : -12c_1 12111123 + b_1 2112111123 \\
&*28 : +12b_1 32112111 - d_1 2132112111 \\
&*29 : +d_2 3211211121 \\
&*31 : -2b_1 232131211
\end{aligned}$$

Commutation relations which contribute:

$$\begin{aligned}
&*1 : -c_1 2133121123 \\
&*4 : -b_3 1331212132 + 3d_1 331212132 \\
&*10 : -d_3 2312333121
\end{aligned}$$

\*11 :  $+c_3 1233312132$   
 \*12 :  $+a_3 1231213233$   
 \*18 :  $+b_3 1231211132$   
 \*24 :  $-c_3 1231212111 + 3d_1 231212111$   
 \*27 :  $-b_1 2112111123$   
 \*30 :  $-d_3 1121112132 + 3c_1 121112132$   
 \*33 :  $+b_1 3231312112$   
 \*34 :  $-c_1 3121121323$

It turns out that the above singular closed braids belong only to two different isotopy classes in the solid torus, namely  $t_1 3213312112$  and  $t_1 2132133121$  (thanks to Stepan Orevkov for verifying this). They are distinguished by the linking number in  $S^3$  of the two knots which are obtained by smoothing the double point  $t_1$  with respect to the orientation. (It is  $+2$  for the first one and  $+3$  for the second one.)

One easily calculates now  $R_1^{split}(rot(\hat{\beta}))$ :

$$\begin{aligned}
 R_a(rot(\hat{\beta})) &= +t_1 2132133121 \\
 R_b(rot(\hat{\beta})) &= 0 \\
 R_c(rot(\hat{\beta})) &= -t_1 3213312112 \\
 R_d(rot(\hat{\beta})) &= -t_1 2132133121 + t_1 3213312112
 \end{aligned}$$

Consequently,  $R_1^{split}(rot(\hat{\beta}))$  is non trivial. This is the simplest possible example, because this is the shortest positive pseudo-Anosov 4-braid which closes to a knot and which contains a half-twist. (Notice that 3-braids are not interesting for us because the tetrahedron equation appears only starting from four strings and there are no commutation relations at all for 3-braids.)

One calculates now (thanks to Stepan Orevkov)

$$\begin{aligned}
 |\lambda_a| &= 1.8105... \\
 \lambda_b &= 1 \text{ (by definition)} \\
 |\lambda_c| &= 2.7551... \\
 |\lambda_d| &= 1 \text{ (here } \Delta R_d(u, t) = (t^5 - t^3)u(t^2 + u)(u - 1))
 \end{aligned}$$

Consequently,  $a$  and  $c$  are the hyperbolic crossings,  $k_{hyp} = 2$  and  $\lambda_{R(\beta)} = 2.2829...$

Notice, that the monodromy  $m_{rot}$  mixes the hyperbolic crossings with the periodic crossings, as it should because  $m_{rot}$  is a cycle. It is amazing that the crossings (with the same homological marking) of a closed braid can not be distinguished by considering only  $H_0(M_{\hat{\beta}+\Delta}; \mathbb{Z})$  but they *can be distinguished* by using homology classes in  $H_1(M_{\hat{\beta}+\Delta}; \mathbb{Z})$ .

It turns out that for the above braid  $R_{xy}(rot(\hat{\beta})) = 0$  without the refinement by names of the crossings. (In order to calculate the weights  $W_1$  and  $W_{n-2=2}$  one has to draw the Gauss diagrams with all homological markings for the eighteen closed braids above.) But we have calculated that  $R_{xy}^{split}(rot(\hat{\beta}))$  is already non trivial for  $x(i) = a$ . Indeed,  $x(i) = a$  appears only in \*13 and \*14. The triple crossing \*13 is of type  $l(2, 1, 1)$  but  $a = hm$  does not become singular for this global type. The triple crossing \*14 is of type  $-l(3, 1, 2)$  and  $a = hm$ . One easily calculates that  $W_1(hm) = 1$  and  $W_2(hm) = 0$ . It follows from Definition 20 that

$$R_{xy,a}^{split}(rot(\hat{\beta})) = x(1 - y)t_21213233123.$$

It is amazing that this is the same singular closed braid up to isotopy as for  $R_a(rot(\hat{\beta}))$ , but the coefficient  $+1$  has changed to  $x(1 - y)$ . The relations between the invariants  $R_1^{split}(rot(\hat{\beta}))$  and  $R_{xy,a}^{split}(rot(\hat{\beta}))$  are an interesting subject for further investigations.

Finally, let us mention that the 1-cocycle  $R_{xy}(rot(\hat{\beta}))$  is still well defined for the closure of positive 3-braids which contain a half-twist if one specializes by  $x+y = 2$ . The value of  $R_{x(2-x)}(rot(\hat{\beta}))$  is non trivial for the pseudo-Anosov 3-braid  $\sigma_2\sigma_1^{-1}\Delta^2 = \sigma_2^2\sigma_1\Delta$ , but we left the verifications to the reader.

## 4 Proofs

Our main results are based on very complicated combinatorics and the interested reader has certainly a hard time to check all the details. We apologize for this. But let us give an unusual advice: don't try to find a better proof by your own, just let us guide patiently through our proof! We believe that there will be conceptually better proofs in the future (compare Question 1). But it has taken nearly 10 years to build the present proof and it is unlikely to find a better one immediately.

On the other side, we can consider the combinatorics in this paper as some discrete analysis: integrating a discrete differential 1-form over a discrete loop in the topological moduli space of a long knot. As already mentioned in the Introduction (Question 1), it would be very important to transform this discrete analysis into real analysis. Nowadays, new invariants in knot theory come usually from some mathematical physics which is transformed into differential geometry (the perturbative approach) and representation theory (the non perturbative approach) and only at the very end into something

which can be calculated in a combinatorial way from a knot diagram. Unfortunately, we have to start with this very end because it seems that in our case all the previous steps are missing for the moment, including the mathematical physics. However, this lack of understanding is partially compensated by the possibility to calculate the invariants in a combinatorial way.

The classical tetrahedron equation is a 3-dimensional generalization of the Yang-Baxter equation. It is a local equation which is fundamental for studying integrable models in  $2 + 1$ -dimensional mathematical physics. This equation has many solutions and the first one was found by Zamolodchikov (see e.g. [43]). But it seems that the present paper is the very first one which considers the tetrahedron equation from a global point of view. The game is to find solutions of this equation which have enough symmetries in order to lead to a 1-cocycle in the knot space but which have still a lack of symmetry so that the 1-cocycle does not become exact. (In anterior work we had constructed lots of exact 1-cocycles, see e.g. [5], [21].)

#### 4.1 Generalities and reductions by using singularity theory

We look at the local tetrahedron equation from the point of view of singularities of the projection of lines. We fix an orthogonal projection  $pr : \mathbb{C} \times \mathbb{R} \rightarrow \mathbb{C}$ . Consider four oriented straight lines which form a braid and such that the intersection of their projection into  $\mathbb{C}$  consists of a single point. We call this an *ordinary quadruple crossing*. After a generic perturbation of the four lines we will see now exactly six ordinary crossings. We assume that all six crossings are positive and we call the corresponding quadruple crossing a *positive quadruple crossing*. Quadruple crossings form smooth strata of codimension 2 in the topological moduli space of lines in 3-space which is equipped with a fixed projection  $pr$ . Each generic point in such a stratum is adjacent to exactly eight smooth strata of codimension 1. Each of them corresponds to configurations of lines which have exactly one ordinary triple crossing besides the remaining ordinary crossings. We number the lines from 1 to 4 from the lowest to the highest (with respect to the projection  $pr$ ). The eight strata of triple crossings glue pairwise together to form four smooth strata which intersect pairwise transversally in the stratum of the quadruple crossing (see e.g. [25]). The strata of triple crossings are determined by the names of the three lines which give the triple crossing. For shorter writing we give them

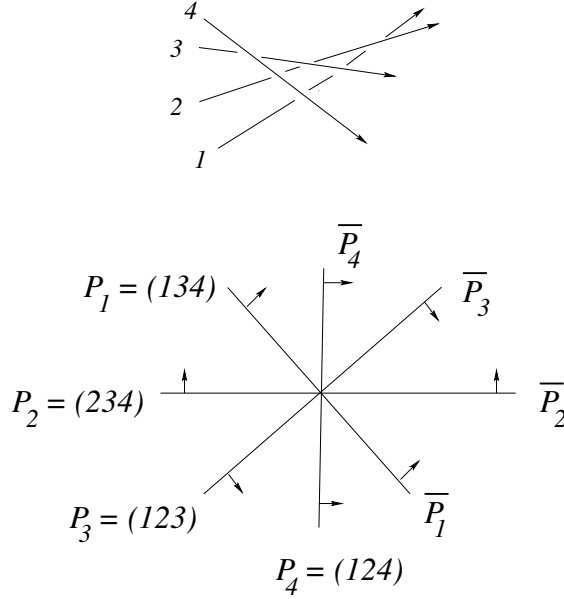


Figure 49: intersection of a normal 2-disc of a positive quadruple crossing with the strata of triple crossings

names from  $P_1$  to  $P_4$  and  $\bar{P}_1$  to  $\bar{P}_4$  for the corresponding stratum on the other side of the quadruple crossing. We show the intersection of a normal 2-disc of the stratum of codimension 2 of a positive quadruple crossing with the strata of codimension 1 in Fig. 49. We give in the figure also the coorientation of the strata of codimension 1, compare Fig. 16. (We could interpret the six ordinary crossings as the edges of a tetrahedron and the four triple crossings likewise as the vertices's or the 2-faces of the tetrahedron.)

Let us consider a small circle in the normal 2-disc and which goes once around the stratum of the quadruple crossing. We call it a *meridian*  $m$  of the quadruple crossing. Going along the meridian  $m$  we see ordinary diagrams of 4-braids and exactly eight diagrams with an ordinary triple crossing. We show this in Fig. 50. (For simplicity we have drawn the triple crossings as triple points, but the branches do never intersect.)

For the classical tetrahedron equation one associates to each stratum  $P_i$  some operator (or some R-matrix) which depends only on the names of the three lines and to each stratum  $\bar{P}_i$  the inverse operator. The tetrahedron equation says now that if we go along the meridian  $m$  then the product of these operators is equal to the identity. Notice, that in the literature (see

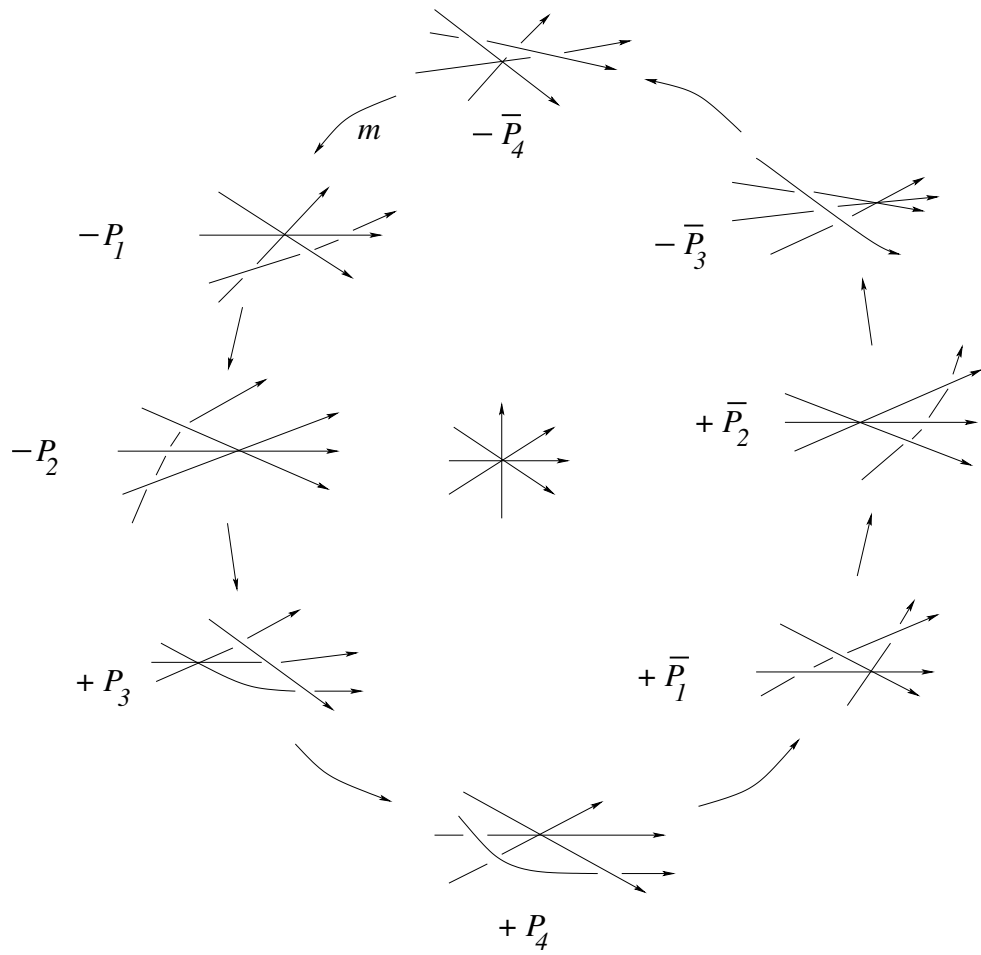


Figure 50: Unfolding of a positive quadruple crossing



e.g. [43]) one considers planar configurations of lines. But this is of course equivalent to our situation because all crossings are positive and hence the lift of the lines into 3-space is determined by the planar picture. Moreover, each move of the lines in the plane which preserves the transversality lifts to an isotopy of the lines in 3-space.

However, the solutions of the classical tetrahedron equation are not well adapted in order to construct 1-cocycles for moduli spaces of knots. There is no natural way to give names to the three branches of a triple crossing in an arbitrary knot isotopy besides in the case of braids. But it is not hard to see that in the case of braids Markov moves would make big trouble (see e.g. [7] for the definition of Markov moves). As well known, a Markov move leads only to a normalization factor in the construction of 0-cocycles (see e.g. [63]). However, the place in the diagram and the moment in the isotopy of a Markov move become important in the construction of 1-cocycles (as already indicated by the lack of control over the Markov moves in Markov's theorem). To overcome this difficulty we search for a solution of the tetrahedron equation which does not use names of the branches.

*The idea is to associate to a triple crossing  $p$  of a diagram of a string link  $K$ , a global element in  $\mathbb{D}_K^1$  instead of a local operator.*

Let us consider a diagram of a string link with a positive quadruple crossing *quad* and let  $p$  be e.g. the positive triple crossing associated to the adjacent stratum  $P_1$ . We consider three cubes:  $I_p^2 \times \mathbb{R} \subset I_{quad}^2 \times \mathbb{R} \subset \mathbb{C} \times \mathbb{R}$ . Here  $I_p^2$  is a small square which contains the triple point  $pr(p)$  and  $I_{quad}^2$  is a slightly bigger square which contains the quadruple point  $pr(quad)$ . We illustrate this in Fig. 51. Let us replace the triple crossing  $p$  in  $I_p^2 \times I$  by some standard linear combination of embedded chord diagrams, say  $L(p)$ . Gluing to  $L(p)$  the rest of the string link  $K$  outside of  $I_p^2 \times I$  gives an element, say  $K(p) \in \mathbb{D}_K^1$ . A triple crossing in an oriented isotopy corresponds to a Reidemeister move of type III.

Let  $m$  be the oriented meridian of the positive quadruple crossing. Our tetrahedron equation in  $\mathbb{D}_K^1$  is now

$$(1) \sum_{p \in m} \text{sign}(p) K(p) = 0$$

where the sum is over all eight triple crossings in  $m$ .

One sees immediately that this is still a local equation because it is sufficient to consider only the part of the embedded chord diagrams which is in  $I_{quad}^2 \times \mathbb{R}$ . This equation has an unique solution, which we call the *standard solution*, compare Section 4.4.

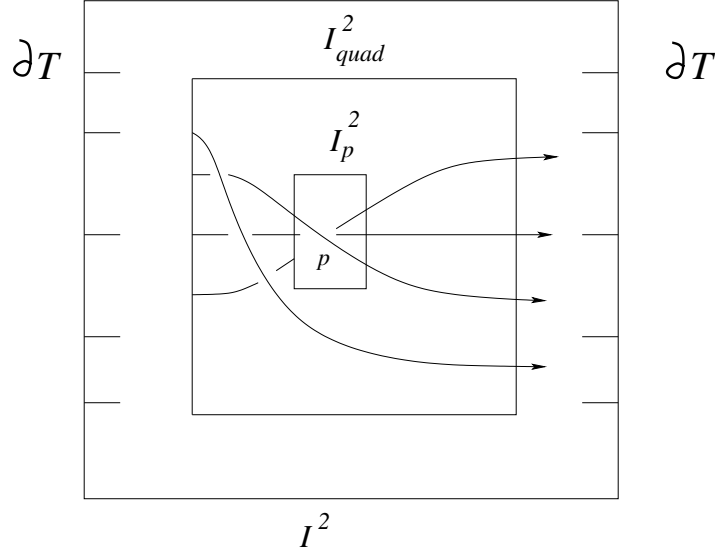


Figure 51: Increasing cubes

We consider then integer valued *weights*  $W(p)$  of the triple crossings which depend on the whole long knot (or string link)  $K$  and not only on the part of it in  $I_{quad}^2 \times \mathbb{R}$ . Moreover, they depend crucially on the point at infinity and they can not be defined for compact knots in  $S^3$ . Therefore we have to consider *twenty four* different positive tetrahedron equations, corresponding to the six different abstract closures of the four lines in  $I_{quad}^2 \times \mathbb{R}$  to a circle and to the four different choices of the point at infinity in each of the six cases. One easily sees that there are exactly *forty eight* local types of quadruple crossings (analog to the eight local types of triple crossings). A major problem is that in all our loops *rot*, *hat*, *drag* we have to deal with each crossing of  $K$  *twice* and the corresponding contributions have tendency to cancel out. Hence we are looking for non symmetric solutions (i.e. the contributions  $sign(p)R_x(p)$  should be in general not invariant under change of orientation, mirror image, rotation by  $\pi$  around the imaginary axes  $i\mathbb{R} \times 0 \subset \mathbb{C} \times \mathbb{R}$  or a composition of these involutions) and which depend non trivially on the point at infinity. This leads to a system of  $24 \times 48 = 1152$  equations in  $\mathbb{D}_K^1$ ! It turns out that such solutions do exist and we call them *solutions of a global tetrahedron equation*. Their existence seems to be a miracle from the combinatorial point of view!

In order to reduce the complexity of the problem we use now singularity

theory for projections  $pr$  of knots into the plan. The infinite dimensional spaces  $M_K$  has a natural *stratification with respect to  $pr$* :

$$M_K = \Sigma^{(0)} \cup \Sigma^{(1)} \cup \Sigma^{(2)} \cup \Sigma^{(3)} \cup \Sigma^{(4)} \dots$$

Here,  $\Sigma^{(i)}$  denotes the union of all strata of codimension  $i$ .

The strata of codimension 0 correspond to the usual generic *diagrams of knots*, i.e. all singularities in the projection are ordinary double points. So, our *discriminant* is the complement of  $\Sigma^{(0)}$  in  $M_K$ . Notice that this discriminant of non-generic diagrams is very different from Vassiliev's discriminant of singular knots [65].

The three types of strata of codimension 1 correspond to the *Reidemeister moves*, i.e. non generic diagrams which have exactly one ordinary triple point, denoted by  $\Sigma_{tri}^{(1)}$ , or one ordinary self-tangency, denoted by  $\Sigma_{tan}^{(1)}$ , or one ordinary cusp, denoted by  $\Sigma_{cusp}^{(1)}$ , in the projection  $pr$ . As already mentioned we call the triple point together with the under-over information (i.e. its embedded resolution) a *triple crossing*.

**Proposition 6** *There are exactly six types of strata of codimension 2. They correspond to non generic diagrams which have exactly either*

- (1) one ordinary quadruple point, denoted by  $\Sigma_{quad}^{(2)}$
  - (2) one ordinary self-tangency with a transverse branch passing through the tangent point, denoted by  $\Sigma_{trans-self}^{(2)}$
  - (3) one ordinary self-tangency in an ordinary flex ( $x = y^3$ ), denoted by  $\Sigma_{self-flex}^{(2)}$
  - (4) two singularities of codimension 1 in disjoint small discs (this corresponds to the transverse intersection of two strata from  $\Sigma^{(1)}$ , i.e. two simultaneous Reidemeister moves at different places of the diagram)
  - (5) one ordinary cusp ( $x^2 = y^3$ ) with a transverse branch passing through the cusp, denoted by  $\Sigma_{trans-cusp}^{(2)}$
  - (6) one degenerate cusp, locally given by  $x^2 = y^5$ , denoted by  $\Sigma_{cusp-deg}^{(2)}$
- We show these strata in Fig. 52.

For a proof as well as for all other necessary preparations from singularity theory see [25] (and also [13]) and references therein (in particular the singularity theory of Thom and Mather).

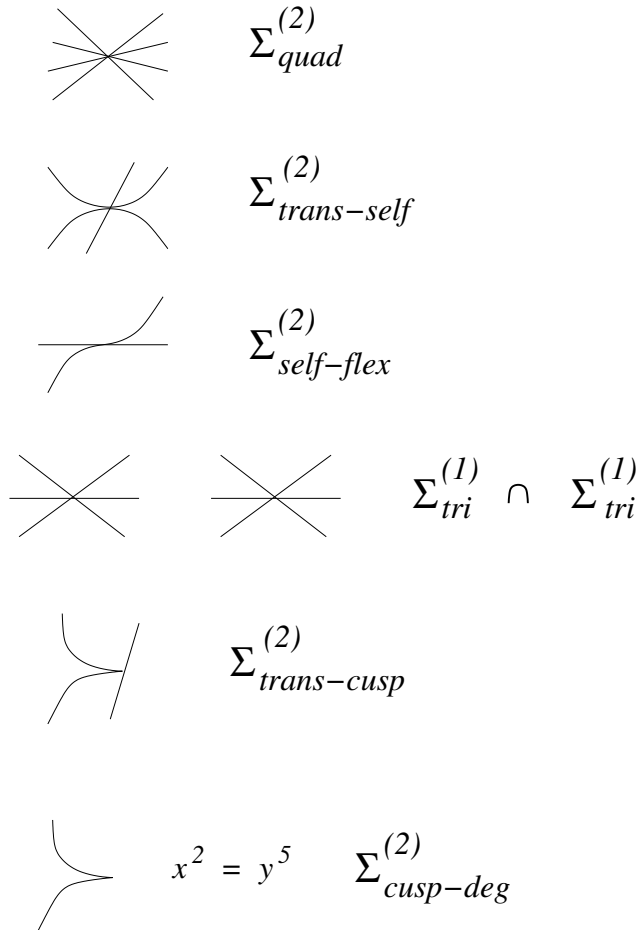


Figure 52: The strata of codimension 2 of the discriminant of non generic projections

The list above of singularities of codimension two can be seen as an analogue for one parameter families of diagrams of the Reidemeister theorem (which gives the list of singularities of codimension one).

A generic arc  $s$  in  $M_K$  intersects  $\Sigma_{tri}^{(1)}$ ,  $\Sigma_{tan}^{(1)}$  and  $\Sigma_{cusp}^{(1)}$  transversally in a finite number of points and it does not intersect at all strata of higher codimension. To each intersection point with  $\Sigma_{tri}^{(1)}$  and  $\Sigma_{tan}^{(1)}$  we associate an element in  $\mathbb{D}_K^1$ . We sum up with signs the contributions over all intersection points in  $s$  and obtain an element  $R_x(s) \in \mathbb{D}_K^1$ .

We use now the strata from  $\Sigma^{(2)}$  to show the invariance of  $R_x(s)$  under all generic homotopies of  $s$  in  $M_K$  which fix the endpoints of  $s$ . A homotopy is *generic* if it intersects  $\Sigma^{(1)}$  transversally besides for a finite number of points in  $s$  where  $s$  has an ordinary tangency with  $\Sigma^{(1)}$ , it intersects  $\Sigma^{(2)}$  transversally in a finite number of points and it doesn't intersect at all  $\Sigma^{(i)}$  for  $i > 2$ . The contributions to  $R_x(s)$  come from discrete points in  $s$  and hence they survive under generic Morse modifications of  $s$ . It follows that if  $R_x(s)$  is invariant under all generic homotopies of  $s$  then it is a 1-cocycle for  $M_K$ .

We see immediately that  $R_x(s)$  is invariant by passing through a tangency of  $s$  with  $\Sigma^{(1)}$ . Indeed, the two intersection points have identical contributions but they enter with different signs and cancel out. In order to show the invariance under generic homotopies we have to study now normal 2-discs for the strata in  $\Sigma^{(2)} \subset M_K$ . For each type of stratum in  $\Sigma^{(2)}$  we have to show that  $R_x(m) = 0$  for the boundary  $m$  of the corresponding normal 2-disc. We call  $m$  a *meridian*.  $\Sigma_{quad}^{(2)}$  is by far the hardest case which leads to the tetrahedron equation (see Section 4.4).

In the case of positive closed braids which contain a half-twist we have to prove the invariance of  $R_{xy}$  and  $R_{x(i)}$  for generic homotopies of loops through the strata  $\Sigma_{quad}^{(2)}$ , corresponding to positive quadruple crossings, and  $\Sigma_{tri}^{(1)} \cap \Sigma_{tri}^{(1)}$ , corresponding to two simultaneous R III moves of local type 1.

**Remark 9** In the case of  $R_{x(i)}$  for 4-braids there are two new strata of codimension 2: a R III move of local type 1 and simultaneously at another place of the diagram a commutation relation, as well as simultaneously two commutation relations. But the definition of  $R_{x(i)}$  doesn't use any weights and consequently  $R_{x(i)}$  is evidently invariant under a homotopy through the strata of the last two types. This implies already that  $R_{xy}$  is a 1-cocycle and that the unordered set of the  $R_{x(i)}$ ,  $i = 1, \dots, k$ , is a 1-cocycle if they are invariant

under generic homotopies of loops through  $\Sigma_{quad}^{(2)}$  and  $\Sigma_{tri}^{(1)} \cap \Sigma_{tri}^{(1)}$ .

Different local types of triple crossings come together in points of  $\Sigma_{trans-self}^{(2)}$ , but one easily sees that the global type of the triple crossings is always preserved. We make now a graph  $\Gamma$  for each global type of a triple crossing in the following way: the vertices's correspond to the different local types of triple crossings. We connect two vertices's by an edge if and only if the corresponding strata of triple crossings are adjacent to a stratum of  $\Sigma_{trans-self}^{(2)}$ . One easily sees that the resulting graph is the 1-skeleton of the 3-dimensional cube  $I^3$  (compare Section 4.6). In particular, it is connected. (Studying the normal discs to  $\Sigma_{trans-self}^{(2)}$  in  $M_K$  one shows that if a 0-cochain is invariant under passing all  $\Sigma_{tan}^{(1)}$  and just one local type of a stratum  $\Sigma_{tri}^{(1)}$  then it is invariant under passing all remaining local types of triple crossings because  $\Gamma$  is connected.) The edges of the graph  $\Gamma = skl_1(I^3)$  correspond to the types of strata in  $\Sigma_{trans-self}^{(2)}$ . The solution of the positive tetrahedron equation tells us what is the contribution to  $R_x$  of a positive triple crossing (i.e. all three involved crossings are positive) . The meridians of the strata from  $\Sigma_{trans-self}^{(2)}$  give equations which allow us to determine the contributions of all other types of triple crossings as well as the contributions of self-tangencies. However, a global phenomenon occurs: each loop in  $\Gamma$  could give an additional equation. Evidently, it suffices to consider the loops which are the boundaries of the 2-faces from  $skl_2(I^3)$ . We call all the equations which come from the meridians of  $\Sigma_{trans-self}^{(2)}$  and from the loops in  $\Gamma = skl_1(I^3)$  the *cube equations* (Section 4.6). (Notice that a loop in  $\Gamma$  is more general than a loop in  $M_K$ . For a loop in  $\Gamma$  we come back to the same local type of a triple crossing but not necessarily to the same whole diagram of  $K$ .)

We need only the following strata from  $\Sigma^{(3)}$  in order to simplify the proof of the invariance of  $R_x$  in generic homotopies which pass through strata from  $\Sigma^{(2)}$ :

- (1) one degenerate quadruple crossing where exactly two branches have an ordinary self-tangency in the quadruple point, denoted by  $\Sigma_{trans-trans-self}^{(3)}$  (see Fig. 53).
- (2) one self-tangency in an ordinary flex with a transverse branch passing through the tangent point, denoted by  $\Sigma_{trans-self-flex}^{(3)}$  (see Fig. 54).

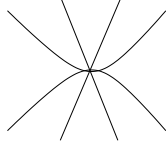


Figure 53: A quadruple crossing with two tangential branches

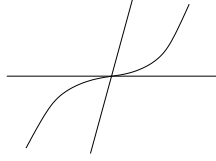


Figure 54: A self-tangency in a flex

- (3) the transverse intersection of a stratum from  $\Sigma^{(1)}$  with a stratum of  $\Sigma_{trans-self}^{(2)}$

Again, for each fixed global type of a quadruple crossing we form a graph with the local types of quadruple crossings as vertices's and the adjacent strata of  $\Sigma_{trans-trans-self}^{(3)}$  as edges. One easily sees that the resulting graph  $\Gamma$  has exactly 48 vertices's and that it is again connected. Luckily, we don't need to study the unfolding of  $\Sigma_{trans-trans-self}^{(3)}$  in much detail. It is clear that each meridional 2-sphere for  $\Sigma_{trans-trans-self}^{(3)}$  intersects  $\Sigma^{(2)}$  transversally in a finite number of points, namely exactly in two strata from  $\Sigma_{quad}^{(2)}$  and in lots of strata from  $\Sigma_{trans-self}^{(2)}$  and from  $\Sigma^{(1)} \cap \Sigma^{(1)}$  and there are no other intersections with strata of codimension 2. If we know now that  $R_x(m) = 0$  for the meridian  $m$  of one of the quadruple crossings, that  $R_x(m) = 0$  for all meridians of  $\Sigma_{trans-self}^{(2)}$  (i.e.  $R_x$  satisfies the cube equations) and for all meridians of  $\Sigma^{(1)} \cap \Sigma^{(1)}$  (i.e.  $R_x$  is invariant under passing simultaneous Reidemeister moves at different places in the diagram) then  $R_x(m) = 0$  for the other quadruple crossing too. It follows that for each of the fixed 24 global types (see Fig. 55, where in each case we have four possibilities for the point at infinity) the 48 tetrahedron equations reduce to a single one, which is called the *positive global tetrahedron equation*. There is no further reduction possible because we are searching for non symmetric solutions and which depend non trivially from the point at infinity!

In the cube equations there are also two local types of edges, correspond-

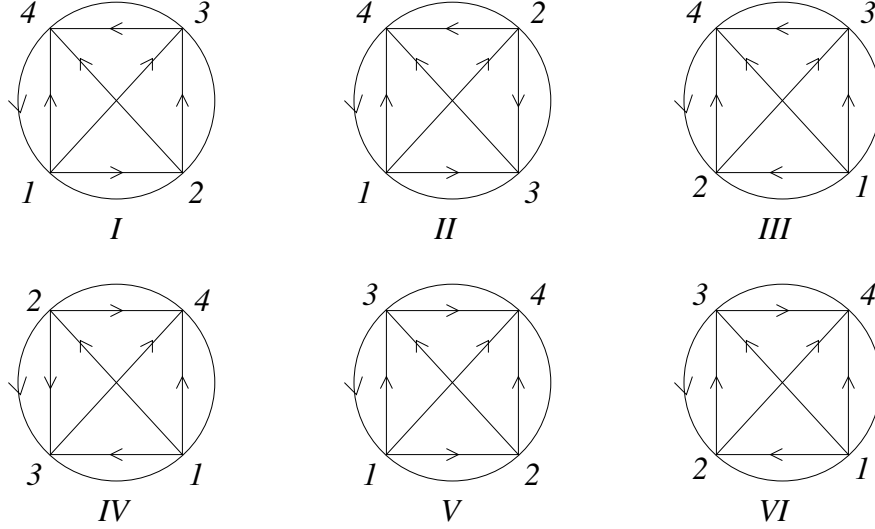


Figure 55: The global types of quadruple crossings

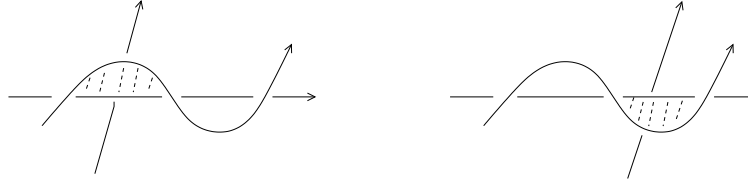


Figure 56: Two different local types of an edge 1-7 in the cube equations and which come together in  $\Sigma_{trans-self-flex}^{(3)}$

ing to the the two different local types of a Reidemeister II move with given orientations, compare Fig. 56. We reduce them to a single type of the edge by using the strata from  $\Sigma_{trans-self-flex}^{(3)}$ . The meridional 2-sphere for  $\Sigma_{trans-self-flex}^{(3)}$  intersects  $\Sigma^{(2)}$  transversally in exactly two strata from  $\Sigma_{trans-self}^{(2)}$ , which correspond to the two different types of the edge, and in lots of strata from  $\Sigma_{self-flex}^{(2)}$  and from  $\Sigma^{(1)} \cap \Sigma^{(1)}$ . Hence, again the invariance under passing one of the two local types of strata from  $\Sigma_{trans-self}^{(2)}$  together with the invariance under passing all strata from  $\Sigma_{self-flex}^{(2)}$  and  $\Sigma^{(1)} \cap \Sigma^{(1)}$  guaranties the invariance under passing the other local type of  $\Sigma_{trans-self}^{(2)}$  too.

The unfolding (i.e. the intersection of a normal disc with the stratification



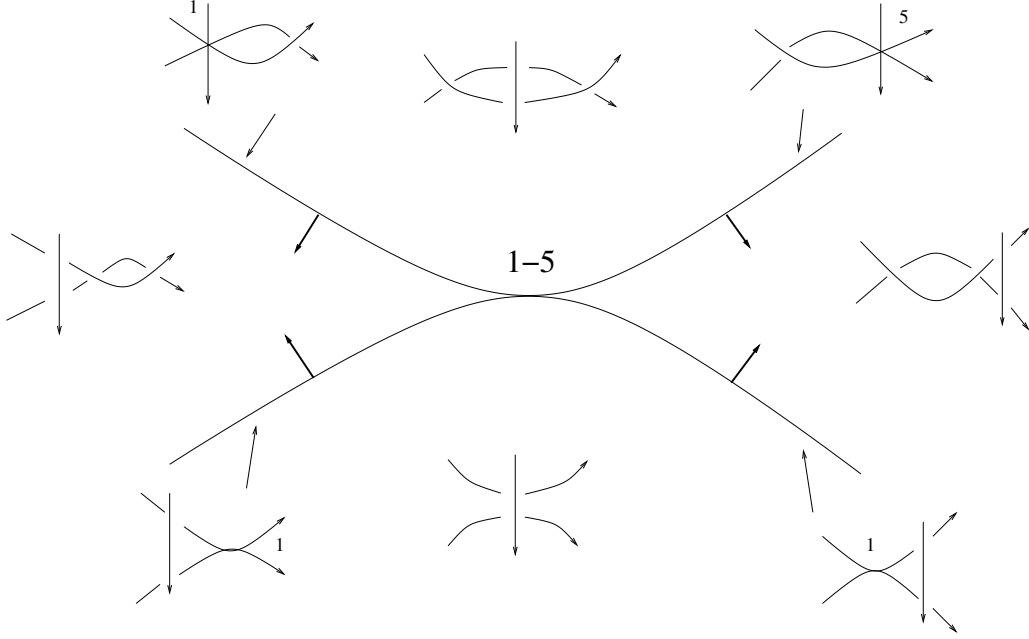


Figure 57: The unfolding of a self-tangency with a transverse branch corresponding to the edge 1 – 5

of  $M_K$ ) of e.g. the edge 1 – 5 of  $\Gamma$  is shown in Fig. 57 (compare [25]). The intersection of a meridional 2-sphere for  $\Sigma^{(1)} \cap \Sigma_{trans-self}^{(2)}$  with  $\Sigma^{(2)}$  consists evidently of the transverse intersections of the stratum  $\Sigma^{(1)}$  with all the strata of codimension 1 in the unfolding of  $\Sigma_{trans-self}^{(2)}$ . It follows again that it is sufficient to prove the invariance under passing  $\Sigma^{(1)} \cap \Sigma^{(1)}$  only for positive triple crossings (i.e. of local type 1) and only for one of the two local types of self-tangencies with a given orientation.

The remaining part of the paper is now organized as follows: we show the invariance of  $R_x$  in the knot case, respectively  $R_{xy}$  and  $R_{x(i)}$  in the braid case, under generic homotopies which pass through the strata from Proposition 6 in the following Subsections: 4.2: (3) and (6), 4.3: (4) in both cases, 4.4: (1) in the knot case, 4.5: (1) in the braid case, 4.6: (2) and the cube equations , 4.7: (5) and the scan property.

(Remember that in the case of  $rot(\hat{\beta}^+ \Delta)$  for positive closed braids which contain a half-twist the strata of the types (2), (3), (5) and (6) do not occur.)

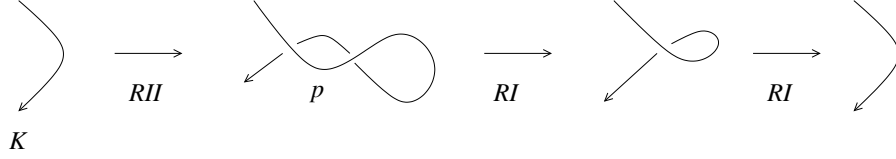


Figure 58: A meridian for a degenerated cusp

$$+ x^{v_2(K)} ( \text{diagram with crossing and dot labeled +} - \text{diagram with crossing and dot labeled -} ) = 0$$

Figure 59:  $R_x$  on the meridian of a degenerated cusp

## 4.2 Reidemeister II moves in a cusp and in a flex

As a warm-up we consider first the less important strata. All signs, weights and contributions  $R_x(p)$  were defined in Section 2.1.

Let's start with  $\Sigma_{cusp-deg}^{(2)}$ . A meridian for one type is shown in Fig. 58. There is a single Reidemeister II move  $p$  which could a priori contribute if it has the right global type. It follows easily from the Polyak-Viro formula, see [56], that in this case  $W_2(d) = v_2(K)$ . The contribution  $R_x(p)$  is shown in Fig. 59 and we see that it vanishes because of the embedded 1T-relation.

The considerations for all other types of  $\Sigma_{cusp-deg}^{(2)}$  are completely analogous.

We show the unfolding and a meridian for one type of  $\Sigma_{self-flex}^{(2)}$  in Fig. 60. There are exactly two Reidemeister II moves,  $p_1$  and  $p_2$ . The third crossings, which are not in the Reidemeister moves, are never f-crossings in the case of long knots (compare Definition 13). If one is a r-crossing for one of the two moves then the other is a r-crossing for the other move with exactly the same f-crossing (compare Definition 12). Consequently,  $W_2(d_1) = W_2(d_2)$ . We show the calculation of  $R_x(m)$  in Fig. 61.

## 4.3 Simultaneous Reidemeister moves

An example of a meridian of  $\Sigma^{(1)} \cap \Sigma^{(1)}$  is shown in Fig. 62. It is clear that e.g. the f-crossings for  $p_1$  do not change when the meridian  $m$  crosses the discriminant at  $p_2$ . Moreover, the linear weight  $W_1(hm)$  (compare Definition 12) is the same for both intersections of  $m$  with the stratum of the discriminant which corresponds to  $p_1$ .

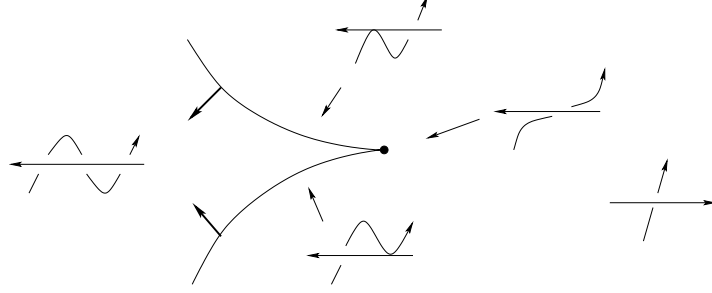


Figure 60: The unfolding for the self-tangency in a flex

$$\begin{aligned}
 & + x W_2(p_1) \left( \begin{array}{c} \text{diagram with a crossing labeled } + \\ \text{diagram with a crossing labeled } - \end{array} \right) \\
 & - x W_2(p_2) \left( \begin{array}{c} \text{diagram with a crossing labeled } + \\ \text{diagram with a crossing labeled } - \end{array} \right) = 0
 \end{aligned}$$

Figure 61:  $R_x$  vanishes on the meridian of a self-tangency in a flex

Let's consider the quadratic weight  $W_2(c)$  (compare Definition 13).

**Lemma 1**  $W_2(d)$  and  $W_2(ml)$  are isotopy invariants for each Reidemeister move of type I, II or III, i.e. they are invariant under any isotopy of the rest of the diagram outside of  $I_p^2 \times \mathbb{R}$ .

The lemma implies that  $W_2(c)$  (for  $c = d$  or  $c = ml$ ) doesn't change under a homotopy of an arc which passes through  $\Sigma^{(1)} \cap \Sigma^{(1)}$ , and hence the contributions to  $R_x$  cancel out as shown in Fig. 63.

*Proof.* It is obvious that  $W_2(c)$  is invariant under Reidemeister moves of type I and II. The latter comes from the fact that both new crossings are simultaneously crossings of type  $f$  or  $r$  and that they have different writhe. As was explained in Section 4.1 the graph  $\Gamma$  implies now that it is sufficient to prove the invariance of  $W_2(d)$ , respectively  $W_2(ml)$ , only under positive Reidemeister moves of type III. There are two global types and for each of them there are three possibilities for the point at infinity. We give names 1, 2, 3 to the crossings and  $a, b, c$  to the points at infinity and we show the six cases in Fig. 64 and Fig. 65. Evidently, we have only to consider the mutual

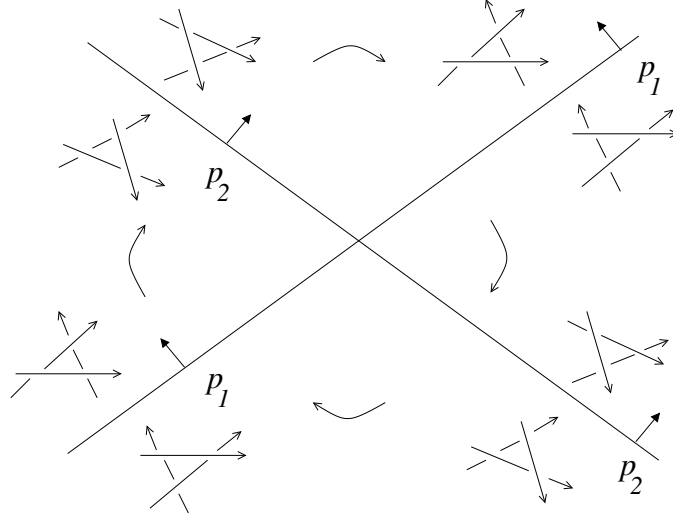


Figure 62: Meridian of two simultaneous Reidemeister III moves

position of the three crossings in the pictures because the contributions with all other crossings do not change.

$r_a$ : there is only 3 which could be a f-crossing but it does not contribute with another crossing in the picture to  $W_2(c)$ .

$r_b$ : no r-crossing at all.

$r_c$ : only 2 could be a f-crossing. In that case it contributes on the left side exactly with the r-crossing 1 and on the right side exactly with the r-crossing 3.

$l_a$ : no f-crossing at all.

$l_b$ : 1 and 2 could be f-crossings but non of them contributes with the crossing 3 to  $W_2(c)$ .

$l_c$ : 1 and 3 could be f-crossings. But the foots of 1 and 3 are arbitrary close. Consequently, they can be f-crossings only simultaneously! In that case 3 contributes with 2 on the left side and 1 with 2 on the right side.

Consequently, we have proven that  $W_2(c)$  is invariant.

□

(One could consider  $W_2(c)$  as a finite type invariant of the tangle in  $(\mathbb{C} \times \mathbb{R}) \setminus (I_p^2 \times \mathbb{R})$ , but which depends on the triple crossing in  $I_p^2 \times \mathbb{R}$ .)

The case of  $R_{xy}(m)$  and  $R_1(m)$  for closed braids is completely analogue and even simpler, because there is no quadratic weight  $W_2$ , respectively no

$$\begin{aligned}
& x^{W_2(d(p_1))} \left( \begin{array}{c} \text{Diagram 1} \\ d(p_1) \end{array} - \begin{array}{c} \text{Diagram 2} \\ d(p_1) \end{array}, \begin{array}{c} \text{Diagram 3} \\ p_2 \end{array} \right) \\
& + x^{W_2(d(p_2))} \left( \begin{array}{c} \text{Diagram 4} \\ d(p_2) \end{array} - \begin{array}{c} \text{Diagram 5} \\ d(p_2) \end{array}, \begin{array}{c} \text{Diagram 6} \\ p_1 \end{array} \right) \\
& - x^{W_2(d(p_1))} \left( \begin{array}{c} \text{Diagram 7} \\ d(p_1) \end{array} - \begin{array}{c} \text{Diagram 8} \\ d(p_1) \end{array}, \begin{array}{c} \text{Diagram 9} \\ p_2 \end{array} \right) \\
& - x^{W_2(d(p_2))} \left( \begin{array}{c} \text{Diagram 10} \\ d(p_2) \end{array} - \begin{array}{c} \text{Diagram 11} \\ d(p_2) \end{array}, \begin{array}{c} \text{Diagram 12} \\ p_1 \end{array} \right) \\
& = 0
\end{aligned}$$

Figure 63: Calculation of  $R_x$  on a meridian of two simultaneous Reidemeister III moves

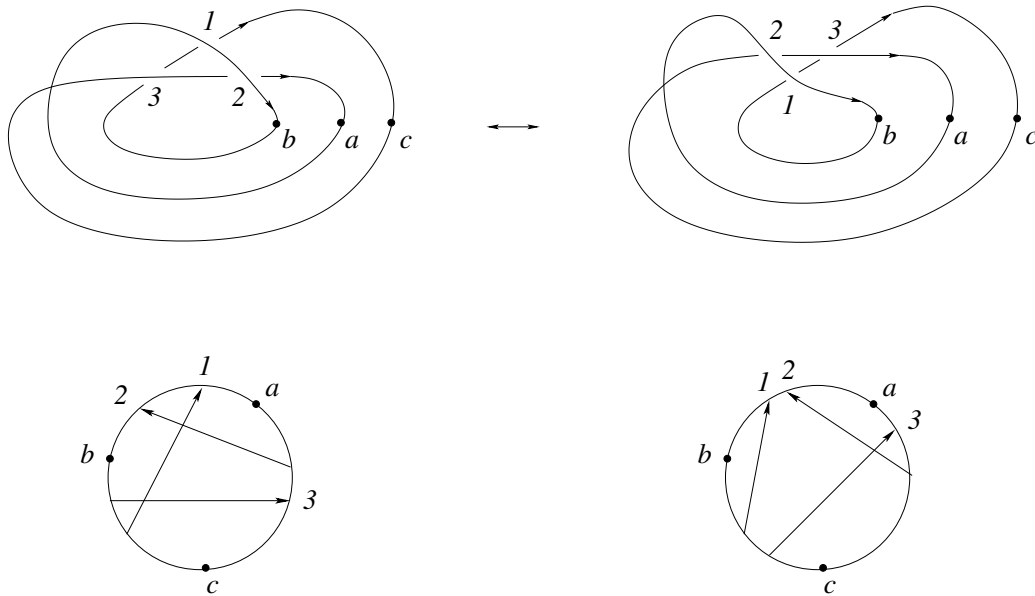


Figure 64:  $RIII$  of type  $r$

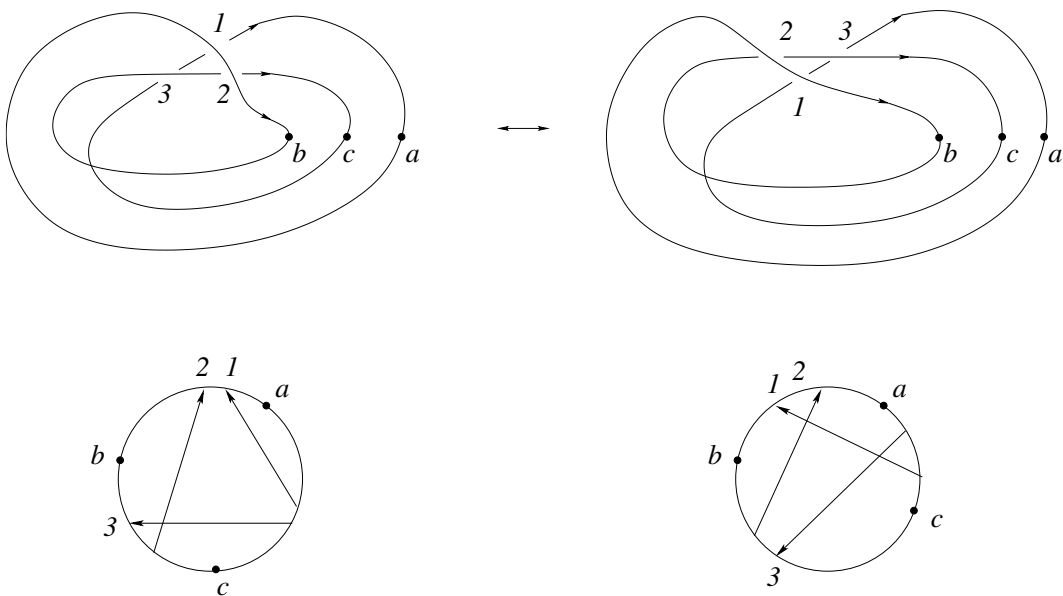


Figure 65:  $RIII$  of type  $l$

weight at all.

## 4.4 Tetrahedron equation for long knots

This one and the next subsection contain the heart of this paper.

As explained in Section 4.1 it suffices to consider global positive quadruple crossings with a fixed point at infinity. We naturally identify crossings in an isotopy outside Reidemeister moves of type I and II. The following lemma is of crucial importance.

**Lemma 2** *The f-crossings for  $d$  of the eight adjacent strata of triple crossings (compare Fig. 50) have the following properties:*

- (1) *the f-crossings in  $P_2$  are identical with those in  $\bar{P}_2$*
- (2) *the f-crossings in  $P_1, \bar{P}_1, P_4$  and  $\bar{P}_4$  are all identical*
- (3) *the f-crossings in  $P_3$  are either identical with those in  $\bar{P}_3$  or there is exactly one new f-crossing in  $\bar{P}_3$  with respect to  $P_3$ . In the latter case the new crossing is always exactly the crossing  $hm = 34$  in  $P_1$  and  $\bar{P}_1$*
- (4) *the new f-crossing in  $\bar{P}_3$  appears if and only if  $P_1$  (and hence also  $\bar{P}_1$ ) is of one of the two global types  $r_a$  or  $l_c$ .*
- (5) *the distinguished crossing  $d$  in  $P_3$  and  $\bar{P}_3$  is always the crossing  $ml$  in  $P_1$  and  $\bar{P}_1$*

*Proof.* We have checked the assertions of the lemma in all twenty four cases (denoted by the global type of the quadruple crossing together with the point at infinity) using Fig. 66-77. These figures are our main instrument. Notice that the crossing  $hm$  in  $P_1$  and  $\bar{P}_1$  is always the crossing 34 and that  $d$  is of type 0 if  $\infty$  is on the right side of it in the figures. The distinguished crossing  $d$  in  $P_3$  is always the crossing 13 which is always the crossing  $ml$  in  $P_1$  too.

We consider just some examples. In particular we show that it is necessary to add the "degenerate" configuration in Fig. 20 and we left the rest of the verification to the reader.

The f-crossings are:

case  $I_1$ . non at all

case  $I_2$ . non at all

case  $I_3$ . In  $P_1, \bar{P}_1$ : 34 (both are the degenerate case). In  $P_4, \bar{P}_4$ : 34 (the third configuration and the first configuration in Fig. 20). In  $P_2, \bar{P}_2$ : 34. In  $P_3$ : non. In  $\bar{P}_3$ : 34.

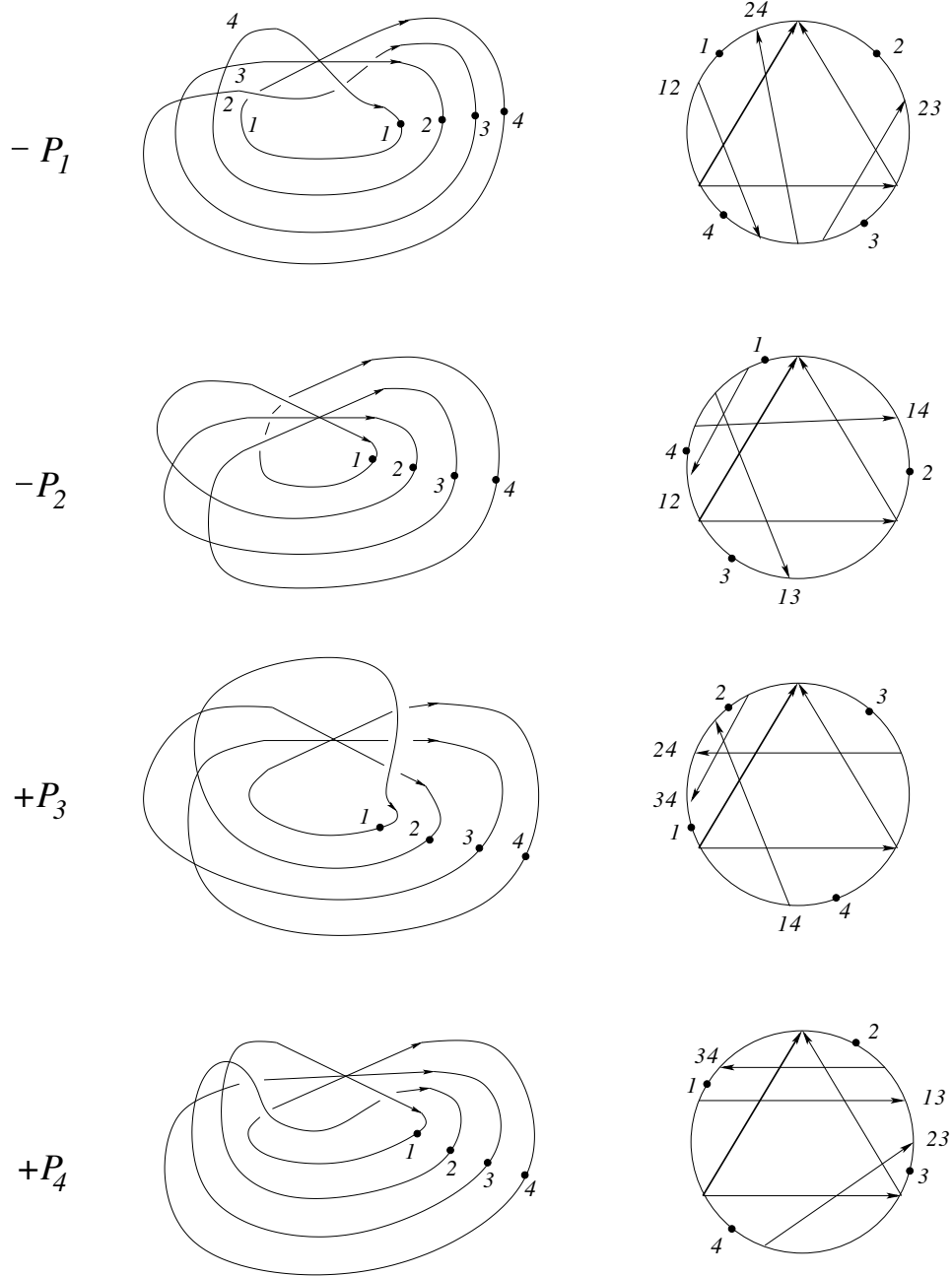


Figure 66: first half of the meridian for global type I



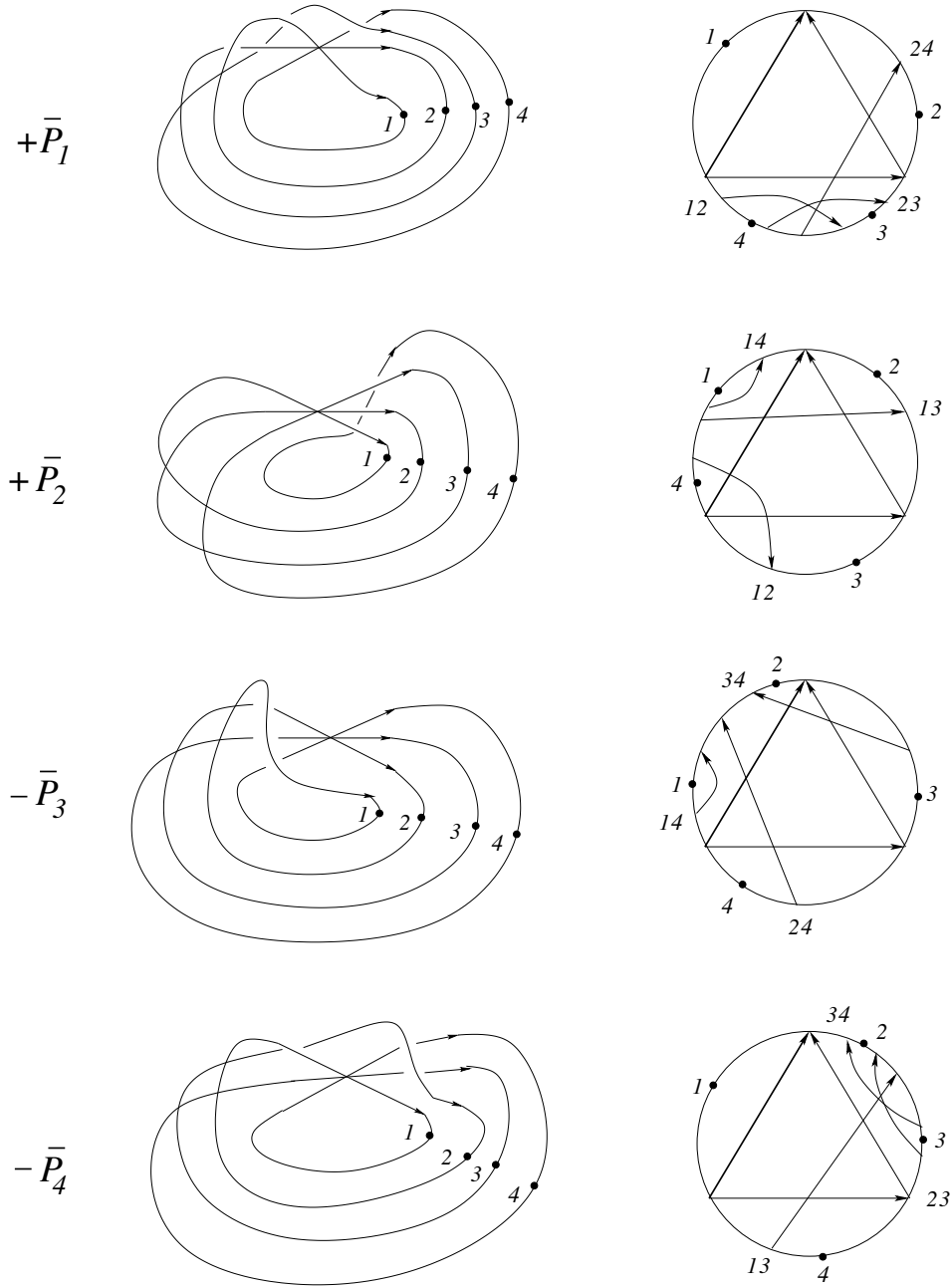


Figure 67: second half of the meridian for global type I

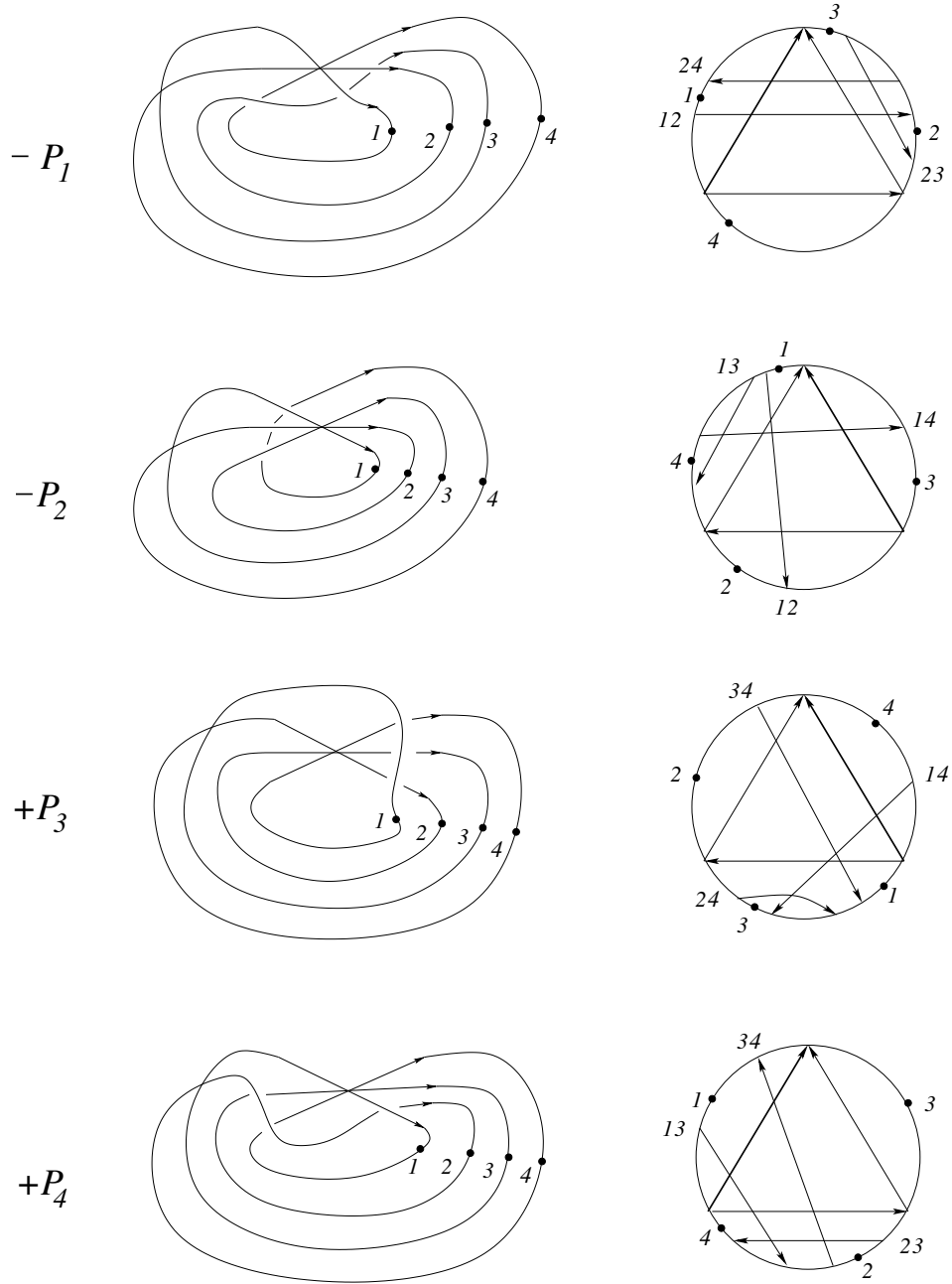


Figure 68: first half of the meridian for global type II

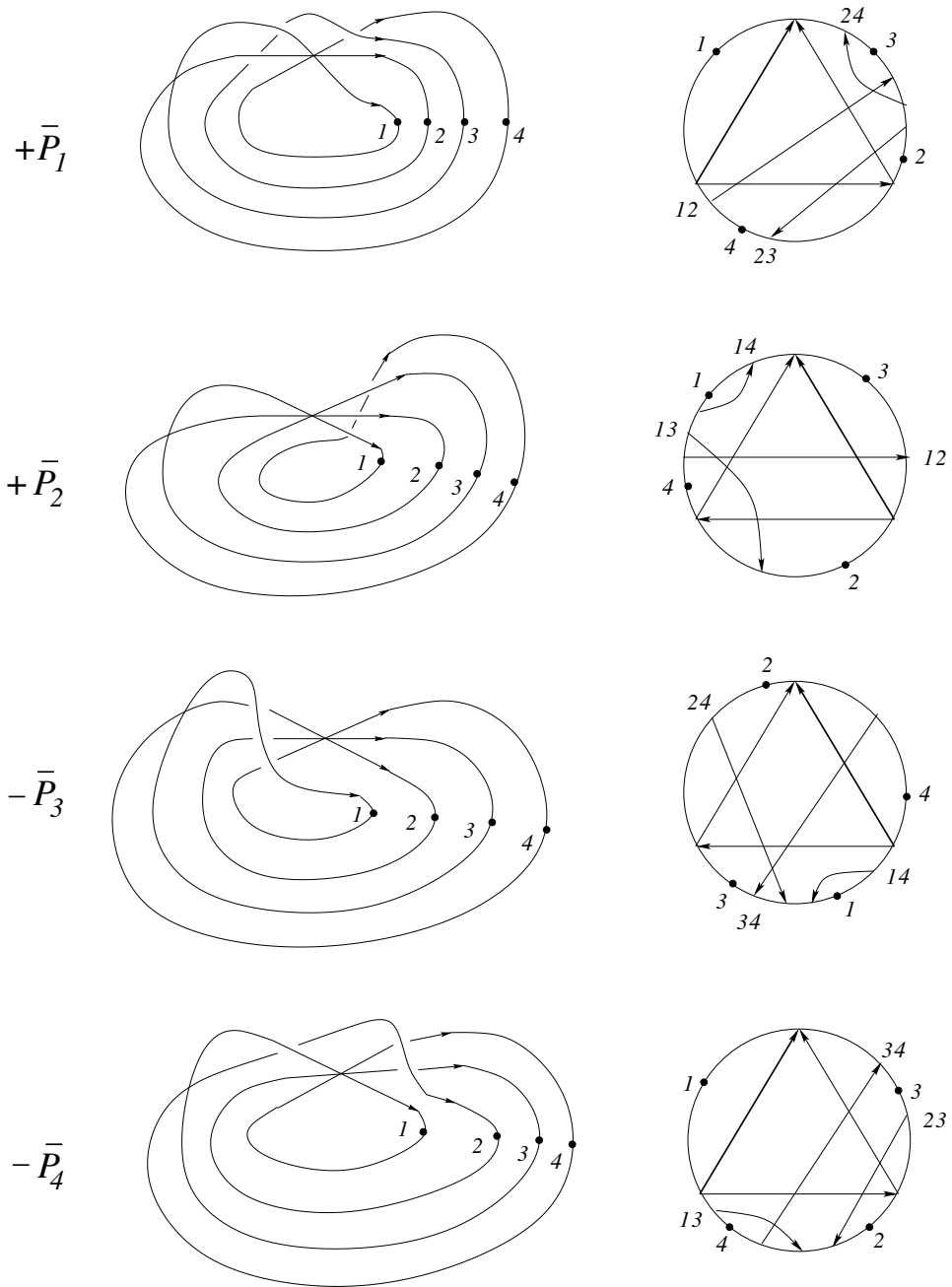


Figure 69: second half of the meridian for global type II

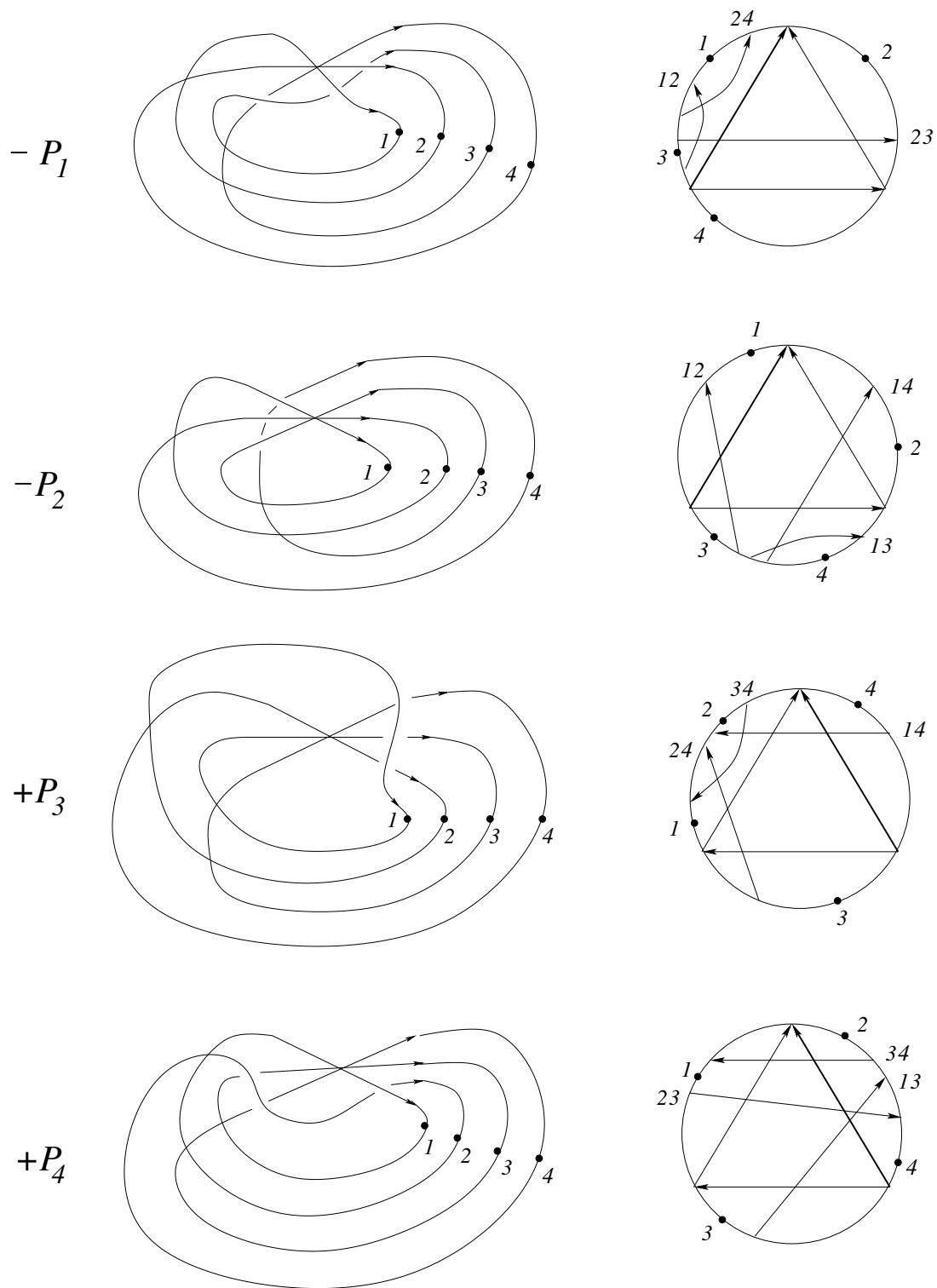


Figure 70: first half of the meridian for global type III

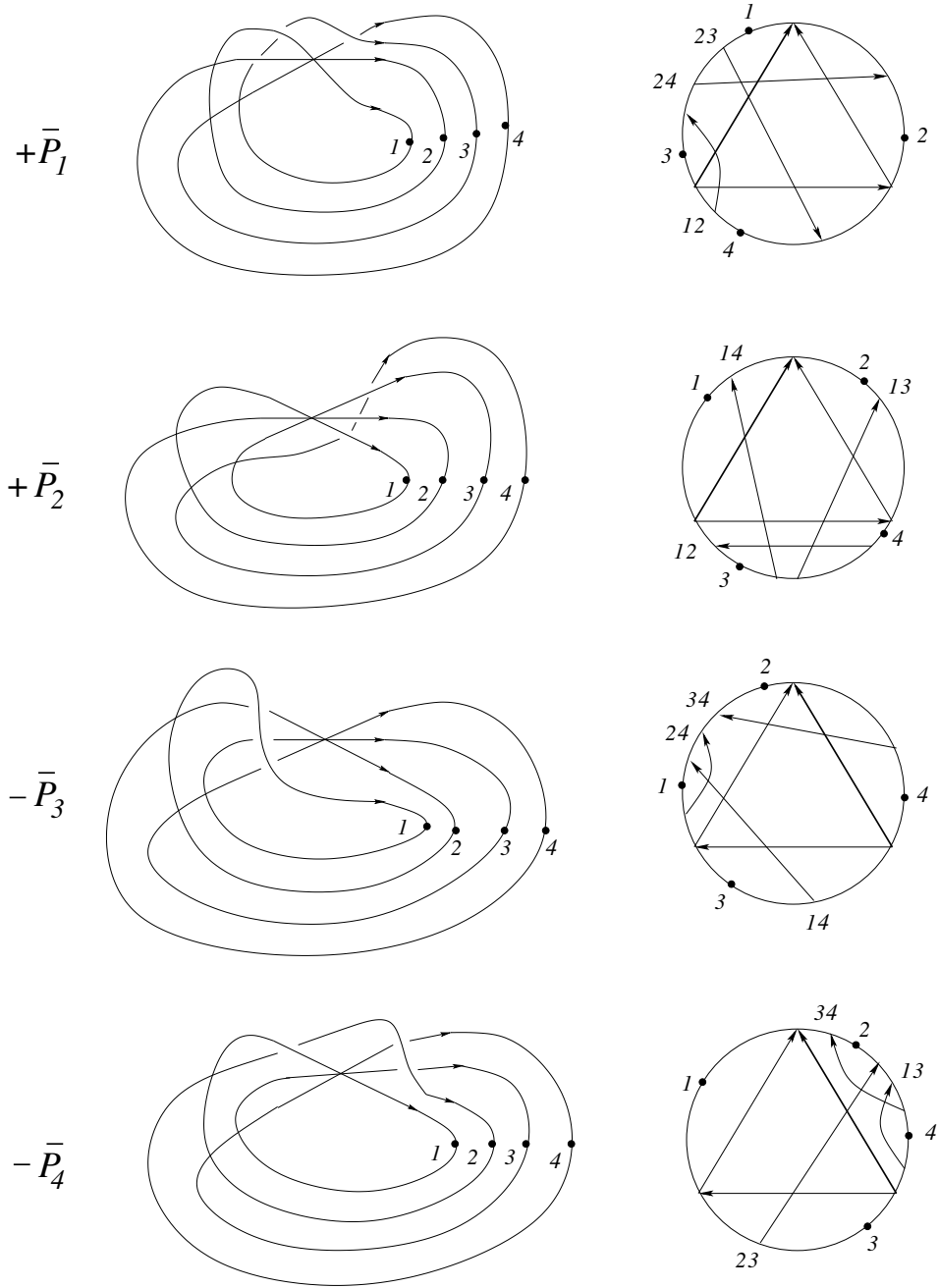


Figure 71: second half of the meridian for global type III

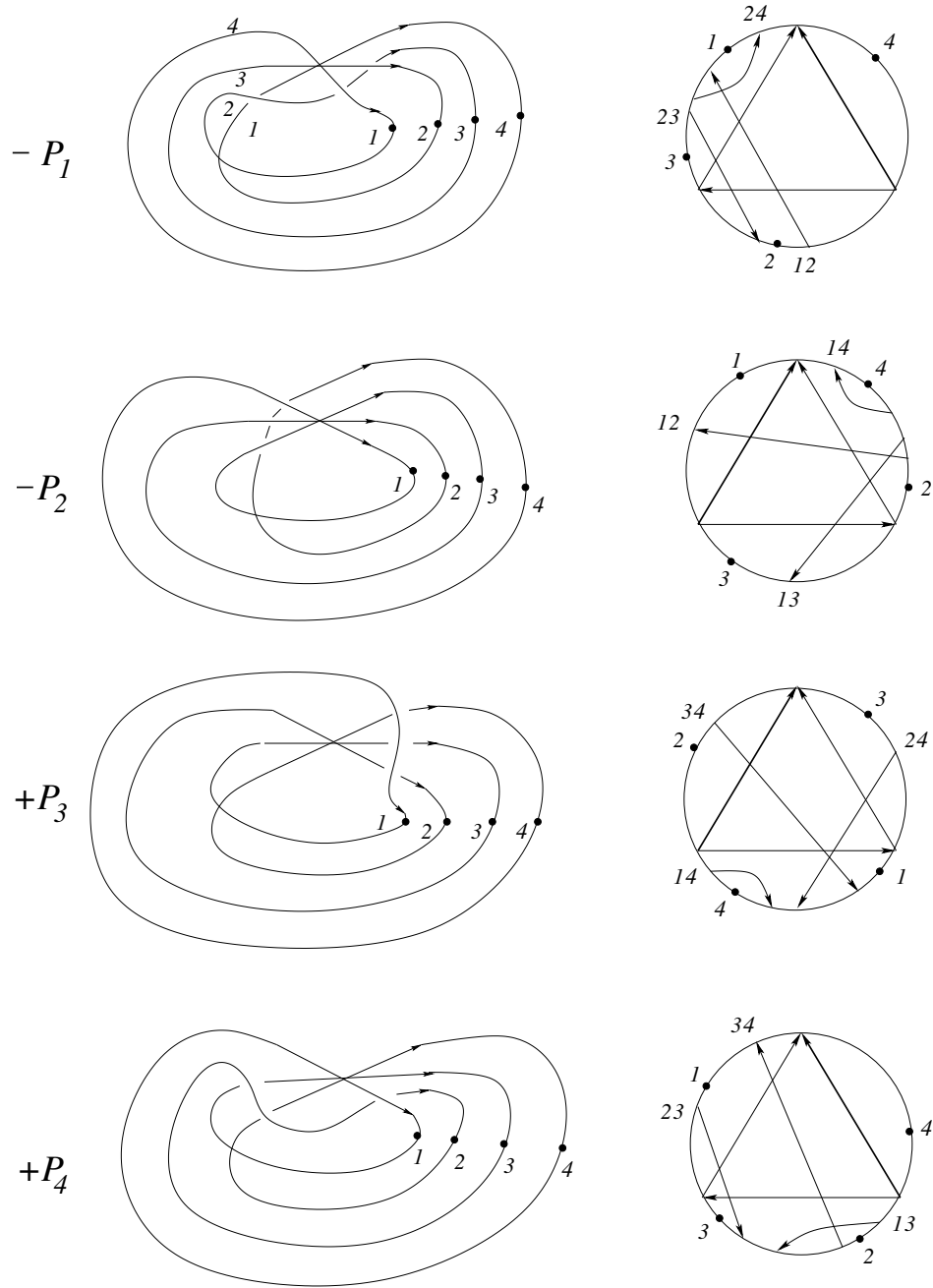


Figure 72: first half of the meridian for global type IV

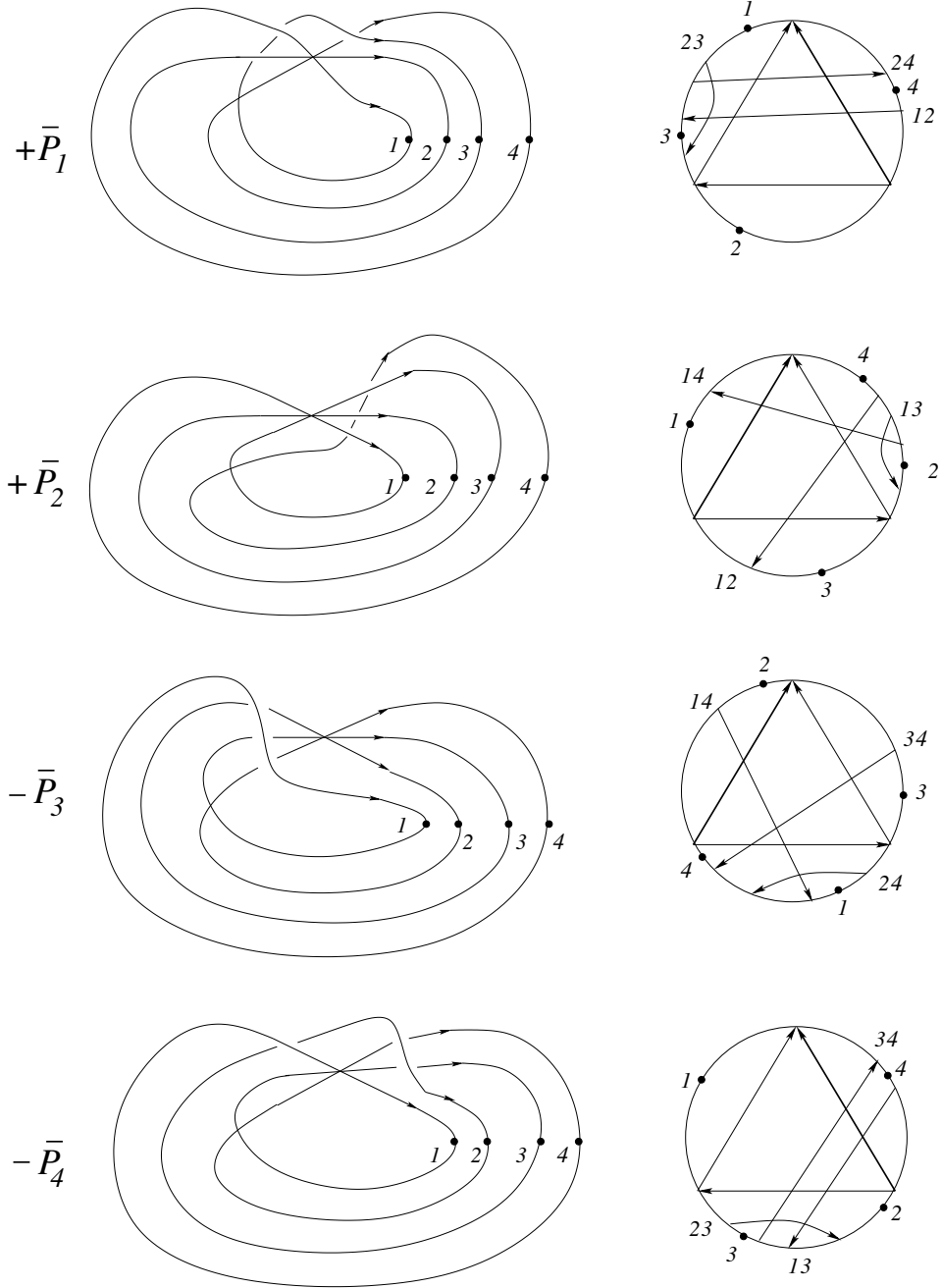


Figure 73: second half of the meridian for global type IV

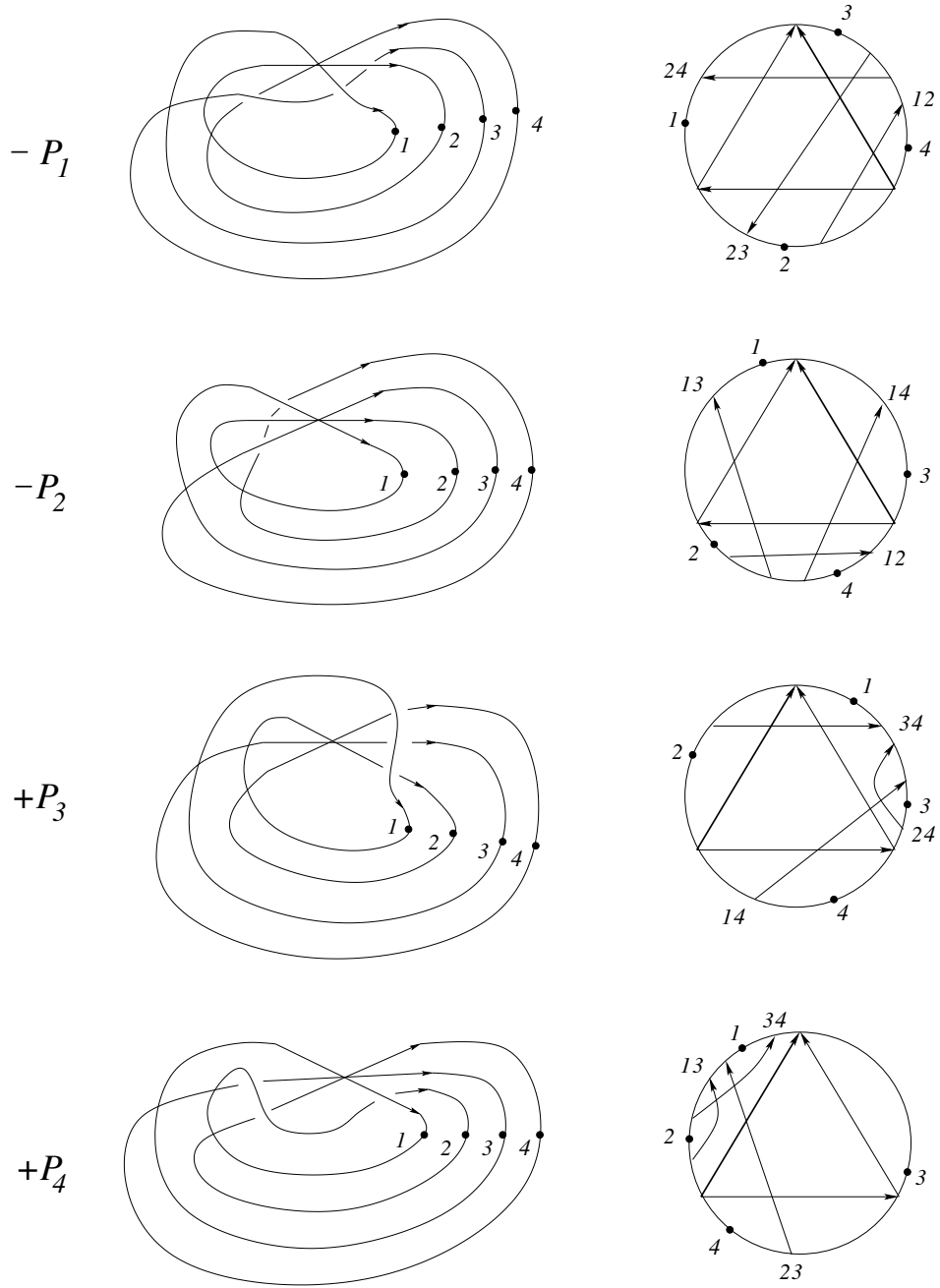


Figure 74: first half of the meridian for global type V



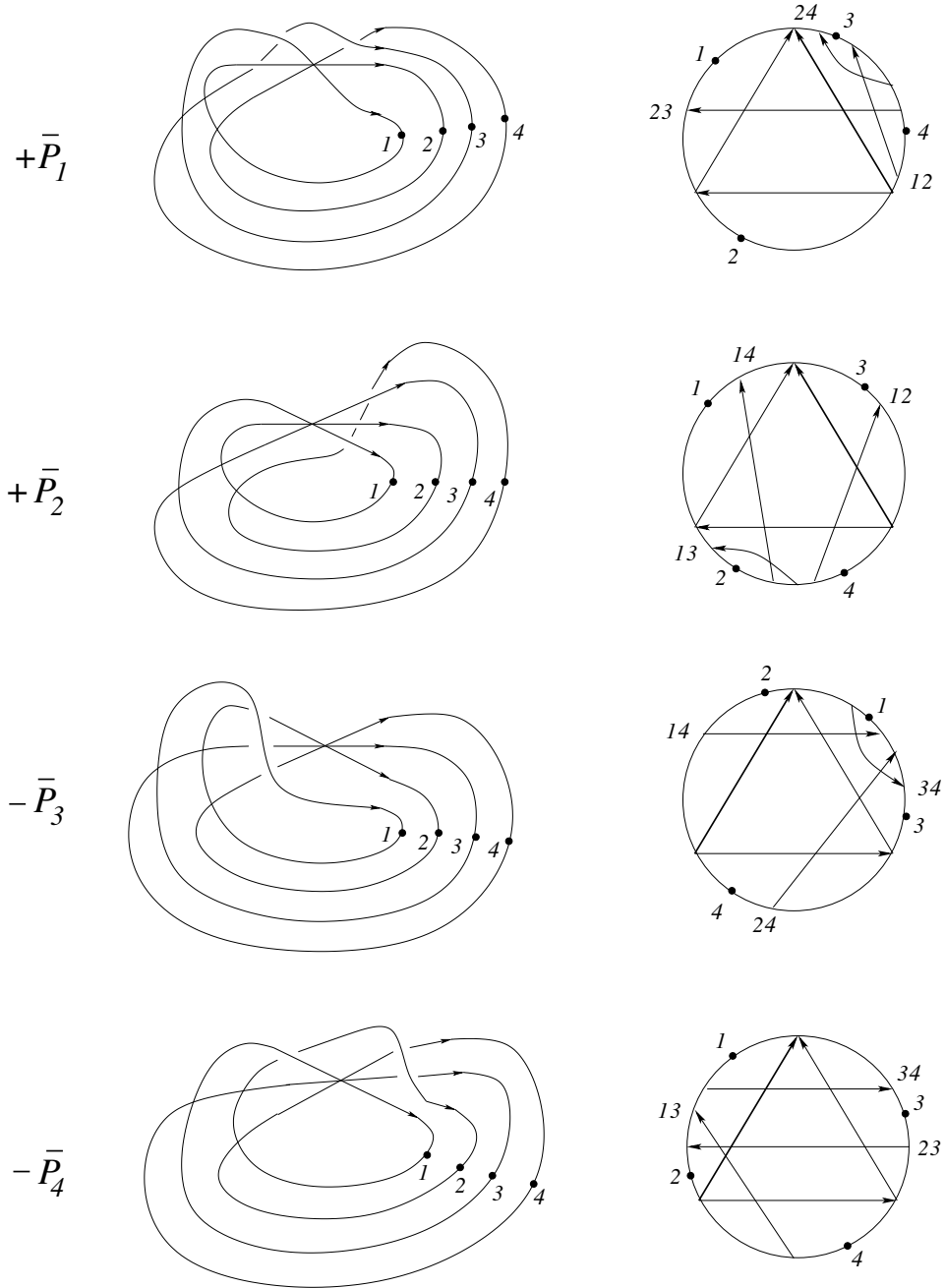


Figure 75: second half of the meridian for global type V

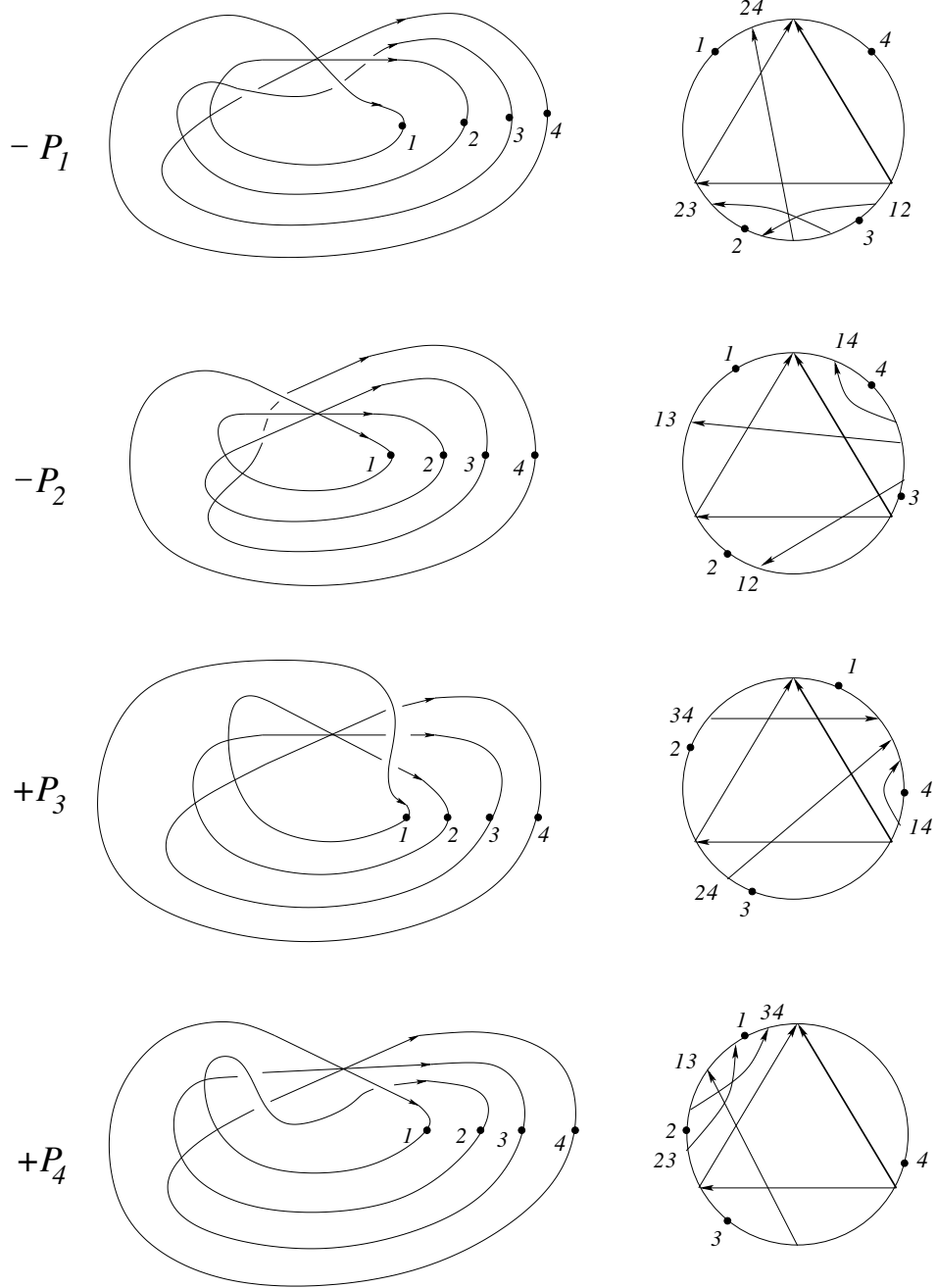


Figure 76: first half of the meridian for global type VI

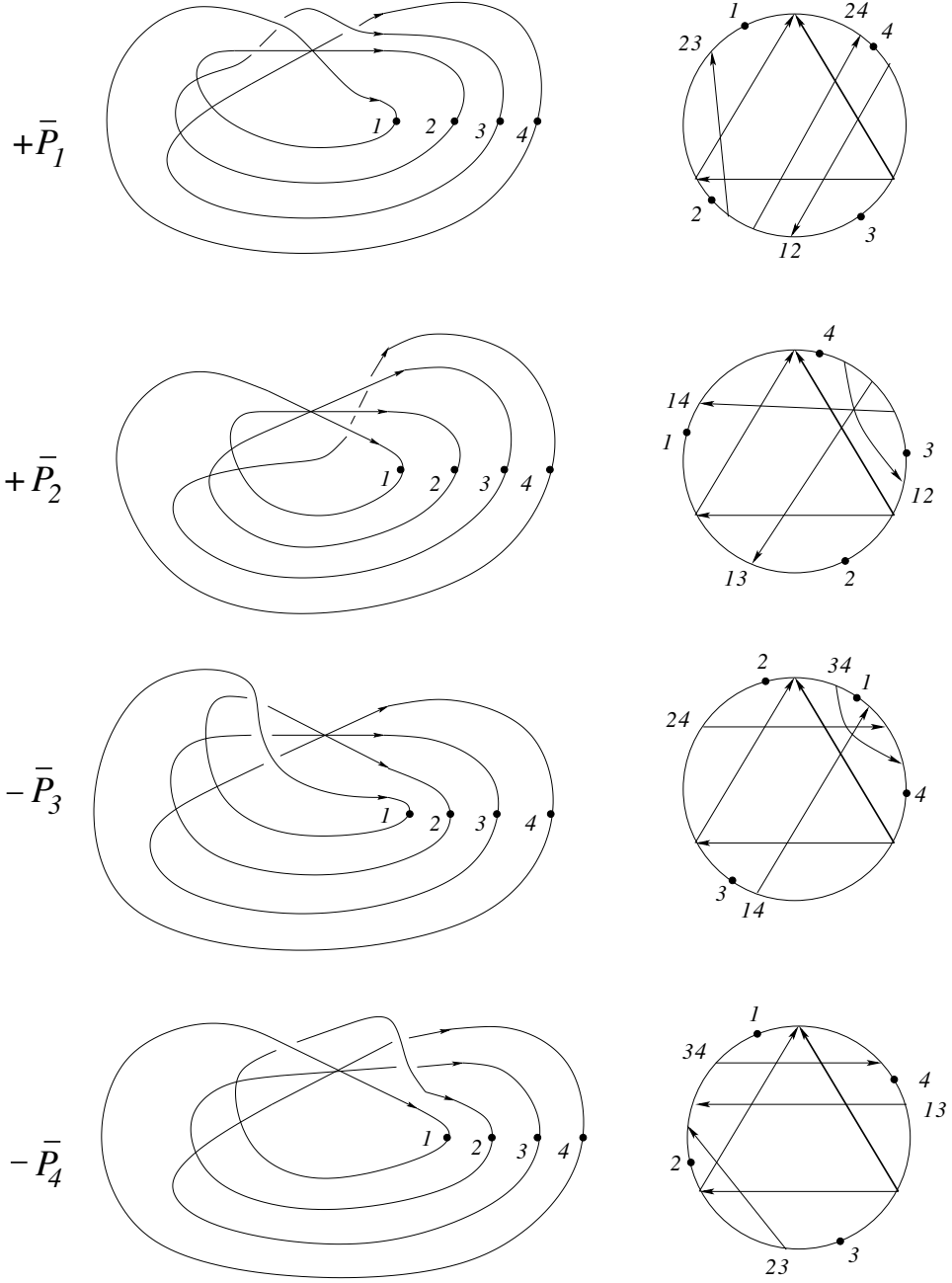


Figure 77: second half of the meridian for global type VI

case  $I_4$ . In  $P_1, \bar{P}_1, P_4, \bar{P}_4$ : 34, 24, 23. In  $P_2, \bar{P}_2$ : non. In  $P_3$ : 23, 24. In  $\bar{P}_3$ : 23, 24, 34.

case  $VI_3$ : In  $P_2$ : 12, 13, 14. In  $\bar{P}_2$ : 12, 13, 14 (12 shows that the fourth configuration in Fig. 20 is necessary too).

case  $VI_1$ : In  $P_3$ : non. In  $\bar{P}_3$ : 34 (shows that the global type  $l_c$  is necessary too).  $\square$

It turns out that Lemma 2 could be used to define already a solution of the global tetrahedron equation (compare [23], Proposition 2). However, this solution is not controllable under moving cusps, compare Section 4.7. This forces us to go one step further and to introduce quadratic weights.

Let us consider now the quadratic weight  $W_2(c)$ . If a f-crossing is one of the six crossings from the positive quadruple crossing than its contribution to  $W_2(c)$  is  $+W_1(f)$ .

We make the following conventions of notations:  $W_2(d)$  and  $W_1(hm)$  for  $P_i$  or  $\bar{P}_i$  are shortly denoted by  $W_2(P_i)$  and  $W_1(P_i)$  respectively  $W_2(\bar{P}_i)$  and  $W_1(\bar{P}_i)$ . If a f-crossing is denoted by the names of the two branches  $ij$ , which define the f-crossing, then  $W_1(ij)$  is the sum over all those r-crossings different from the six crossings of the quadruple crossing (i.e. this are the r-crossings which are not drawn in the figures). Consequently,  $W_1(f)$  is the sum of  $W_1(ij)$  and a correction term which comes from the r-crossings amongst the six crossings of the positive quadruple crossing.

In the case that the f-crossings in  $P_3$  and  $\bar{P}_3$  are not the same we get now  $W_2(\bar{P}_3) = W_2(P_3) + W_1(f)$

where  $f$  is the new f-crossing in  $\bar{P}_3$ . But luckily the new f-crossing  $f$  is always just the crossing  $hm$  in  $P_1$  (compare the previous lemma).

The following lemma is a "quadratic refinement" of the previous lemma.

**Lemma 3** (1)  $W_2(P_1) = W_2(\bar{P}_1) = W_2(P_4) = W_2(\bar{P}_4)$

(2)  $W_2(P_2) = W_2(\bar{P}_2)$

(3) Let  $P_i$  for some  $i \in \{1, 2\}$  be of one of the global types  $r_a$  or  $l_c$ . Then  $W_1(P_i) = W_1(\bar{P}_i)$ .

(4) If the f-crossings in  $P_3$  and  $\bar{P}_3$  coincide then  $W_2(P_3) = W_2(\bar{P}_3)$

(5) Let  $f$  be the new f-crossing in  $\bar{P}_3$  with respect to  $P_3$  and let  $f = hm$  be the corresponding crossing in  $P_1$ . Then  $W_2(\bar{P}_3) - W_2(P_3) = W_1(f)$  and  $W_1(f) = W_1(P_1) = W_1(\bar{P}_1)$ .

(6) Let  $P_i$  for some  $i \in \{3, 4\}$  be of one of the global types  $r_a$  or  $l_c$ . Then either simultaneously  $W_1(P_3) = W_1(\bar{P}_3)$  and  $W_1(P_4) = W_1(\bar{P}_4)$  or simultaneously  $W_1(P_3) = W_1(\bar{P}_3) + 1$  and  $W_1(\bar{P}_4) = W_1(P_4) + 1$ .

*Proof.* The proof is by inspection of all f-crossings, all r-crossings and all hm-crossings in all twenty four cases in the figures. We give it below in details. (Those strata which can never contribute are dropped.) We skip also the  $W_1(ij)$  and  $W_2(ij)$  contributions because they are always determined by  $ij$  and cancel out.

It shows in particular that it is necessary to add the degenerate configurations in Fig. 20 and Fig. 19.

$I_1$ : nothing at all

$$I_2: W_2(P_1) = W_2(\bar{P}_1) = W_2(P_4) = W_2(\bar{P}_4) = 0. \quad W_2(P_2) = W_2(\bar{P}_2) = 0.$$

$$I_3: W_2(P_1) = W_2(\bar{P}_1) = W_2(P_4) = W_2(\bar{P}_4) = 2. \quad W_2(P_2) = W_2(\bar{P}_2) = 2. \\ W_1(P_1) = W_1(\bar{P}_1) = 2. \quad W_1(P_2) = W_1(\bar{P}_2) = 2. \quad W_2(P_3) = 0 \text{ and } W_2(\bar{P}_3) = \\ W_2(\bar{P}_3, f) = 2.$$

$$I_4: W_2(P_1) = W_2(\bar{P}_1) = W_2(P_4) = W_2(\bar{P}_4) = 4. \quad W_1(P_1) = W_1(\bar{P}_1) = \\ 1. \quad W_1(P_3) = W_1(\bar{P}_3) = 1. \quad W_1(P_4) = W_1(\bar{P}_4) = 2. \quad W_2(\bar{P}_3) - W_2(P_3) = \\ W_2(\bar{P}_3, f) = 1.$$

$$II_1: W_1(P_2) = W_1(\bar{P}_2) = 0.$$

$$II_2: W_2(P_1) = W_2(\bar{P}_1) = W_2(P_4) = W_2(\bar{P}_4) = 2. \quad W_1(P_3) = 1 \text{ and } \\ W_1(\bar{P}_3) = 0. \quad W_1(P_4) = 1 \text{ and } W_1(\bar{P}_4) = 2.$$

$$II_3: W_2(P_1) = W_2(\bar{P}_1) = W_2(P_4) = W_2(\bar{P}_4) = 0. \quad W_2(P_2) = W_2(\bar{P}_2) = 0.$$

$$II_4: W_2(P_1) = W_2(\bar{P}_1) = W_2(P_4) = W_2(\bar{P}_4) = 3. \quad W_1(P_1) = W_1(\bar{P}_1) = 2. \\ W_1(P_2) = W_1(\bar{P}_2) = 2. \quad W_2(\bar{P}_3) - W_2(P_3) = W_2(\bar{P}_3, f) = 2. \quad W_1(P_4) = \\ W_1(\bar{P}_4) = 1.$$

$$III_1: W_1(P_3) = W_1(\bar{P}_3) = W_1(P_4) = W_1(\bar{P}_4) = 0.$$

$$III_2: W_2(P_1) = W_2(\bar{P}_1) = W_2(P_4) = W_2(\bar{P}_4) = 0. \quad W_2(P_2) = W_2(\bar{P}_2) = 0. \\ W_1(P_3) = W_1(\bar{P}_3) = 0.$$

$$III_3: W_2(P_2) = W_2(\bar{P}_2) = 3. \quad W_1(P_2) = W_1(\bar{P}_2) = 1.$$

$$III_4: W_2(P_1) = W_2(\bar{P}_1) = W_2(P_4) = W_2(\bar{P}_4) = 2. \quad W_1(P_1) = W_1(\bar{P}_1) = \\ 2. \quad W_2(P_2) = W_2(\bar{P}_2) = 2. \quad W_1(P_2) = W_1(\bar{P}_2) = 2. \quad W_2(\bar{P}_3) - W_2(P_3) = \\ W_2(\bar{P}_3, f) = 2.$$

$$IV_1: W_1(P_1) = W_1(\bar{P}_1) = 0. \quad W_2(\bar{P}_3) - W_2(P_3) = W_2(\bar{P}_3, f) = 0. \\ W_1(P_3) = W_1(\bar{P}_3) = 1. \quad W_1(P_4) = W_1(\bar{P}_4) = 0.$$

$$IV_2: W_2(P_2) = W_2(\bar{P}_2) = 3.$$

$IV_3$ :  $W_1(P_1) = W_1(\bar{P}_1) = 1$ .  $W_1(P_2) = W_1(\bar{P}_2) = 1$ .  $W_2(P_2) = W_2(\bar{P}_2) = 2$ .  $W_2(\bar{P}_3) - W_2(P_3) = W_2(\bar{P}_3, f) = 1$ .

$IV_4$ :  $W_2(P_1) = W_2(\bar{P}_1) = W_2(P_4) = W_2(\bar{P}_4) = 0$ .  $W_2(P_2) = W_2(\bar{P}_2) = 0$ .  $W_1(P_3) = W_1(\bar{P}_3) = 1$ .  $W_2(P_3) = W_2(\bar{P}_3) = 1$ .

$V_1$ :  $W_1(P_1) = W_1(\bar{P}_1) = 0$ .  $W_1(P_2) = W_1(\bar{P}_2) = 0$ .  $W_2(\bar{P}_3) - W_2(P_3) = W_2(\bar{P}_3, f) = 0$ .

$V_2$ : nothing at all

$V_3$ :  $W_2(P_1) = W_2(\bar{P}_1) = W_2(P_4) = W_2(\bar{P}_4) = 0$ .  $W_2(P_2) = W_2(\bar{P}_2) = 0$ .  $W_2(P_3) = W_2(\bar{P}_3) = 0$ .

$V_4$ :  $W_2(P_1) = W_2(\bar{P}_1) = W_2(P_4) = W_2(\bar{P}_4) = 4$ .  $W_2(P_3) = W_2(\bar{P}_3) = 4$ .  $W_2(P_4) = W_2(\bar{P}_4) = 4$ .  $W_1(P_3) = 3$ .  $W_1(\bar{P}_3) = 2$ .  $W_1(P_4) = 1$ .  $W_1(\bar{P}_4) = 2$ .

$VI_1$ :  $W_1(P_1) = W_1(\bar{P}_1) = 0$ .  $W_1(P_2) = W_1(\bar{P}_2) = 0$ .  $W_1(P_4) = W_1(\bar{P}_4) = 0$ .  $W_2(\bar{P}_3) - W_2(P_3) = W_2(\bar{P}_3, f) = 0$ .

$VI_2$ :  $W_1(P_3) = 1$ .  $W_1(\bar{P}_3) = 0$ .  $W_1(P_4) = 0$ .  $W_1(\bar{P}_4) = 1$ .

$VI_3$ :  $W_2(P_2) = W_2(\bar{P}_2) = 4$ .

$VI_4$ :  $W_2(P_1) = W_2(\bar{P}_1) = W_2(P_4) = W_2(\bar{P}_4) = 0$ .  $W_2(P_2) = W_2(\bar{P}_2) = 0$ .  $W_2(P_3) = W_2(\bar{P}_3) = 0$ .

□

We take now into account also  $W_2(ml)$ .

**Lemma 4** *We have to consider only the triple crossings of global type  $r_a$  and  $l_c$ .*

(1)  $ml = 12$  in  $P_3, P_4, \bar{P}_3, \bar{P}_4$ .

(2)  $13 = d$  in  $P_3, -\bar{P}_3$  and  $13 = ml$  in  $P_1, \bar{P}_1$ .

(3) *The  $f$ -crossings for  $ml$  in  $P_2$  and in  $\bar{P}_2$  are the same.  $W_2(ml)$  in  $P_2$  is always equal to  $W_2(ml)$  in  $\bar{P}_2$ .  $W_1(hm)$  in  $P_2$  is always equal to  $W_1(hm)$  in  $\bar{P}_2$ .*

(4) *The  $f$ -crossings for  $ml$  in  $P_1$  and in  $\bar{P}_1$  are the same.  $W_2(ml)$  in  $P_1$  is always equal to  $W_2(ml)$  in  $\bar{P}_1$ .*

(5)  $W_2(P_3) = W_2(ml)$  in  $P_1$ .

(6) *the sum of  $x^{W_2(ml)+W_1(hm)} - x^{W_2(ml)}$  over  $+P_3 - \bar{P}_3 + P_4 - \bar{P}_4$  is 0. (Here it can happen that only  $+P_3 - \bar{P}_3$  or  $+P_4 - \bar{P}_4$  are of the right global type  $r_a$  or  $l_c$ .)*

*Proof.* (1) and (2) are evident. By inspection of the f-crossings and the r-crossings we have

$I_3$ :  $W_2(ml) = 0$  in  $P_1$  and in  $\bar{P}_1$ .  $W_2(ml) = 0$  in  $P_2$  and in  $\bar{P}_2$ .  $W(hm) = 2$  in  $P_2$  and in  $\bar{P}_2$ .

$I_4$ :  $W_2(ml) = 3$  in  $P_1$  and in  $\bar{P}_1$ .  $W_2(P_3) = 3 = W_2(ml)$  in  $P_1$ .  $P_3$ :  $x^{W_2(12)+W_1(23)+1} - x^{W_2(12)}$ ,  $\bar{P}_3$ :  $x^{W_2(12)+W_1(23)+1+W_1(24)+2} - x^{W_2(12)+W_1(24)+2}$ ,  $P_4$ :  $x^{W_2(12)+W_1(23)+1+W_1(24)+2} - x^{W_2(12)+W_1(23)+1}$ ,  $\bar{P}_4$ :  $x^{W_2(12)+W_1(24)+2} - x^{W_2(12)}$ .

$II_1$ :  $W_2(ml) = 1$  in  $P_2$  and in  $\bar{P}_2$ .  $W_1(hm) = 0$  in  $P_2$  and in  $\bar{P}_2$ .

$II_2$ :  $P_3$ :  $x^{W_2(12)+W_1(23)+1} - x^{W_2(12)}$ ,  $\bar{P}_3$ :  $x^{W_2(12)+W_1(23)+1+W_1(24)} - x^{W_2(12)+W_1(24)+1}$ ,  $P_4$ :  $x^{W_2(12)+W_1(23)+1+W_1(24)} - x^{W_2(12)+W_1(23)+1}$ ,  $\bar{P}_4$ :  $x^{W_2(12)+W_1(24)+1} - x^{W_2(12)}$ .

$II_4$ :  $W_2(ml) = 0$  in  $P_2$  and in  $\bar{P}_2$ .  $W_1(hm) = 2$  in  $P_2$  and in  $\bar{P}_2$ .  $P_4$ :  $x^{W_2(12)+W_1(34)+2+W_1(24)+1} - x^{W_2(12)+W_1(34)+2}$ ,  $\bar{P}_4$ :  $x^{W_2(12)+W_1(34)+2+W_1(24)+1} - x^{W_2(12)+W_1(34)+2}$ .

$III_1$ :  $P_3$ :  $x^{W_2(12)+W_1(23)} - x^{W_2(12)}$ ,  $\bar{P}_3$ :  $x^{W_2(12)+W_1(23)+W_1(24)} - x^{W_2(12)+W_1(24)}$ ,  $P_4$ :  $x^{W_2(12)+W_1(23)+W_1(24)} - x^{W_2(12)+W_1(23)}$ ,  $\bar{P}_4$ :  $x^{W_2(12)+W_1(24)} - x^{W_2(12)}$ .

$III_2$ :  $P_3$ :  $x^{W_2(12)+W_1(23)} - x^{W_2(12)}$ ,  $\bar{P}_3$ :  $x^{W_2(12)+W_1(23)} - x^{W_2(12)}$ .

$III_3$ :  $W_2(ml) = 3$  in  $P_2$  and in  $\bar{P}_2$ .  $W_1(hm) = 1$  in  $P_2$  and in  $\bar{P}_2$ .

$III_4$ :  $W_2(ml) = 0$  in  $P_1$  and in  $\bar{P}_1$ .  $W_2(P_3) = 0 = W_2(ml)$  in  $P_1$ .  $W_2(ml) = 0$  in  $P_2$  and in  $\bar{P}_2$ .  $W_1(hm) = 2$  in  $P_2$  and in  $\bar{P}_2$ .

$IV_1$ :  $W_2(ml) = 1$  in  $P_1$  and in  $\bar{P}_1$ .  $W_2(P_3) = 1 = W_2(ml)$  in  $P_1$ .  $P_3$ :  $x^{W_2(12)+W_1(23)+1} - x^{W_2(12)}$ ,  $\bar{P}_3$ :  $x^{W_2(12)+W_1(23)+W_1(24)+1} - x^{W_2(12)+W_1(24)}$ ,  $P_4$ :  $x^{W_2(12)+W_1(23)+W_1(24)+1} - x^{W_2(12)+W_1(23)+1}$ ,  $\bar{P}_4$ :  $x^{W_2(12)+W_1(24)} - x^{W_2(12)}$ .

$IV_3$ :  $W_2(ml) = 0$  in  $P_1$  and in  $\bar{P}_1$ .  $W_2(ml) = 0$  in  $P_2$  and in  $\bar{P}_2$ .  $W_1(hm) = 1$  in  $P_2$  and in  $\bar{P}_2$ .

$IV_4$ :  $P_3$ :  $x^{W_2(12)+W_1(23)} - x^{W_2(12)}$ ,  $\bar{P}_3$ :  $x^{W_2(12)+W_1(23)} - x^{W_2(12)}$ .

$V_1$ :  $W_2(ml) = 0$  in  $P_1$  and in  $\bar{P}_1$ .  $W_2(ml) = 0$  in  $P_2$  and in  $\bar{P}_2$ .  $W_1(hm) = 0$  in  $P_2$  and in  $\bar{P}_2$ .

$V_4$ :  $P_3$ :  $x^{W_2(12)+W_1(23)+3} - x^{W_2(12)}$ ,  $\bar{P}_3$ :  $x^{W_2(12)+W_1(23)+2+W_1(24)+2} - x^{W_2(12)+W_1(24)+2}$ ,  $P_4$ :  $x^{W_2(12)+W_1(23)+3+W_1(24)+1} - x^{W_2(12)+W_1(23)+3}$ ,  $\bar{P}_4$ :  $x^{W_2(12)+W_1(24)+2} - x^{W_2(12)}$ .

$VI_1$ :  $W_2(ml) = 0$  in  $P_1$  and in  $\bar{P}_1$ .  $W_2(P_3) = 0 = W_2(ml)$  in  $P_1$ .  $W_2(ml) = 0$  in  $P_2$  and in  $\bar{P}_2$ .  $W_1(hm) = 0$  in  $P_2$  and in  $\bar{P}_2$ .  $P_4$ :  $x^{W_2(12)+W_1(34)+W_1(24)} - x^{W_2(12)+W_1(34)}$ ,  $\bar{P}_4$ :  $x^{W_2(12)+W_1(34)+W_1(24)} - x^{W_2(12)+W_1(34)}$ .

$$\begin{aligned}
R_x(\gamma) = & \sum_{\substack{p \text{ of type} \\ r_a \text{ and } l_c}} \text{sign}(p) (x^{W_2(ml) + W_1(hm)} - x^{W_2(ml)}) \quad \begin{array}{c} \nearrow \\ \text{---} \bullet \text{---} \searrow \\ + \end{array} \\
& + \sum_{\substack{d(p) \\ \text{of type } 0}} \text{sign}(p) x^{W_2(d)} \left( \begin{array}{c} \nearrow \\ \text{---} \bullet \text{---} \searrow \\ + \end{array} - \begin{array}{c} + \\ \nearrow \bullet \searrow \\ \text{---} \end{array} \right)
\end{aligned}$$

Figure 78: The 1-cochain  $R_x(\gamma)$  on positive triple crossings

$$\begin{aligned}
VI_2: P_3: & x^{W_2(12) + W_1(23) + 1} - x^{W_2(12)}, \bar{P}_3: x^{W_2(12) + W_1(23) + 1 + W_1(24)} - x^{W_2(12) + W_1(24) + 1}, \\
P_4: & x^{W_2(12) + W_1(23) + 1 + W_1(24)} - x^{W_2(12) + W_1(23) + 1}, \bar{P}_4: x^{W_2(12) + W_1(24) + 1} - x^{W_2(12)}.
\end{aligned}$$

□

Let  $\gamma$  be an oriented generic arc in  $M_K$  which intersects  $\Sigma^{(1)}$  only in positive triple crossings.

**Definition 29** *The evaluation of the 1-cochain  $R_x$  on  $\gamma$  is defined in Fig. 78 where the first sum is over all triple crossings of the global types  $r_a$  and  $l_c$ . The second sum is over all triple crossings  $p$  which have a distinguished crossing  $d$  of type 0.*

**Proposition 7** *Let  $m$  be the meridian for a positive quadruple crossing. Then  $R_x(m) = 0$ .*

*Proof.* The distinguished crossing  $d$  is the same for  $P_1, \bar{P}_1, P_4$  and  $\bar{P}_4$  and which share the same  $W_2(d)$  as follows from (1) in Lemma 3. We calculate their contribution to the second sum for  $R_x$  in Fig. 79, which turns out to be 0.

Making the distinguished crossing  $d$  singular in  $P_2$  and  $\bar{P}_2$  leads to isotopic singular knots. The same is true for  $P_3$  and  $\bar{P}_3$ . It follows now from (2) in Lemma 3 that the contributions of  $P_2$  and  $\bar{P}_2$  to the second sum in  $R_x$  cancel out. The same is true for  $P_3$  and  $\bar{P}_3$  if they share the same f-crossings, as follows from (4) in Lemma 3.

The double point in the first sum of  $R_x$  corresponds to the crossing  $ml$  and hence the corresponding singular knots in  $P_i$  and  $\bar{P}_i$  are always isotopic



$$\begin{aligned}
& -x^{W_2(d)} \left( \begin{array}{c} \text{Diagram 1} \\ 1 \end{array} - \begin{array}{c} \text{Diagram 2} \\ 2 \end{array} \right) \\
& + x^{W_2(d)} \left( \begin{array}{c} \text{Diagram 3} \\ 3 \end{array} - \begin{array}{c} \text{Diagram 2} \\ 2 \end{array} \right) \\
& + x^{W_2(d)} \left( \begin{array}{c} \text{Diagram 4} \\ 4 \end{array} - \begin{array}{c} \text{Diagram 3} \\ 3 \end{array} \right) \\
& - x^{W_2(d)} \left( \begin{array}{c} \text{Diagram 4} \\ 4 \end{array} - \begin{array}{c} \text{Diagram 1} \\ 1 \end{array} \right) \\
& = 0
\end{aligned}$$

Figure 79: The standard solution

$$\begin{aligned}
& - (x^{W_2(ml) + W_I(hm)} - x^{W_2(ml)}) \cdot \text{Diagram 1} \\
& + (x^{W_2(ml) + W_I(hm)} - x^{W_2(ml)}) \cdot \text{Diagram 2} \\
& + (x^{W_2(ml)} - x^{W_2(ml) + W_I(hm)}) \cdot (\text{Diagram 3} - \text{Diagram 4}) \\
& = 0
\end{aligned}$$

Figure 80: The cancellation of  $R_x(m)$  in  $-P_1 + \bar{P}_1 + P_3 - \bar{P}_3$  for the global types  $r_a$  and  $l_c$  of  $P_1$

for  $i \in \{2, 3, 4\}$ . It follows now from (3) in Lemma 3 and (3) in Lemma 4 that the contributions of  $P_2$  and  $\bar{P}_2$  to the first sum in  $R_x$  cancel always out.

It follows from (4) in Lemma 2 that  $P_1$  and  $\bar{P}_1$  do not contribute to the first sum if  $P_3$  and  $\bar{P}_3$  share the same f-crossings, because  $P_1$  and  $\bar{P}_1$  have not the right global type. If there is a new f-crossing in  $\bar{P}_3$  then it follows from (5) in Lemma 3 and (4) and (5) in Lemma 4 that the contributions of  $-P_1 + \bar{P}_1 + P_3 - \bar{P}_3$  to  $R_x(m)$  cancel out as shown in Fig. 80 (remember that according to Lemma 2 the distinguished crossing  $d$  in  $P_3$  and  $\bar{P}_3$  is always the crossing  $ml$  in  $P_1$  and  $\bar{P}_1$ ).

It follows from (6) in Lemma 3 that we can have only simultaneously  $W_1(P_3) = W_1(\bar{P}_3) + 1$  and  $W_1(\bar{P}_4) = W_1(P_4) + 1$ . But the crossing  $ml$  in  $P_3$  and  $P_4$  is for both strata the crossing 12. Notice that if  $ml = 12$  becomes singular then all other branches of the quadruple crossing are over the branches of the double point  $ml$  and hence all four singular knots are isotopic already locally. It follows now from (6) in Lemma 4 that the contributions of  $+P_3 - \bar{P}_3 + P_4 - \bar{P}_4$  cancel out as illustrated in Fig. 81.  $\square$

**Remark 10** *Let us summarize the combinatorial structure of  $R_x$  which leads to  $R_x(m) = 0$  for the meridian  $m$  of a positive quadruple crossing.*

$$\begin{aligned}
& + (x^{W_2(ml) + W_1(hm)} - x^{W_2(ml)}) \cdot \text{diagram}_1 \\
& - (x^{W_2(ml) + W_1(hm)} - x^{W_2(ml)}) \cdot \text{diagram}_2 = 0
\end{aligned}$$

Figure 81: The cancellation of  $R_x(m)$  in  $+P_3 - \bar{P}_3 + P_4 - \bar{P}_4$  for the global types  $r_a$  and  $l_c$

$$v_2(K) = \text{diagram}_1 \quad v_2(K) = \text{diagram}_2$$

Figure 82: Polyak-Viro formulas for the Vassiliev invariant  $v_2$

(1) The strata  $P_1, \bar{P}_1, P_4, \bar{P}_4$  share the same distinguished crossing  $d$  and their contributions with  $d$  singular cancel out (this was called the standard solution).

(2) All contributions of  $P_2$  and  $\bar{P}_2$  cancel out.

(3) The strata  $P_3$  and  $\bar{P}_3$  contribute non trivially with  $d$  singular if and only if  $P_1$  and  $\bar{P}_1$  are of global type  $r_a$  or  $l_c$  and in this case the contributions of  $P_3$  and  $\bar{P}_3$  with  $d$  singular cancel out with those of  $P_1$  and  $\bar{P}_1$  with  $ml$  singular.

(4) The contributions of  $P_3$  and  $\bar{P}_3$  with  $ml$  singular cancel always out with those from  $P_4$  and  $\bar{P}_4$  with  $ml$  singular too.

The lack of symmetry of  $R_x$  is apparent:  $-P_2 + \bar{P}_2$ , where the triple crossing is on the top, does never contribute at all, but  $+P_3 - \bar{P}_3$ , where the triple crossing is on the bottom, can contribute highly non trivially both for  $d$  singular and for  $ml$  singular. Its contribution for  $d$  singular cancels out with the contribution for  $ml$  singular in  $-P_1 + \bar{P}_1$  and its contribution with  $ml$  singular cancels out with the contribution for  $ml$  singular in  $+P_4 - \bar{P}_4$ .

**Remark 11** In fact, the coefficients of  $R_x$  can be generalized to 2-variable

polynomials by considering in addition a second type of f-crossings, called *h-crossings*, together with a new variable  $y$ : the head of the *h-crossing* of type 1 is in the arc from the foot of the crossing  $c$  to the point at infinity. In order to define the *r-crossings* of the *h-crossings* we use the second formula of Polyak-Viro for  $v_2(K)$  (see Fig. 82). Now, also the crossing  $hm$  becomes singular exactly for the global types  $r_b$  and  $l_a$ . The solution of the tetrahedron equation is still non symmetric because only the global type  $r_c$  does never contribute. The new 1-cocycle doesn't have any longer a scan property. Its specialization for  $y = 1$  coincides with  $R_x$ . But the verifications for the tetrahedron equation and the cube equations become so complicated that we will come back to them in a separate paper.

There are of course also "dual" solutions  $R_x$  by using symmetries as taking mirror images, the orientation change and the rotation by  $\pi$  around the imaginary axes  $i\mathbb{R} \times 0 \subset \mathbb{C} \times \mathbb{R}$  for the definition of the weights  $W_1$  and  $W_2$ .

**Question 3** *Can one define 1-cocycle invariants by using weights of degrees higher than two? (Gauss diagram formulas for finite type invariants of higher degrees for long knots are contained in [14].)*

## 4.5 Tetrahedron equation for closed braids and the Tetrahex equation

Let us consider first the positive tetrahedron equation for closed  $n$ -braids in the solid torus for  $n > 3$  (there isn't any tetrahedron equation for  $n < 4$ ).

We consider  $R_{xy}$  from Definitions 18, 19, 20 and 21.

**Proposition 8** *Let  $m$  be the meridian for a positive quadruple crossing. Then  $R_{xy}(m) = 0$ .*

*Proof.* The combinatorial structure of  $R_{xy}(m) = 0$  is similar to those described in Remark 9 but symetrized with respect to turning everything over. However, the proof is much simpler because there are only linear weights. We use again Fig. 66-77. It is clear again that we need only to consider the  $q$ -crossings from Definition 18 which belong to the six crossings involved in the quadruple crossing. The parts of the singular closed braids near the quadruple crossing are denoted as singular 4-braids (by using moreover our notation conventions). We give the details of the proof for simplicity only for  $n = 4$ . In this case each of the four arcs in the circle of the Gauss diagram

for the quadruple crossing represents the positive generator of  $H_1(V; \mathbb{Z}) \cong \mathbb{Z}$ . The general case is completely analogous but splits into much more sub cases, corresponding to all decompositions of  $n$  into four positive integers and to the attaching of these integers to the arcs in the circle. We left its verification to the reader.

The global type I is shown in Fig. 55. Each of the four arcs in the circle represents a positive homology class in the solid torus. Therefore only the crossing 14 can have the homological marking 1 and it is a d-crossing for  $-P_1, \bar{P}_1, P_4, -\bar{P}_4$  which are all of type  $r$ . There aren't any crossings which contribute to  $W_1(d)$  neither to  $W_{n-2=2}(d)$  and there is no triple crossing of global type  $l$  which contributes to  $R_{xy}$ . Hence  $R_{xy}(m) = 0$  by (1) of Remark 9 (this is again the standard solution, see Fig. 79).

The global type II is shown in Fig. 55 too. Only the crossings 14 and 23 can have marking 1. The crossing 23 is not a d-crossing and it can not be a q-crossing for 14 (under a small perturbation the corresponding two arrows will never intersect). There are no q-crossings in  $W_2(14)$  and we have again the standard solution for  $-P_1, \bar{P}_1, P_4, -\bar{P}_4$ .

$-P_2$  is of type  $l(3, 2, 1)$ :  $-x^{W_1(23)}(y^{W_2(23)+1} - y^{W_2(23)})12t_1321$

$\bar{P}_2$ :  $+x^{W_1(23)}(y^{W_2(23)+2} - y^{W_2(23)+1})12t_1321$

$P_3$  is of type  $l(3, 1, 2)$ :  $+x^{W_1(23)}(y^{W_2(23)+1} - y^{W_2(23)})12t_1321$

$-\bar{P}_3$ :  $-x^{W_1(23)}(y^{W_2(23)+2} - y^{W_2(23)+1})12t_1321$

It follows that  $R_{xy}(m) = 0$ .

The global type III is shown in Fig. 55. Only the crossings 24 and 12 can have marking 1 and only 24 is a d-crossing, namely for  $-P_2$  and  $\bar{P}_2$ . But they share the same weights, because 12 in  $-P_2$  doesn't cut  $d = 24$  in the right direction. Consequently, the contributions of  $-P_2$  and  $\bar{P}_2$  cancel out.  $-P_1$  and  $\bar{P}_1$  have not the right global type and do not contribute.

$P_3$  is of type  $l(3, 2, 1)$ :  $+x^{W_1(12)+1}(y^{W_2(12)+1} - y^{W_2(12)})t_121321$

$-\bar{P}_3$ :  $-x^{W_1(12)}(y^{W_2(12)+1} - y^{W_2(12)})t_121321$

$P_4$  is of type  $l(2, 1, 1)$ :  $y^{W_2(12)+1}(x^{W_1(12)} - x^{W_1(12)+1})t_121321$

$-\bar{P}_4$ :  $-y^{W_2(12)}(x^{W_1(12)} - x^{W_1(12)+1})t_121321$

It follows that  $R_{xy}(m) = 0$ .

The global type IV is shown in Fig. 55. Only the crossings 13 and 24 can have marking 1. The crossing 13 is a d-crossing for  $P_3$  and  $-\bar{P}_3$  and the crossing 24 is a d-crossing for  $-P_2$  and  $\bar{P}_2$ . Again, the two crossings with marking 1 can never intersect.

$-P_1$  is of type  $l(3, 2, 1)$ :  $-x^{W_1(13)}(y^{W_2(13)+1} - y^{W_2(13)})1t_23212$

$\bar{P}_1$ :  $+x^{W_1(13)}(y^{W_2(13)+1} - y^{W_2(13)})23t_1213$

$$\begin{aligned}
-P_2: & -x^{W_1(24)}y^{W_2(24)}(1232t_12 - 1231t_21) \\
\bar{P}_2: & +x^{W_1(24)}y^{W_2(24)+1}(1232t_12 - 1231t_21) \\
P_3: & +x^{W_1(13)}y^{W_2(13)}(23t_1213 - 1t_23212) \\
-\bar{P}_3: & -x^{W_1(13)}y^{W_2(13)+1}(23t_1213 - 1t_23212) \\
P_4 \text{ is of type } l(3, 1, 2): & +x^{W_1(24)}(y^{W_2(24)+1} - y^{W_2(24)})1231t_21 \\
-\bar{P}_4: & -x^{W_1(24)}(y^{W_2(24)+1} - y^{W_2(24)})1232t_12
\end{aligned}$$

It follows that  $R_{xy}(m) = 0$ .

The global type V is shown in Fig. 55. Only the crossings 13 and 34 can have marking 1.  $-P_1$  and  $\bar{P}_1$  are of the type  $l(2, 1, 1)$  which contributes.  $P_4$  and  $-\bar{P}_4$  have not the right type.

$$\begin{aligned}
-P_1: & -y^{W_2(13)}(x^{W_1(13)} - x^{W_1(13)+1})1t_23212 \\
\bar{P}_1: & +y^{W_2(13)}(x^{W_1(13)} - x^{W_1(13)+1})23t_1213 \\
-P_2 \text{ is of type } l(3, 1, 2): & -x^{W_1(34)}(y^{W_2(34)+1} - y^{W_2(34)})12312t_1 \\
\bar{P}_2: & +x^{W_1(34)}(y^{W_2(34)+1} - y^{W_2(34)})12312t_1 \\
P_3 \text{ is of type } r(1, 2, 3): & +x^{W_1(13)+1}y^{W_2(13)}(23t_1213 - 1t_23212) \\
-\bar{P}_3: & -x^{W_1(13)}y^{W_2(13)}(23t_1213 - 1t_23212)
\end{aligned}$$

It follows that  $R_{xy}(m) = 0$ .

The global type VI is shown in Fig. 55. Only the crossings 12, 23 and 34 can have marking 1. Non of them is a d-crossing.  $-P_2$  and  $P_3$  are both of type  $l(2, 1, 1)$  and contribute. In  $-P_1$  and  $\bar{P}_1$  the crossing  $hm = 34$ . This crossing is over all other crossings of the quadruple crossing and the weights in  $-P_1$  and  $\bar{P}_1$  are identical. Consequently, the contributions of  $-P_1$  and  $\bar{P}_1$  cancel out.

$$\begin{aligned}
-P_2: & -y^{W_2(23)}(x^{W_1(23)} - x^{W_1(23)+1})12t_1321 \\
\bar{P}_2: & +y^{W_2(23)}(x^{W_1(23)} - x^{W_1(23)+1})12t_1321 \\
P_3: & +y^{W_2(12)}(x^{W_1(12)} - x^{W_1(12)+1})t_121321 \\
-\bar{P}_3: & -y^{W_2(12)+1}(x^{W_1(12)} - x^{W_1(12)+1})t_121321 \\
P_4 \text{ is of type } l(3, 2, 1): & +x^{W_1(12)}(y^{W_2(12)+1} - y^{W_2(12)})t_121321 \\
-\bar{P}_4: & -x^{W_1(12)+1}(y^{W_2(12)+1} - y^{W_2(12)})t_121321
\end{aligned}$$

It follows that  $R_{xy}(m) = 0$  and this finishes the proof of Proposition 8.

□

We have proven the invariance of  $R_{xy}(\gamma)$  under generic homotopies of  $\gamma$  in  $M_{\hat{\beta}+\Delta}$  through the strata of the types (1) and (4) of Proposition 6. This finishes the proof of Proposition 1.

**Remark 12** *All the eliminations of singular closed braids in the meridian  $m$  are supported by local planar isotopies near to the quadruple crossing and hence all crossings have different names. It follows that our solution  $R_{xy}$*

splits into a solution for each fixed double point coming from a crossing with homological marking 1 and with given name  $x(i)$ . Consequently, in analogy to  $R_1^{split}$  the class  $[R_{xy}^{split}] \in H^1(M_{\hat{\beta}+\Delta}; \text{Sym}_k(\mathbb{D}_\beta^1))$  is also well defined.

**Question 4** Can  $R_{xy}^{split}$  be further refined by using also names for the crossings which are used to define the weights  $W_1$  and  $W_{n-2}$ ?

Let us consider now the *tetrahex equation*. The meridian  $m$  of the positive quadruple crossing is represented by the following loop:

$$\begin{aligned} &1(323)12 \rightarrow_{*1} 123(212) \rightarrow_{*2} 12(31)21 \rightarrow_{*3} (121)321 \rightarrow_{*4} 21(232)1 \rightarrow_{*5} \\ &2(13)231 \rightarrow_{*6} 2312(31) \rightarrow_{*7} 23(121)3 \rightarrow_{*8} (232)123 \rightarrow_{*9} 32(31)23 \rightarrow_{*10} \\ &321(323) \rightarrow_{*11} 3(212)32 \rightarrow_{*12} 312(13)2 \rightarrow_{*13} (13)2132 \rightarrow_{*14} 132312 \end{aligned}$$

Here,  $*1 = -P_1$ ,  $*2 = -P_2$ ,  $*4 = P_3$ ,  $*5 = P_4$ ,  $*8 = \bar{P}_1$ ,  $*9 = \bar{P}_2$ ,  $*11 = -\bar{P}_3$ ,  $*12 = -\bar{P}_4$ ,

$*3 : \sigma_3 = 14, \sigma_1 = 23$ ,  $*6 : \sigma_3 = 24, \sigma_1 = 13$ ,  $*7 : \sigma_3 = 12, \sigma_1 = 34$ ,  $*10 : \sigma_3 = 23, \sigma_1 = 14$ ,  $*13 : \sigma_3 = 13, \sigma_1 = 24$ ,  $*14 : \sigma_3 = 34, \sigma_1 = 12$ .

The unfolding together with the co-orientations is shown in Fig. 83, where the strata which correspond to commutations are drawn in red. Notice that the co-orientations on the smooth strata which correspond to commutations do not fit in  $\Sigma_{quad}^{(2)}$ . However, we see from the signs in the contributions of the commutations to  $R_1$  that we could make them fit if we would define the co-orientation by taking into account also the homological markings of the two crossings which commute. Notice also that we could change the cyclical order (with respect to the remaining strata) of the smooth stratum  $(*6 \cup *13)$  with the smooth stratum  $(*7 \cup *14)$  in the meridian  $m$ .

We consider now the 1-cochain  $R_1$  from Definitions 22, 23 and 24.

**Proposition 9** Let  $m$  be the meridian for a positive quadruple crossing. Then  $R_1(m) = 0$ .

*Proof.* We use again Fig. 66-77 and Fig. 55 and we know already the global types of the corresponding triple crossings from the proof of Proposition 8. Notice that  $-P_2$  and  $\bar{P}_2$  have always the same global type and differ just by one branch which goes under the triple crossing. Consequently, their contributions cancel out. The same is true for  $P_3$  and  $-\bar{P}_3$  which differ just by one branch which goes over the triple crossing.

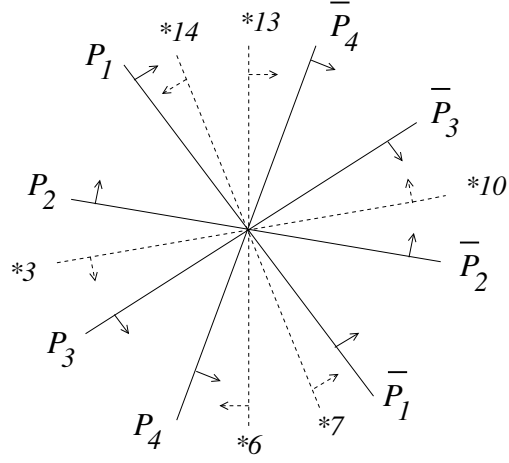


Figure 83: Unfolding for the tetrahex equation

$$\begin{array}{rcl}
 - & \begin{array}{c} \text{Diagram 1: A crossing of two strands with a dot at the intersection.} \end{array} & + \begin{array}{c} \text{Diagram 2: A crossing of two strands with a dot at the intersection.} \end{array} \\
 - & \begin{array}{c} \text{Diagram 3: A crossing of two strands with a dot at the intersection.} \end{array} & + \begin{array}{c} \text{Diagram 4: A crossing of two strands with a dot at the intersection.} \end{array} \\
 + & \begin{array}{c} \text{Diagram 5: A crossing of two strands with a dot at the intersection.} \end{array} & - \begin{array}{c} \text{Diagram 6: A crossing of two strands with a dot at the intersection.} \end{array} \\
 & & = 0
 \end{array}$$

Figure 84: Type I



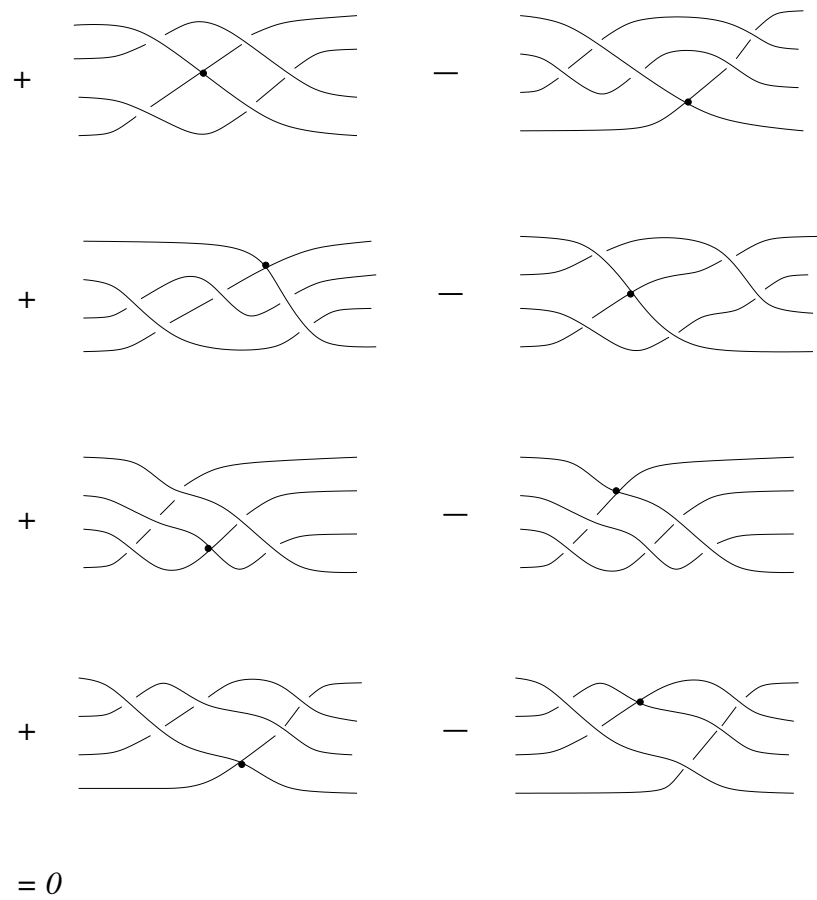


Figure 85: Type II

$$\begin{array}{cc}
+ & \begin{array}{c} \text{Diagram 1: A crossing of two strands with a dot on the upper-right strand.} \end{array} & - & \begin{array}{c} \text{Diagram 2: A crossing of two strands with a dot on the lower-left strand.} \end{array} \\
- & \begin{array}{c} \text{Diagram 3: A crossing of two strands with a dot on the upper-left strand.} \end{array} & + & \begin{array}{c} \text{Diagram 4: A crossing of two strands with a dot on the lower-right strand.} \end{array} \\
- & \begin{array}{c} \text{Diagram 5: A crossing of two strands with a dot on the upper-left strand.} \end{array} & + & \begin{array}{c} \text{Diagram 6: A crossing of two strands with a dot on the upper-right strand.} \end{array} \\
+ & \begin{array}{c} \text{Diagram 7: A crossing of two strands with a dot on the lower-right strand.} \end{array} & - & \begin{array}{c} \text{Diagram 8: A crossing of two strands with a dot on the lower-left strand.} \end{array} \\
= 0
\end{array}$$

Figure 86: Type III

$$\begin{array}{cc}
- \text{ [Diagram 1] } & + \text{ [Diagram 2] } \\
- \text{ [Diagram 3] } & + \text{ [Diagram 4] } \\
- \text{ [Diagram 5] } & + \text{ [Diagram 6] } \\
- \text{ [Diagram 7] } & + \text{ [Diagram 8] } \\
= 0
\end{array}$$

The figure shows a sequence of eight diagrams arranged in four rows, each representing a term in a sum. Each diagram consists of several horizontal lines that are crossed by a series of diagonal lines, creating a complex web of intersections. A single black dot is placed at a specific intersection point in each diagram. The diagrams are grouped by minus and plus signs, indicating a signed sum. The final result of the sum is stated as  $= 0$ .

Figure 87: Type IV

$$\begin{array}{cc}
- & \text{[Diagram 1]} & + & \text{[Diagram 2]} \\
+ & \text{[Diagram 3]} & - & \text{[Diagram 4]} \\
+ & \text{[Diagram 5]} & - & \text{[Diagram 6]} \\
- & \text{[Diagram 7]} & + & \text{[Diagram 8]} \\
= 0
\end{array}$$

The figure shows a sum of eight diagrams, each representing a configuration of four strands with a crossing. The strands are labeled 1, 2, 3, and 4 from top to bottom. The diagrams are arranged in a 4x2 grid. The first row shows two diagrams with a crossing between strands 2 and 3. The second row shows two diagrams with a crossing between strands 1 and 2. The third row shows two diagrams with a crossing between strands 3 and 4. The fourth row shows two diagrams with a crossing between strands 1 and 3. The signs alternate in a checkerboard pattern: (-, +), (+, -), (+, -), (-, +).

Figure 88: Type V

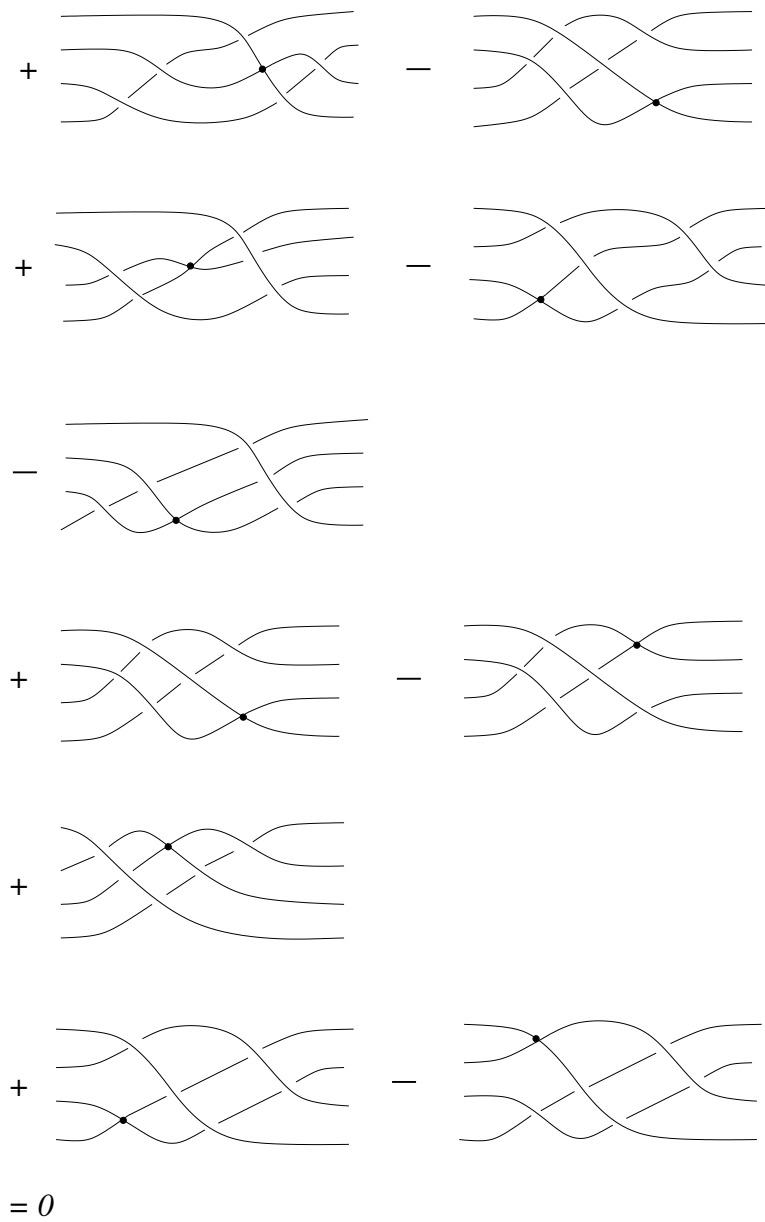


Figure 89: Type VI

*Global type I:* only 14 has marking 1.

$$-P_1: -12t_3212, \bar{P}_1: +231t_213, P_4: -213t_231, -\bar{P}_4: +32t_1232, *3: +12t_3121, \\ *10: -323t_123$$

It follows that  $R_1(m) = 0$  as shown in Fig. 84.

*Global type II:* only 14 and 23 have marking 1.

$$-P_1: +13t_2312, \bar{P}_1: -232t_123, P_4: +212t_321, -\bar{P}_4: -31t_2132, *3: +123t_121 - \\ 12t_3121, *10: +323t_123 - 32t_3123$$

It follows that  $R_1(m) = 0$  as shown in Fig. 85.

*Global type III:* only 12 and 24 have marking 1.

$$P_4: +2123t_21 - 21t_2321, -\bar{P}_4: -312t_132 + 3t_12132, *6: -21t_3231, *7: \\ +2132t_31, *13: +312t_132, *14: -3t_12132$$

It follows that  $R_1(m) = 0$  as shown in Fig. 86.

*Global type IV:* only 13 and 24 have marking 1.

$$-P_1: -1t_23212, \bar{P}_1: +23t_1213, P_4: -2123t_21, -\bar{P}_4: +312t_132, *6: -2t_13231 + \\ 21t_3231, *13: -312t_132 + 3121t_32$$

It follows that  $R_1(m) = 0$  as shown in Fig. 87.

*Global type V:* only 13 and 34 have marking 1.

$$-P_1: -123t_212 + 1t_23212, \bar{P}_1: +2312t_13 - 23t_1213, *6: +23t_1231, *7: \\ -2312t_13, *13: -312t_312, *14: +1t_32132$$

It follows that  $R_1(m) = 0$  as shown in Fig. 88.

*Global type VI:* only 12, 23 and 34 have marking 1.

$$-P_1: +123t_212, \bar{P}_1: -2312t_13, P_4: +21t_2321, -\bar{P}_4: -3t_12132, *3: -12t_1321, \\ *7: +12323t_1 - 1232t_31, *10: +32t_3123, *14: +3t_12312 - t_312312$$

It follows that  $R_1(m) = 0$  as shown in Fig. 89.

□

*Proof of Theorem 2.* It follows from Proposition 6, Remark 9, Section 4.3 and Proposition 9 that  $R_1$  is a 1-cocycle in  $M_{\hat{\beta}+\Delta}$ . It follows from Remark 12 that  $R_1^{split}$  is a 1-cocycle too and it follows from the example in Section 3.2 that it is not always trivial.

□

**Remark 13** *It follows immediately from e.g. the case of global type I in Proposition 9 that  $R_1$  does not split into a solution of the tetrahedron equation and of the hexagon equation. Indeed, the last two singular braids in Fig. 84 (the only one which come from the commutations) do not cancel out with each other.*

**Remark 14** *In fact, there is also a 1-cocycle  $R_2$  for closed positive 4-braids which contain a half-twist, and such that all double points have homological marking 2. The sign issues are quite different for this 1-cocycle because there are two different configurations for the commutation of two crossings of marking 2 (the arrows in the Gauss diagram cross and can be distinguished) in difference with the commutation of two crossings with marking 1 in  $R_1$  (the arrows do not cross and can not be distinguished). It turns out that the value of the 1-cocycle  $R_2$  is non trivial already for  $\text{rot}(\hat{\beta})$  with  $\beta = \sigma_3^2 \sigma_1 \sigma_2 \sigma_1 \Delta \in B_4^+$ , even without the splitting by the names of the crossings:  $R_2(\text{rot}(\hat{\beta})) = -2[t_3 1212111132]$ . But we will come back to this in a separate paper.*

## 4.6 Cube equations

In the case of long knots we have to consider now all other local types of triple crossings together with the self-tangencies. We know already the singularizations for the local type 1 from the solution of the tetrahedron equation and we will determine the singularizations of all other local types from the cube equations. The local types of triple crossings were shown in Fig. 16. The diagrams which correspond to the edges of the graph  $\Gamma$  (compare Section 4.1) are shown in Fig. 90. The projection of a triple crossing  $p$  into the plan separates the plan near  $p$  into three couples of a region and its dual. The regions correspond exactly to the three edges adjacent to the vertex corresponding to the local type of the triple crossing (we can forget about the three dual regions because of  $\Sigma_{trans-self-flex}^{(3)}$  as was explained in Section 4.1). We show the corresponding graph  $\Gamma$  now in Fig. 91. The unfolding of e.g. the edge 1 – 5 is shown in Fig. 57 (compare [25]).

**Observation 2** *The diagrams corresponding to the two vertices's of an edge differ just by the two crossings of the self-tangency which replace each other in the triangle as shown in Fig. 92. Consequently, the two vertices of an edge have always the same global type and always different local types and the two crossings which are interchanged can only be simultaneously f-crossings. Moreover, the two self-tangencies in the unfolding (of an edge) can contribute non trivially to  $R_x$  if they have different weights  $W_2(d)$  or if their singularizations are not isotopic. The latter happens exactly for the edges "1-6", "3-5", "4-7" and "2-8" (where the third branch passes between the two branches of the self-tangency).*

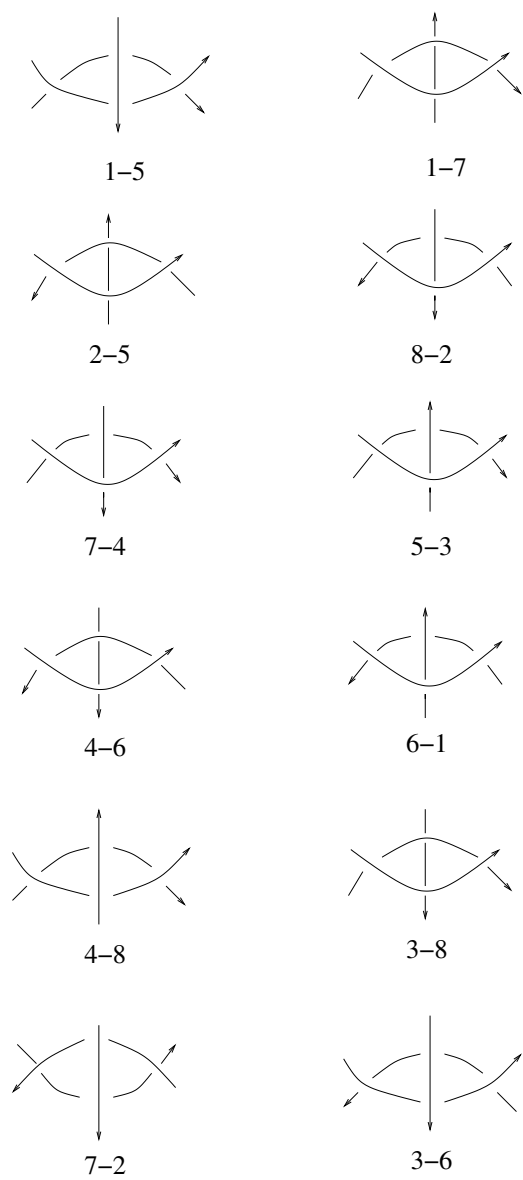


Figure 90: The twelve edges of the graph  $\Gamma$



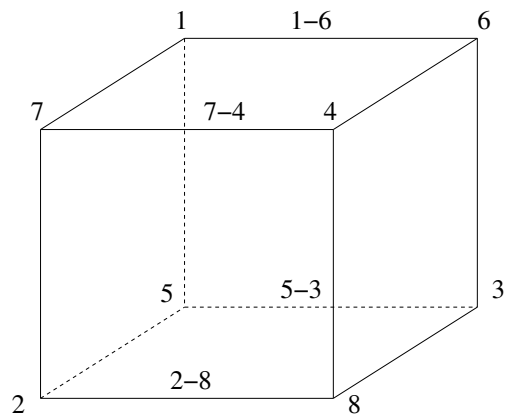


Figure 91: The graph  $\Gamma$

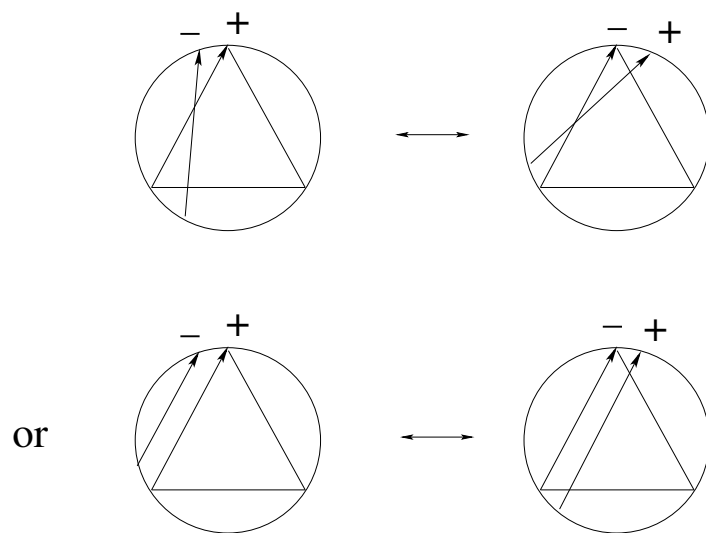


Figure 92: Two crossings replace each other for an edge of  $\Gamma$

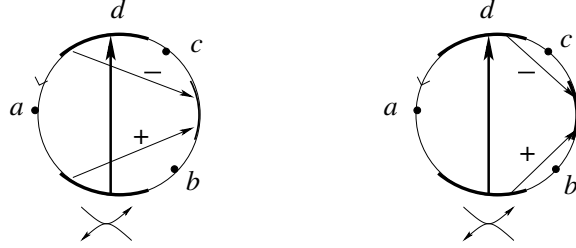


Figure 93: The two self-tangencies for the edge  $l7 - 2$

It follows that we have to solve the cube equations for the graph  $\Gamma$  exactly six times: one solution for each global type of triple crossings. We show the Gauss diagrams for the edges of  $\Gamma$  in Fig. 94 up to Fig. 101.

**Proposition 10** *Let  $m$  be a meridian of  $\Sigma_{trans-self}^{(2)}$  or a loop in  $\Gamma$ . Then  $R_x(m) = 0$  for the contributions given in Definition 14.*

*Proof.* First of all we observe that the two vertices of an edge (i.e. triple crossings) share the same f-crossings. The f-crossings could only change if the foot of a f-crossing slides over the head of the crossing  $d$ . But this is not the case as it was shown in Fig. 92. Indeed, the foot of the crossing which changes in the triangle can not coincide with the head of  $d$  because the latter coincides always with the head of another crossing.

It suffices of course to consider only the four crossings involved in an edge because the position of the triple crossings and the self-tangencies with respect to all other crossings do not change.

We start with the solutions for triple crossings of global type  $l$ . In the figures we show the Gauss diagrams of the two triple crossings together with the points at infinity and the Gauss diagram of just one of the two self-tangencies. The Gauss diagram of the second self-tangency is derived from the first one in the following way: the two arrows slide over the arrow  $d$  but their mutual position does not change. We show an example in Fig. 93. Notice that in the thick part of the circle there aren't any other heads or foots of arrows.

To each figure of an edge corresponds a second figure. In the first line on the left we have the singularization at  $ml$  which is already known. Of course we draw only the case when the triple crossing contributes, i.e. global type  $l_c$ . This determines the new singularization at  $ml$  on the right. We put the

singularizations in rectangles for better visualizing them. In the second line we give the corresponding singularizations at  $d$  for the global type  $l_b$ .

The fourth arrow which is not in the triangle is always almost identical with an arrow of the triangle. Consequently, in the case  $l_c$  it can not be a r-crossing with respect to  $hm$ . In the case  $l_b$  it could be a r-crossing with respect to some f-crossing. But the almost identical arrow in the triangle would be a r-crossing for the same f-crossing too. Their contributions cancel out, because they have different writhe.

It can happen for the type  $l_c$  that the crossing  $hm$  becomes a new f-crossing with respect to  $ml$  for the new triple crossing. This forces to use the coefficient  $w(hm)$  in the definition of the weights for the new triple crossing.

The type  $l_a$  does never contribute.

The mutual position of the two arrows for a self-tangency does not change. Only the position with respect to the distinguished crossing  $d$  changes. It remains to consider the edges "1-5", "4-8", "2-7" and "3-6" for  $l_c$ , where one of the two self-tangencies has a new f-crossing with respect to the other self-tangency. But one sees immediately from the figures that this new f-crossing is exactly the crossing  $hm$  in the triple crossings. In this case, exactly one of the self-tangencies contributes with the factor  $w(hm)x^{W_2(ml)+w(hm)W_1(hm)}$  and the other contributes with the factor  $w(hm)x^{W_2(ml)}$ . The singularizations are isotopic in this case and enter the equation for the singularization at the crossing  $ml$  of the triple crossings. Hence sometimes the self-tangencies contribute non trivially to the first line (when  $W_2(d)$  is different for the two self-tangencies but the singularizations are isotopic) and sometimes they contribute non trivially to the second line (when the third branch passes between the branches of the self-tangency and consequently the singularizations of the self-tangencies are not isotopic but have the same weight  $W_2(d)$ ). Sometimes the self-tangencies do not contribute at all (if the singularizations are isotopic and have the same weight  $W_2(d)$  or if they don't have the right global type).

We proceed then in exactly the same way for the global type  $r$ . But notice the difference which comes from the fact that we have broken the symmetry: the global type  $r_a$  contributes both with  $ml$  singular and with  $d$  singular. Exactly the same arguments as previously apply in the case  $r_b$  too. In the case  $r_c$  there are no contributions at all. The differences appear in the case  $r_a$ . Here sometimes the fourth crossing, which is not in the triangle, is a r-crossing with respect to  $hm$  for exactly one of the two triple crossings. If there could be confusion then we write the local type of the triple crossing in brackets behind the weight (but remember that we don't take yet into

account the correction term for the local type from Definition 14).

We examine now the figures (don't forget the degenerate configurations in the definition of the weights):

edge "1-7": type 1 and type 7 share the same  $W_1(hm)$  and  $W_2(d)$ , but  $W_2(ml)(7) = W_2(ml)(1) + W_1(hm)$

edge "1-5":  $W_1(hm)(5) = W_1(hm)(1) + 1$ ,  $W_2(d)(5) = W_2(d)(1) + 1$ , they share the same  $W_2(ml)$

edge "1-6":  $W_1(hm)(6) = W_1(hm)(1) - 1$ ,  $W_2(d)(6) = W_2(d)(1) - 1$ , they share the same  $W_2(ml)$

edge "7-4":  $W_1(hm)(4) = W_1(hm)(7) - 1$ ,  $W_2(d)(4) = W_2(d)(7) + 1$ , they share the same  $W_2(ml)$

edge "7-2":  $W_1(hm)(2) = W_1(hm)(7) + 1$ ,  $W_2(d)(2) = W_2(d)(7) - 1$ , they share the same  $W_2(ml)$

edge "5-2": same  $W_1(hm)$ , but  $W_2(d)(2) = W_2(d)(5) - 2$  and  $W_2(ml)(2) = W_2(ml)(5) + (W_1(hm) - 1)$

edge "5-3":  $W_1(hm)(3) = W_1(hm)(5) - 1$ ,  $W_2(d)(3) = W_2(d)(5) - 1$ , they share the same  $W_2(ml)$

edge "3-8": they share the same  $W_1(hm)$  and  $W_2(d)$ , but  $W_2(ml)(8) = W_2(ml)(3) + W_1(hm)$

edge "3-6":  $W_1(hm)(6) = W_1(hm)(3) - 1$ ,  $W_2(d)(6) = W_2(d)(3) - 1$ , they share the same  $W_2(ml)$

edge "4-8":  $W_1(hm)(8) = W_1(hm)(4) + 1$ ,  $W_2(d)(8) = W_2(d)(4) - 1$ , they share the same  $W_2(ml)$

edge "4-6": same  $W_1(hm)$ , but  $W_2(d)(6) = W_2(d)(4) - 2$  and  $W_2(ml)(6) = W_2(ml)(4) - (W_1(hm) + 1)$

edge "8-2":  $W_1(hm)(8) = W_1(hm)(2) - 1$ ,  $W_2(d)(8) = W_2(d)(2) + 1$ , they share the same  $W_2(ml)$ .

The weights have to be the same for both vertices of an edge. This forces the constant correction terms for the weights given in Definition 14 and one easily verifies by using the above calculations that the coefficients from Definition 14 satisfy the cube equations.

For the self-tangencies "8-2" as well as "1-6" both self-tangencies in the unfolding have the same  $W_2(d)$  as the triple crossing in type 8 respectively type 1. In the self-tangencies "7-4" and "5-3" both have the same  $W_2(d)$  as the triple crossing in type 7 respectively type 3. In the remaining cases  $W_2(d)$  is either the same too for the two self-tangencies or they differ exactly by  $W_1(hm)$  of the triple crossing.

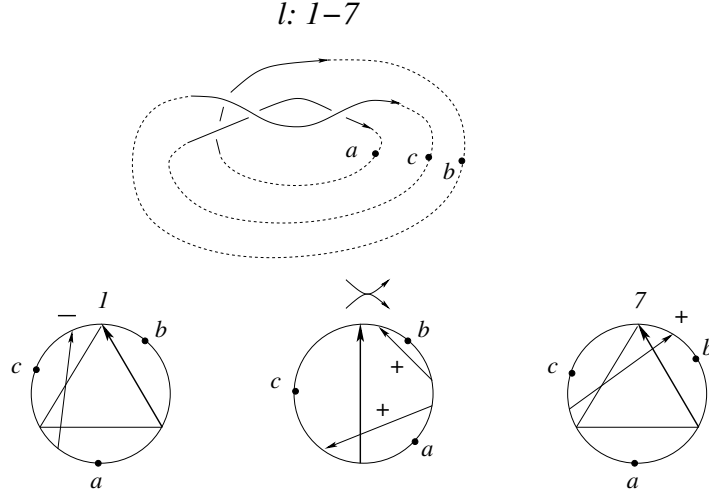


Figure 94:  $l1 - 7$

After establishing the singularizations for all eight local types of triple crossings we have to verify that the solution is consistent for the loops in  $\Gamma$ . We have to do this for the boundary of the three different types of 2-faces "1-7-2-5", "1-6-4-7" and "7-4-8-2" of the cube, i.e. we have just to check that the remaining fourth edge leads to the same result. The remaining 2-faces, which are parallel to these three, are completely analogous.

A part of the proof is in the figures Fig. 102 up to Fig. 111, where we have already incorporated the constant correction terms from Definition 14. All the remaining cases are quit similar and we leave them to the reader.

□

Notice that we haven't used here at all the embedded 1T-relation.

**Proposition 11** *In the case of closed braids the 1-cocycle  $R_1$  can not be extended to a solution of the cube equations (which degenerate for closed braids to the equator of the cube with respect to the poles, which are the triple crossings of the local type 2 and of the local type 6).*

*Proof.* Let us consider the global type  $r(1, 3, 2)$ . The edge  $r1 - 7$  determines the contribution of  $r(1, 3, 2)$  of local type 7:  $(\sigma_1 t_2^+ \sigma_1) \sigma_1^{-1} = \sigma_2 (\sigma_2^{-1} \sigma_1 t_2^+)$ . We consider now the edge  $r7 - 4$ . The distinguished crossing  $d$  is positive for the local type 7 but it is negative for the local type 4 and therefore we have to use also both self-tangencies (because we can not distinguish them).

$l:1-5$

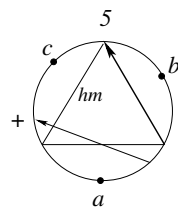
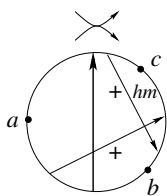
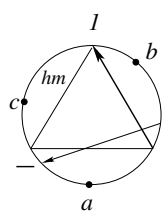
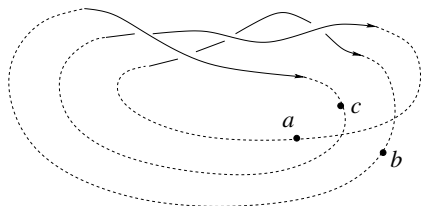


Figure 95:  $l1 - 5$

$l:1-6$

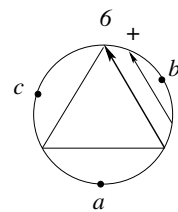
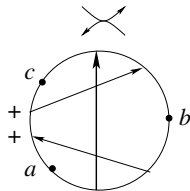
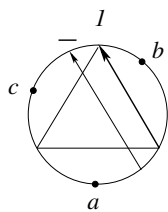
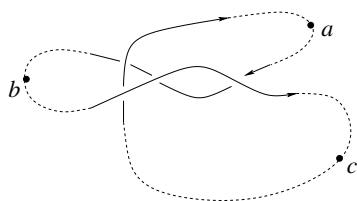


Figure 96:  $l1 - 6$

$l: 7-2$

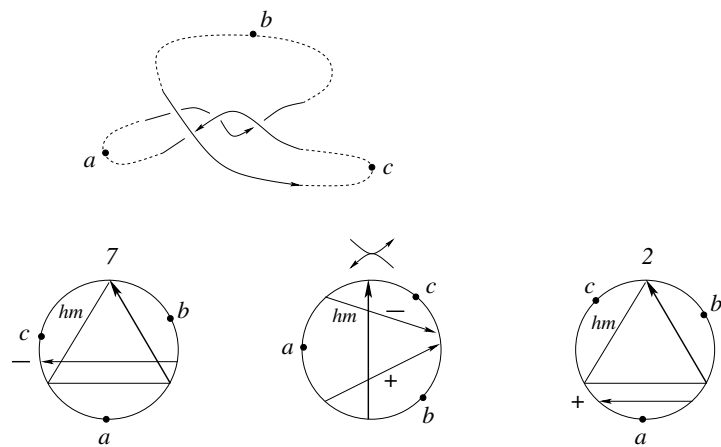


Figure 97:  $l7 - 2$

$l: 7-4$

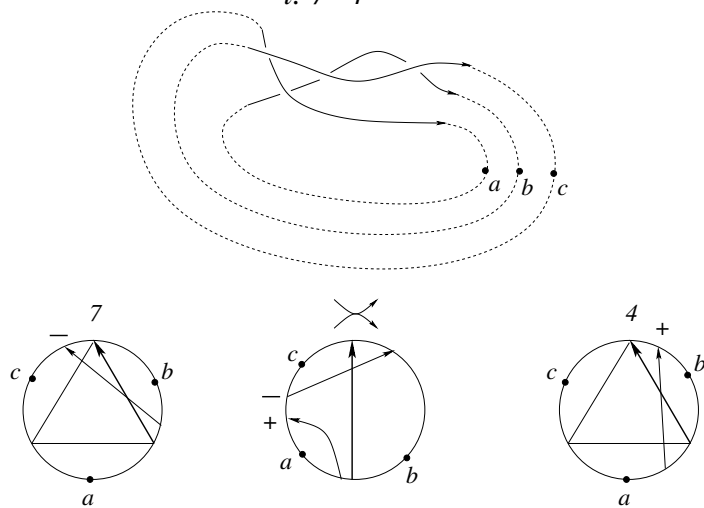


Figure 98:  $l7 - 4$

$r: 1-7$

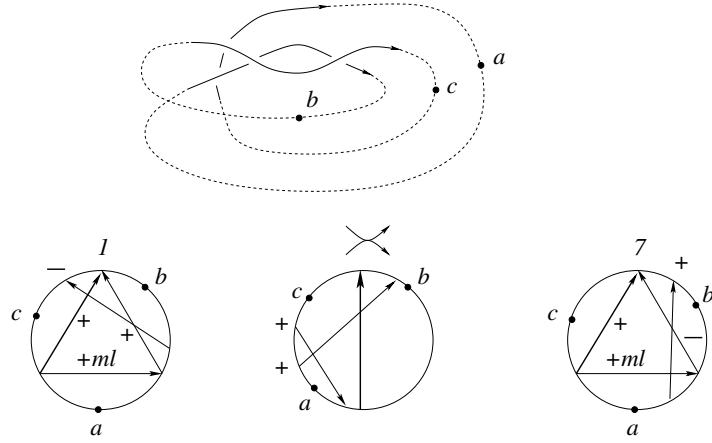


Figure 99:  $r1 - 7$

$r: 1-5$

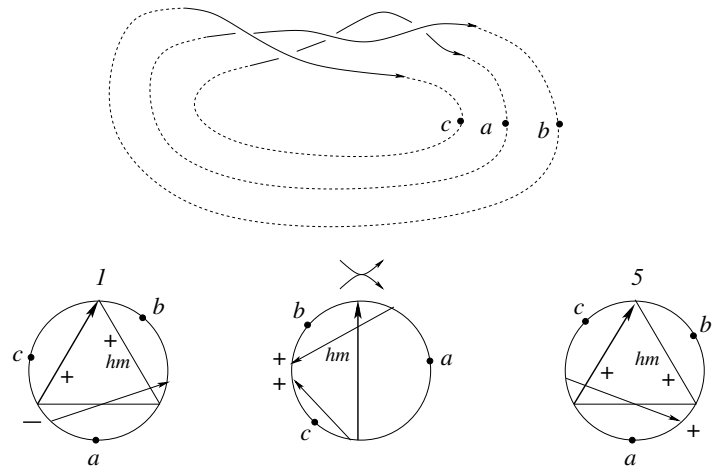


Figure 100:  $r1 - 5$



$r: 1-6$

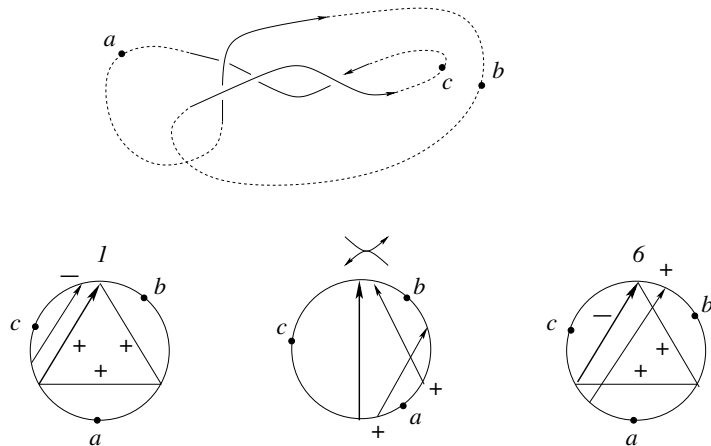


Figure 101:  $r1 - 6$

In any case there will be an odd number of singular braids with a positive double point as well as an odd number with a negative double point in the corresponding equation. Hence, they can not cancel out. (Forgetting the sign of the double point does not help, because the sum of the writhe of the remaining crossings will be different too.)

□

In fact, in difference to  $R_1$  the 1-cocycle  $R_{xy}$  for closed braids could be extended to a solution of the cube equations. But we don't know whether this is really useful.

## 4.7 Moving cusps and scan-property

We have to deal now with the irreducible strata of codimension two which contain a diagram with a cusp. We can assume that in the local picture there is exactly one crossing, before the small curl from the cusp appears. Notice that in this case the local types 2 and 6 can evidently not occur as triple crossings. There are exactly sixteen possible local types. We list them in Fig. 112...Fig. 115, where we move the branch from the right to the left. For each local type we have exactly two global types, corresponding to the position of the point at infinity. We give in the figure also the Gauss diagrams of the triple crossing and of one of the self-tangencies. Notice that in each

$$\begin{aligned}
& - (x^{W_2(ml) + W_l(hm)} - x^{W_2(ml)}) \left( \begin{array}{c} \text{diagram with box and } + \end{array} \right) \\
& = - (x^{W_2(ml) + W_l(hm)} - x^{W_2(ml)}) \left( \begin{array}{c} \text{diagram with box and } + \end{array} \right) \\
& - x^{W_2(d)} \left( \begin{array}{c} \text{diagram with box and } + \end{array} \right) - \begin{array}{c} \text{diagram with box and } + \end{array} \\
& + x^{W_2(d)} \left( \begin{array}{c} \text{diagram with } + \end{array} - \begin{array}{c} \text{diagram with } - \end{array} \right) \\
& = - x^{W_2(d)} \left( - \begin{array}{c} \text{diagram with box and } - \end{array} + \begin{array}{c} \text{diagram with box and } - \end{array} \right) \\
& + x^{W_2(d)} \left( \begin{array}{c} \text{diagram with } + \end{array} - \begin{array}{c} \text{diagram with } - \end{array} \right)
\end{aligned}$$

$ll-6$

Figure 102: Singularization for  $ll-6$

$$\begin{aligned}
& + ( x^{W_2(ml)} - x^{W_2(ml) - W_1(hm)} ) \left( \text{diagram 1} \right) \\
& = + ( x^{W_2(ml)} - x^{W_2(ml) - W_1(hm)} ) \left( \text{diagram 2} \right) \\
& + x^{W_2(d)} ( \text{diagram 3} - \text{diagram 4} ) = \\
& + x^{W_2(d)} ( \text{diagram 5} - \text{diagram 6} )
\end{aligned}$$

15-2

Figure 103: Singularization for  $l5 - 2$

Gauss diagram of a triple crossing one of the three arcs is empty besides just one head or foot of an arrow. Let us denote each stratum of  $\Sigma_{trans-cusp}^{(2)}$  simply by the global type of the corresponding triple crossing.

First of all we show that it is necessary to use the quadratic weight  $W_2$  for the construction of  $R_x$ . Indeed, assume that we replace  $W_2$  by a linear weight  $W$  (which is just the sum of the writhes of the f-crossings). This implies that we have to replace  $W_2$  by  $W$  for the self-tangencies too and that we have to replace the linear weight  $W_1$  for the types  $r_a$  and  $l_c$  by the constant weight 1. We show the meridian of a stratum  $\Sigma_{r_a}^{(2)}$  of local type 1 in Fig. 116. The calculation of  $R_x(m)$  with linear weight is shown in Fig. 117. We have no control over the resulting singular knot because it depends on the place of the cusp in the knot diagram. This forces us indeed to use the quadratic weights  $W_2(d)$  and  $W_2(ml)$  in the definition of  $R_x$  to overcome this problem (see Proposition 11).

**Lemma 5** *If  $R_x(m) = 0$  for  $\Sigma_{trans-cusp}^{(2)}$  with one orientation of the moving branch then it is also 0 for the other orientation of the moving branch.*

*Proof.* It suffices to notice that the contributions of the two Reidemeister II moves shown in Fig. 118 obviously cancel out.

$$\begin{aligned}
& (x^{W_2(ml)+W_I(hm)} - x^{W_2(ml)}) \left( \text{diagram with box and crossing} \right) \\
&= (x^{W_2(ml)+W_I(hm)} - x^{W_2(ml)}) \left( \text{diagram with box and crossing} \right) \\
& x^{W_2(d)} \left( \text{diagram with box and crossing} - \text{diagram with box and crossing} \right) \\
&= x^{W_2(d)} \left( \text{diagram with box and crossing} - \text{diagram with box and crossing} \right) \\
& \quad \quad \quad ll-7 \\
& - (x^{W_2(ml)+W_I(hm)} - x^{W_2(ml)}) \left( \text{diagram with box and crossing} \right) \\
& + (x^{W_2(ml)+W_I(hm)} - x^{W_2(ml)}) \left( \text{diagram with box and crossing} - \text{diagram with box and crossing} \right) \\
&= - (x^{W_2(ml)+W_I(hm)} - x^{W_2(ml)}) \left( \text{diagram with box and crossing} \right) \\
& - x^{W_2(d)} \left( \text{diagram with box and crossing} - \text{diagram with box and crossing} \right) \\
&= - x^{W_2(d)} \left( \text{diagram with box and crossing} - \text{diagram with box and crossing} \right) \\
& \quad \quad \quad ll-5
\end{aligned}$$

Figure 104: Singularizations for  $l1 - 7$  and  $l1 - 5$

$$- (x^{W_2(ml) + W_I(hm)} - x^{W_2(ml)}) \quad \begin{array}{c} \text{Diagram 1} \end{array}$$

$$= - (x^{W_2(ml) + W_I(hm)} - x^{W_2(ml)}) \quad \begin{array}{c} \text{Diagram 2} \end{array}$$

$$- x^{W_2(d)} ( \quad \begin{array}{c} \text{Diagram 3} \end{array} - \quad \begin{array}{c} \text{Diagram 4} \end{array} )$$

$$= - x^{W_2(d)} ( \quad \begin{array}{c} \text{Diagram 5} \end{array} - \quad \begin{array}{c} \text{Diagram 6} \end{array} )$$

$l3-8$

$$+ (x^{W_2(ml) + W_I(hm)} - x^{W_2(ml)}) \quad \begin{array}{c} \text{Diagram 7} \end{array}$$

$$= + (x^{W_2(ml) + W_I(hm)} - x^{W_2(ml)}) ( \quad \begin{array}{c} \text{Diagram 8} \end{array} )$$

$$+ x^{W_2(d)} ( \quad \begin{array}{c} \text{Diagram 9} \end{array} - \quad \begin{array}{c} \text{Diagram 10} \end{array} )$$

$$= + x^{W_2(d)} ( \quad \begin{array}{c} \text{Diagram 11} \end{array} - \quad \begin{array}{c} \text{Diagram 12} \end{array} )$$

$l4-6$

Figure 105: Singularizations for  $l3-8$  and  $l4-6$

$$\begin{aligned}
& - (x^{W_2(ml)} - x^{W_2(ml) - W_I(hm)}) \left( \text{diagram with box, crossing, and '+' sign} \right) \\
& = - (x^{W_2(ml) - W_I(hm)} - x^{W_2(ml)}) \left( \text{diagram with box, crossing, and '+' sign} - \text{diagram with box, crossing, and '-' sign} \right) \\
& - (x^{W_2(ml)} - x^{W_2(ml) - W_I(hm)}) \left( \text{diagram with box, crossing, and '-' sign} \right) \\
& - x^{W_2(d)} \left( - \text{diagram with box, crossing, and '+' sign} + \text{diagram with box, crossing, and '+' sign} \right) \\
& = - x^{W_2(d)} \left( \text{diagram with box, crossing, and '+' sign} - \text{diagram with box, crossing, and '+' sign} \right)
\end{aligned}$$

$l7-2$

Figure 106: Singularization for  $l7 - 2$

$$\begin{aligned}
& + (x^{W_2(ml)} - x^{W_2(ml) - W_1(hm)}) \left( \text{diagram} \right) \\
& = + (x^{W_2(ml)} - x^{W_2(ml) - W_1(hm)}) \left( \text{diagram} \right) \\
& + x^{W_2(d)} ( \text{diagram} - \text{diagram} ) \\
& + x^{W_2(d)} ( \text{diagram} - \text{diagram} ) \\
& = + x^{W_2(d)} ( \text{diagram} - \text{diagram} ) \\
& + x^{W_2(d)} ( \text{diagram} - \text{diagram} )
\end{aligned}$$

$l7-4$

Figure 107: Singularization for  $l7 - 4$

$$\begin{aligned}
& - (x^{W_2(ml)} - x^{W_2(ml) - W_1(hm)}) \left( \text{diagram with box and crossing, sign } - \right) \\
& = - (x^{W_2(ml)} - x^{W_2(ml) - W_1(hm)}) \left( \text{diagram with box and crossing, sign } - \right) \\
& - x^{W_2(d)} ( \text{diagram with box and crossing, sign } - \text{ } - \text{diagram with box and crossing, sign } - \text{ } ) \\
& + x^{W_2(d)} ( \text{diagram with box and crossing, sign } + \text{ } - \text{diagram with box and crossing, sign } - \text{ } ) \\
& = - x^{W_2(d)} ( \text{diagram with box and crossing, sign } + \text{ } - \text{diagram with box and crossing, sign } + \text{ } ) \\
& + x^{W_2(d)} ( \text{diagram with box and crossing, sign } + \text{ } - \text{diagram with box and crossing, sign } - \text{ } )
\end{aligned}$$

$l8-2$

Figure 108: Singularization for  $l8 - 2$



$$\begin{aligned}
& + (x^{W_2(ml)} - x^{W_2(ml) - W_I(hm)}) \left( \begin{array}{c} \text{Diagram 1: A box containing a crossing with a '+' sign} \end{array} \right) \\
& + (x^{W_2(ml) - W_I(hm)} - x^{W_2(ml)}) \left( \begin{array}{c} \text{Diagram 2: A crossing with a '+' sign} \\ \text{Diagram 3: A crossing with a '-' sign} \end{array} \right) \\
& = + (x^{W_2(ml)} - x^{W_2(ml) - W_I(hm)}) \left( \begin{array}{c} \text{Diagram 4: A box containing a crossing with a '-' sign} \end{array} \right) \\
& + x^{W_2(d)} \left( \begin{array}{c} \text{Diagram 5: A box containing a crossing with a '-' sign} \\ \text{Diagram 6: A box containing a crossing with a '-' sign} \end{array} \right) \\
& = + x^{W_2(d)} \left( \begin{array}{c} \text{Diagram 7: A box containing a crossing with a '-' sign} \\ \text{Diagram 8: A box containing a crossing with a '-' sign} \end{array} \right)
\end{aligned}$$

$l4-8$

Figure 109: Singularization for  $l4 - 8$

$$- (x^{W_2(ml) + W_I(hm) - W_2(ml)}) \left( \begin{array}{c} \text{Diagram 1} \end{array} \right) = - (x^{W_2(ml) + W_I(hm) - W_2(ml)}) \left( \begin{array}{c} \text{Diagram 2} \end{array} \right)$$

$$- x^{W_2(d)} \left( \begin{array}{c} \text{Diagram 3} \end{array} \right) - \left( \begin{array}{c} \text{Diagram 4} \end{array} \right) + x^{W_2(d)} \left( \begin{array}{c} \text{Diagram 5} \end{array} \right) - \left( \begin{array}{c} \text{Diagram 6} \end{array} \right)$$

$$= - x^{W_2(d)} \left( \begin{array}{c} \text{Diagram 7} \end{array} \right) - \left( \begin{array}{c} \text{Diagram 8} \end{array} \right) + x^{W_2(d)} \left( \begin{array}{c} \text{Diagram 9} \end{array} \right) - \left( \begin{array}{c} \text{Diagram 10} \end{array} \right)$$

$r1-6$

$$- (x^{W_2(ml) - W_2(ml) - W_I(hm)}) \left( \begin{array}{c} \text{Diagram 11} \end{array} \right) = - (x^{W_2(ml) - W_2(ml) - W_I(hm)}) \left( \begin{array}{c} \text{Diagram 12} \end{array} \right)$$

$$- (x^{W_2(ml) - W_2(ml) - W_I(hm)}) \left( \begin{array}{c} \text{Diagram 13} \end{array} \right) - \left( \begin{array}{c} \text{Diagram 14} \end{array} \right)$$

$$- x^{W_2(d)} \left( \begin{array}{c} \text{Diagram 15} \end{array} \right) - \left( \begin{array}{c} \text{Diagram 16} \end{array} \right) = - x^{W_2(d)} \left( \begin{array}{c} \text{Diagram 17} \end{array} \right) - \left( \begin{array}{c} \text{Diagram 18} \end{array} \right)$$

$r7-2$

Figure 110: Singularizations for  $r1 - 6$  and  $r7 - 2$

$$\begin{aligned}
& + (x^{W_2(ml) + W_I(hm) - W_2(ml)}) \left( \text{diagram with box and } + \right) = + (x^{W_2(ml) + W_I(hm) - W_2(ml)}) \left( \text{diagram with box and } + \right) \\
& + x^{W_2(d)} \left( \text{diagram with box and } + \right) - \text{diagram with box and } + = x^{W_2(d)} \left( \text{diagram with box and } + \right) - \text{diagram with box and } + \\
& \quad \quad \quad r1-7 \\
& - (x^{W_2(ml) + W_I(hm) - W_2(ml)}) \left( \text{diagram with box and } + \right) \\
& + (x^{W_2(ml) + W_I(hm) - W_2(ml)}) \left( \text{diagram with box and } + \right) - \left( \text{diagram with box and } - \right) \\
& = - (x^{W_2(ml) + W_I(hm) - W_2(ml)}) \left( \text{diagram with box and } - \right) \\
& - x^{W_2(d)} \left( \text{diagram with box and } + \right) - \text{diagram with box and } + = - x^{W_2(d)} \left( \text{diagram with box and } + \right) - \text{diagram with box and } + \\
& \quad \quad \quad r1-5
\end{aligned}$$

Figure 111: Singularizations for  $r1 - 7$  and  $r1 - 5$

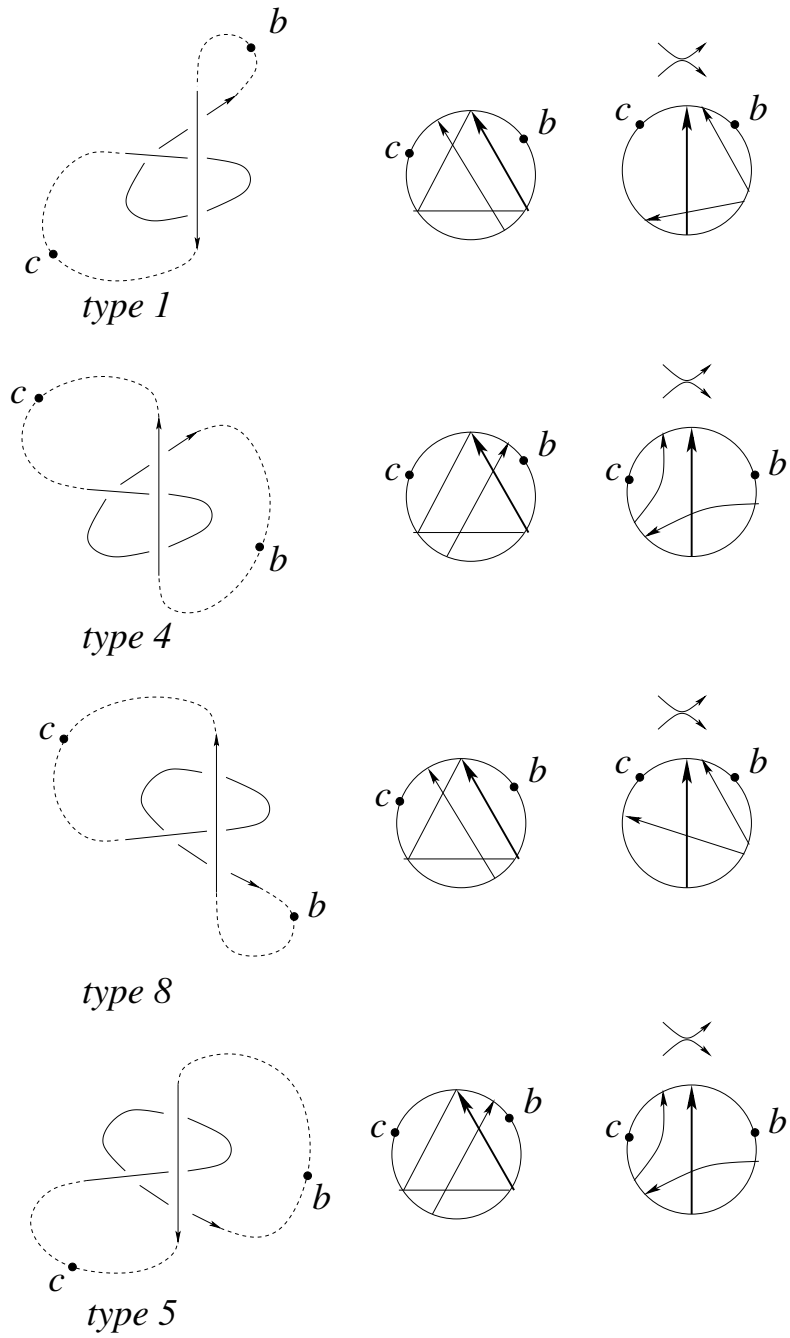


Figure 112: the strata  $\Sigma_{l_c}^{(2)}$  and  $\Sigma_{l_b}^{(2)}$

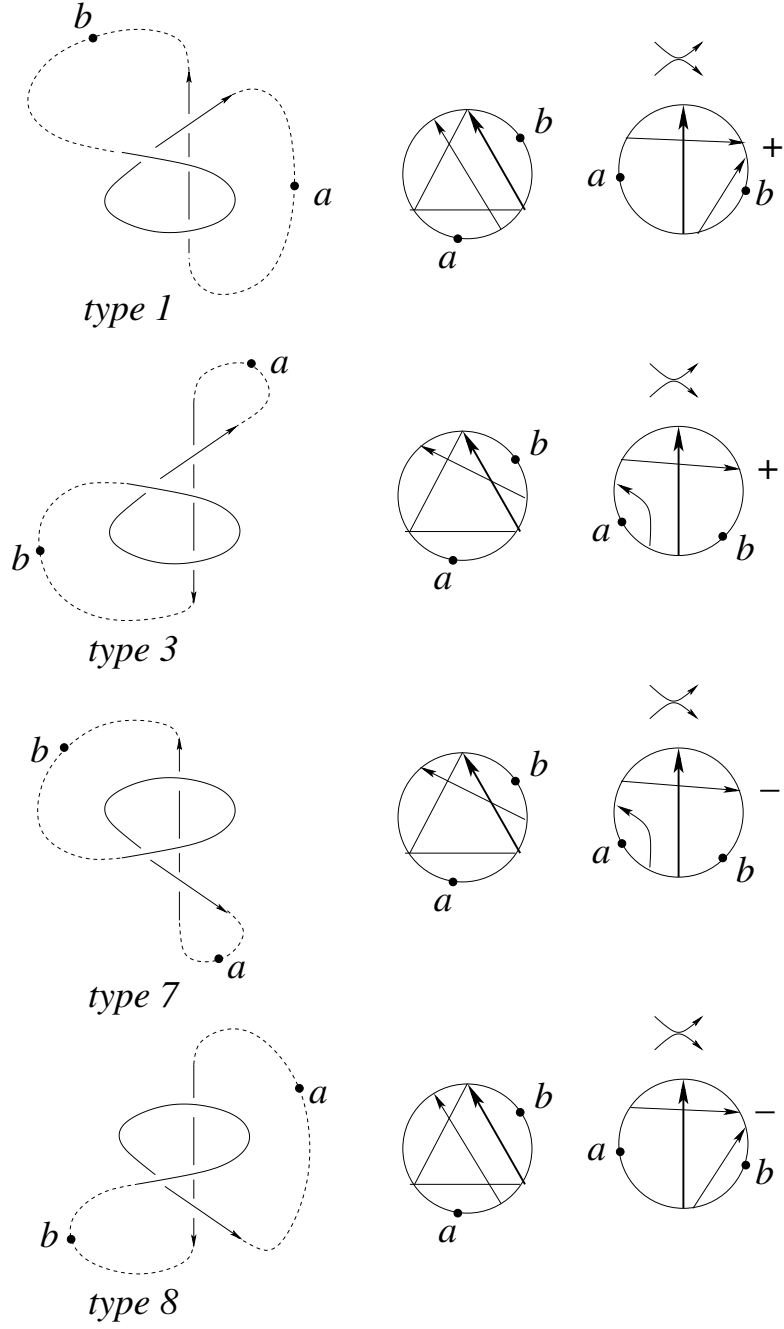


Figure 113: the strata  $\Sigma_{l_a}^{(2)}$  and  $\Sigma_{l_b}^{(2)}$

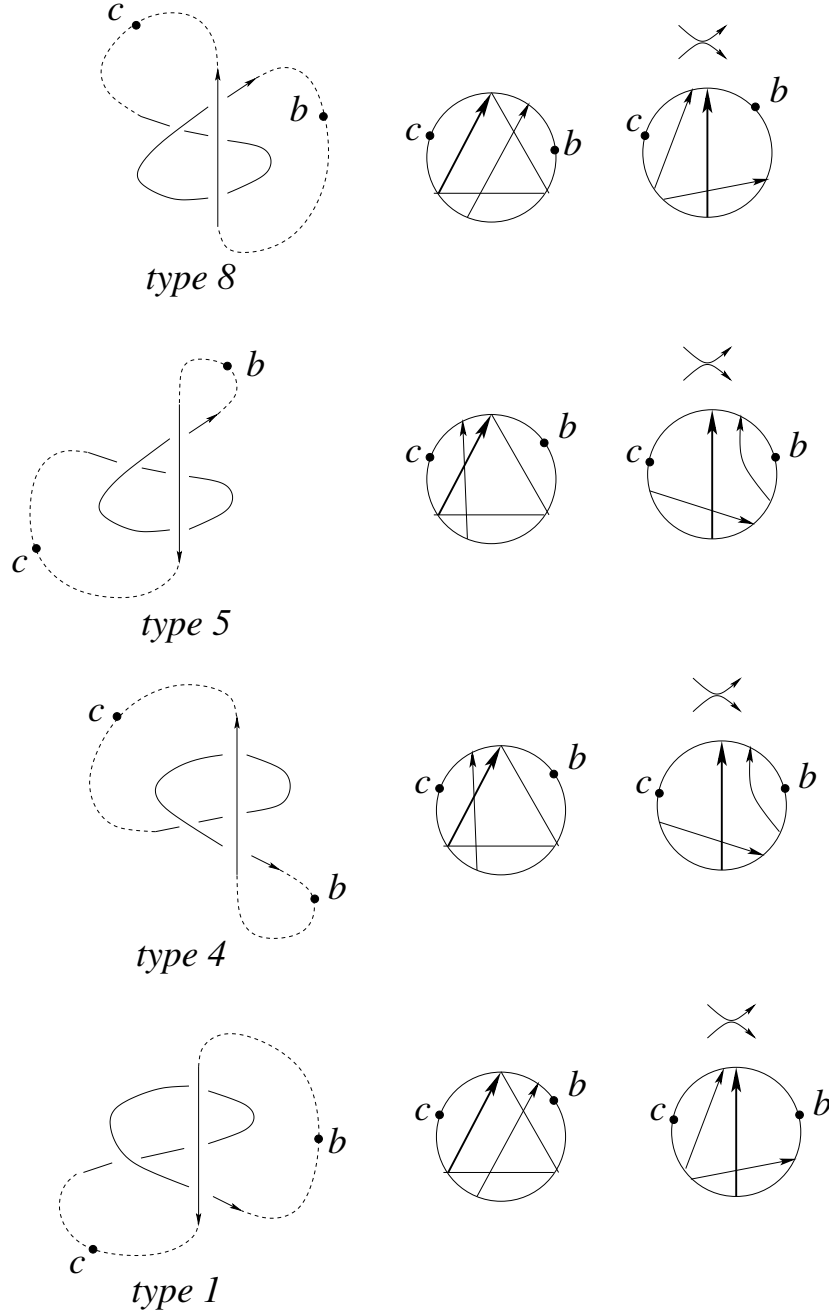


Figure 114: the strata  $\Sigma_{r_b}^{(2)}$  and  $\Sigma_{r_c}^{(2)}$

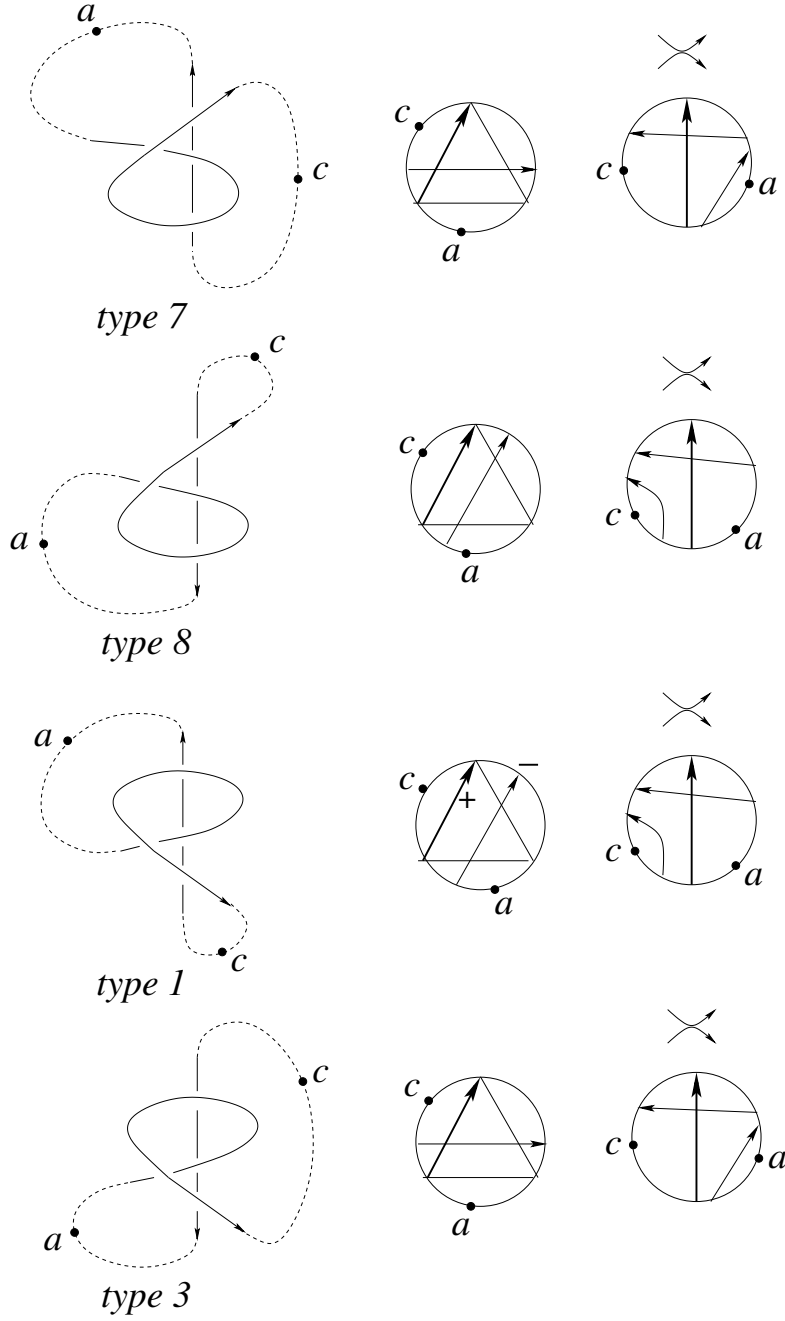


Figure 115: the strata  $\Sigma_{r_a}^{(2)}$  and  $\Sigma_{r_c}^{(2)}$

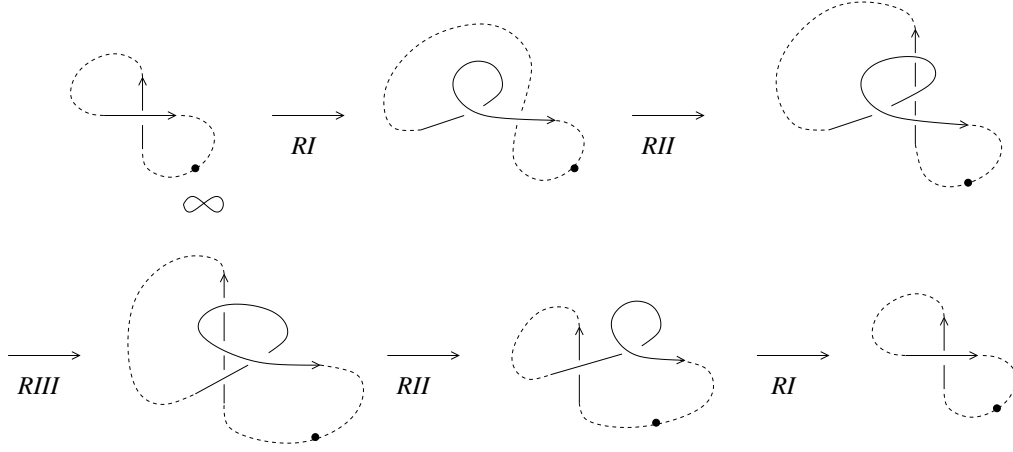


Figure 116: The meridian of a stratum  $\Sigma_{r_a}^{(2)}$  of local type 1

$$\begin{aligned}
& + x^{W(d)} \left( \begin{array}{c} \uparrow \\ \text{Diagram 1} \\ \downarrow \end{array} - \begin{array}{c} \uparrow - \\ \text{Diagram 2} \\ \downarrow \end{array} \right) \\
& - (x^{W(ml)+1} - x^{W(ml)}) \begin{array}{c} \uparrow \\ \text{Diagram 3} \\ \downarrow \end{array} - x^{W(d)} \left( \begin{array}{c} \uparrow \\ \text{Diagram 4} \\ \downarrow \end{array} - \begin{array}{c} \uparrow \\ \text{Diagram 5} \\ \downarrow \end{array} \right) \\
& - x^{W(d)} \left( \begin{array}{c} \uparrow \\ \text{Diagram 6} \\ \downarrow \end{array} - \begin{array}{c} \uparrow - \\ \text{Diagram 7} \\ \downarrow \end{array} \right) \\
& = (x^{W(ml)} - x^{W(ml)+1}) - \begin{array}{c} \uparrow \\ \text{Diagram 8} \\ \downarrow \end{array} = + (x^{W(ml)} - x^{W(ml)+1}) \begin{array}{c} \uparrow \\ \text{Diagram 9} \\ \downarrow \end{array} \neq 0
\end{aligned}$$

Figure 117: Calculation of  $R_x(m)$  with linear weight on the meridian of  $\Sigma_{r_a}^{(2)}$



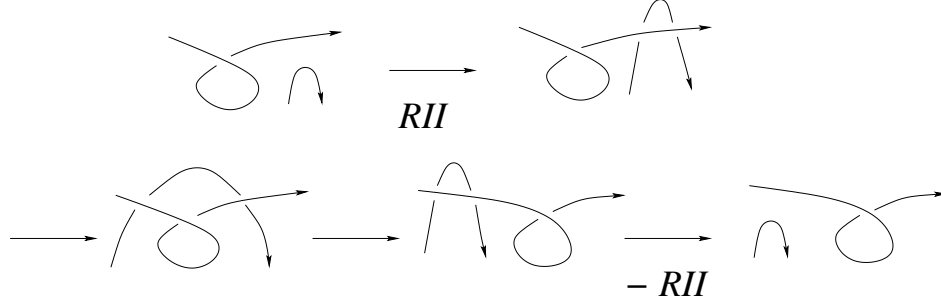


Figure 118: Two Reidemeister *II* moves with canceling contributions

□

**Proposition 12** *Let  $m$  be a meridian of  $\Sigma_{trans-cusp}^{(2)}$ . Then  $R_x(m) = 0$  for  $\Sigma_{l_c}^{(2)}$  because of the embedded 1T-relation.  $R_x(m) = 0$  for all other strata of  $\Sigma_{trans-cusp}^{(2)}$  without using the embedded 1T-relation.*

*Proof.* For the type  $\Sigma_{l_c}^{(2)}$  only the triple crossing contributes to  $R_x(m)$ , namely by  $x^{W_2(ml)+W_1(hm)} - x^{W_2(ml)}$  times the knot with the double point in  $ml$ . Notice that  $W_1(hm)$  can be non trivial. It follows now from Lemma 5 that it is sufficient to consider the local types 1 and 8. We show them in Fig. 119. But  $ml$  is just the new crossing created from the cusp and the embedded 1T-relation applies.

We show that  $R_x(m) = 0$  for  $\Sigma_{l_b}^{(2)}$ , respectively  $\Sigma_{r_a}^{(2)}$  of local type 1 in Fig. 120. Let us consider in detail the more complicated case of  $\Sigma_{r_a}^{(2)}$ . We observe first that  $W_1(hm) = 0$ . Indeed,  $d$  of the triple crossing contributes  $+1$  and the negative crossing from the self-tangency contributes  $-1$  and there are no other crossings at all which contribute to  $W_1(hm)$ . Hence  $x^{W_2(ml)+W_1(hm)} - x^{W_2(ml)} = 0$  and the triple crossing does not contribute with  $ml$  which becomes singular. On the other hand,  $W_2(d) = W_2(ml) + W_1(hm) = W_2(ml)$  for the triple crossing because there are no foots of arrows in the segment from the undercross to the overcross of  $hm$  (this is exactly the small curl). Let  $d'$  be the distinguished crossing of the self-tangencies. One easily sees (compare Fig. 115) that  $W_2(d') = W_2(ml) + W_1(hm) = W_2(ml)$  too. It follows that the weights of degree 2 are all the same and they are simply denoted by  $W_2$  in Fig. 120.

All other cases are completely analogous and are left to the reader.

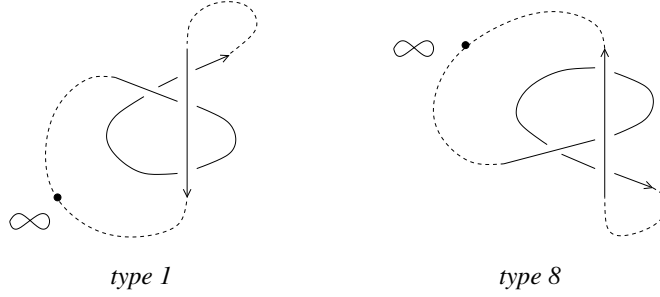


Figure 119: The strata  $\Sigma_{l_c}^{(2)}$  of type 1 and 8

□

We have proven that  $R_x(\gamma)$  is invariant under all generic homotopies of  $\gamma$  in  $M_K$  through the six types of strata of Proposition 6 and hence  $R_x$  is a 1-cocycle.

**Lemma 6** *Let  $T$  be a diagram of a string link and let  $t$  be a Reidemeister move of type II for  $T$ . Then the contribution of  $t$  to  $R_x$  does not change if a branch of  $T$  is moved under  $t$  from one side of  $t$  to the other.*

*Proof.* Besides  $d$  of  $t$  there are two crossings involved with the branch which goes under  $t$ . Moving the branch under  $t$  from one side to the other slides the heads of the corresponding arrows over  $d$ , see e.g. Fig. 94 and Fig. 99 as well as Fig. ?? and Fig. ?. Consequently, the f-crossings do not change. Notice that the mutual position of the two arrows does not change. Consequently, there are no new r-crossings and  $W_2(d)$  does not change neither. On the other hand it is clear that the singularizations of  $t$  on both sides are even planar isotopic.

□

We are now ready to prove the scan-property claimed in Theorem 1.

*Proof.* Let  $T$  be a diagram of a string link and let  $s$  be an isotopy which connects  $T$  with a diagram  $T'$ . We consider the loop

$-s \circ -scan(T') \circ s \circ scan(T)$  in  $M_T$ . This loop is contractible in  $M_T$  because  $s$  and  $scan$  commute. Consequently,  $R_x$  vanishes on this loop, because  $R_x$  is a 1-cocycle. It suffices to prove now that each contribution of a Reidemeister move  $t$  in  $s$  cancels out with the contribution of the same move  $t$  in  $-s$  (the signs of the contributions are of course opposite). The difference for the two Reidemeister moves is in a branch which has moved under  $t$ . It follows

$$\begin{aligned}
& +x W_2(d) \left( \begin{array}{c} \uparrow \\ \diagup \quad \diagdown \\ \bullet^+ \\ \downarrow \end{array} - \begin{array}{c} \uparrow \\ \diagup \quad \diagdown \\ \bullet^- \\ \downarrow \end{array} \right) \\
& -x W_2(d) \left( \begin{array}{c} \uparrow \\ \diagup \quad \diagdown \\ \bullet^+ \\ \downarrow \end{array} - \begin{array}{c} \uparrow \\ \diagup \quad \diagdown \\ \bullet^+ \\ \downarrow \end{array} \right) \\
& -x W_2(d) \left( \begin{array}{c} \uparrow \\ \diagup \quad \diagdown \\ \bullet^+ \\ \downarrow \end{array} - \begin{array}{c} \uparrow \\ \diagup \quad \diagdown \\ \bullet^- \\ \downarrow \end{array} \right) = 0 \\
& \qquad \qquad \qquad \Sigma_{l_b}^{(2)}
\end{aligned}$$

$$\begin{aligned}
& +x W_2(d) \left( \begin{array}{c} \uparrow \\ \diagup \quad \diagdown \\ \bullet^+ \\ \downarrow \end{array} - \begin{array}{c} \uparrow \\ \diagup \quad \diagdown \\ \bullet^- \\ \downarrow \end{array} \right) \\
& -x W_2(d) \left( \begin{array}{c} \uparrow \\ \diagup \quad \diagdown \\ \bullet^+ \\ \downarrow \end{array} - \begin{array}{c} \uparrow \\ \diagup \quad \diagdown \\ \bullet^+ \\ \downarrow \end{array} \right) \\
& -x W_2(d) \left( \begin{array}{c} \uparrow \\ \diagup \quad \diagdown \\ \bullet^+ \\ \downarrow \end{array} - \begin{array}{c} \uparrow \\ \diagup \quad \diagdown \\ \bullet^- \\ \downarrow \end{array} \right) = 0 \\
& \qquad \qquad \qquad \Sigma_{r_a}^{(2)}
\end{aligned}$$

Figure 120:  $R_x(m) = 0$  for  $\Sigma_{l_b}^{(2)}$  and  $\Sigma_{r_a}^{(2)}$

that the singular string links in the contributions are always planar isotopic. Hence it suffices to study the weights. If  $t$  is a positive triple crossing then the weights are the same just before the branch moves under  $t$  and just after it has moved under  $t$ . Indeed, this follows from the fact that for the positive global tetrahedron equation the contribution from the stratum  $-P_2$  cancels always out with that from the stratum  $\bar{P}_2$  (compare the Section 4.4). If we move the branch further away then the invariance follows from the already proven fact that the values of the 1-cocycles do not change if the loop passes through a stratum of  $\Sigma^{(1)} \cap \Sigma^{(1)}$  (compare Section 4.3). We use now again the graph  $\Gamma$ . The meridian  $m$  which corresponds to an arbitrary edge of  $\Gamma$  is a contractible loop in  $M_T$ , no matter what is the position of the branch which moves under everything. Let's take an edge where one vertex is a triple crossing of local type 1. We know from Lemma 6 that the contributions of the self-tangencies in  $s$  do not depend on the position of the moving branch. Consequently the contribution of the other vertex of the edge doesn't change neither because the contributions from all four Reidemeister moves together sum up to 0. Using the fact that the graph  $\Gamma$  is connected we obtain the invariance with respect to the position of the moving branch for all Reidemeister moves  $t$  of type III and II. We know from Proposition 12 that Reidemeister moves of type I do not change  $R_x(scan(T))$  neither.

□

Notice that  $R_x$  does not have the scan-property for a branch which moves over everything else because the contributions of the strata  $P_3$  and  $-\bar{P}_3$  in the positive tetrahedron equation do not cancel out at all. Of course, the "dual" 1-cocycle will have the scan property for a branch which moves over everything. It is an interesting question whether or not the two 1-cocycles represent the same cohomology class.

We have proven that  $R_x$  has the scan-property. It is not always trivial as shows the example in Section 3.1. This finishes the proof of Theorem 1.

## References

- [1] Agol I.: Ideal triangulations of pseudo-Anosov mapping tori, *Topology and geometry in dimension three*, Contemp. Math. 560 (2011) 1-17

- [2] Band G., Boyland P.: The Burau estimate for the entropy of a braid, *Algebr. Geom. Topol.* 7 (2007) 1345-1378
- [3] Bar-Natan D. : On the Vassiliev knot invariants, *Topology* 34 (1995) 423-472
- [4] Bar-Natan D. : Vassiliev homotopy string link invariants, *J. Knot Theory Ramif.* 4 (1995) 13-32
- [5] Bar-Natan D. (with Jana Archibald, Karene Chu, Thomas Fiedler): Some HOMFLYPT one parameter knot theory computations, [www.toronto.edu/drornb/misc/](http://www.toronto.edu/drornb/misc/)
- [6] Bar-Natan D., Thang T. Q. Le, Thurston D.: Two applications of elementary knot theory to Lie algebras and Vassiliev invariants, *Geometry & Topology* 7 (2003) 1-31
- [7] Birman J. : Braids , Links and Mapping class groups, *Annals of Mathematics Studies* 82 , Princeton University Press (1974)
- [8] Birman J., Gebhardt V., Gonzáles-Meneses J.: Conjugacy in Garside groups III: Periodic braids, *J. of Algebra* 316 (2007) 746-776
- [9] Budney R., Conant J., Scannell K., Sinha D.: New perspectives on self-linking, *Advances in Math.* 191 (2005) 78-113
- [10] Budney R., Cohen F.: On the homology of the space of knots, *Geometry & Topology* 13 (2009) 99-139
- [11] Budney R. : Topology of spaces of knots in dimension 3, *Proceedings London Math. Soc.* 101 (2010) 477-496
- [12] Burde G., Zieschang H.: *Knots*, de Gruyter Studies in Mathematics 5, Berlin (1985)
- [13] Carter J.S., Saito M.: Reidemeister moves for surface isotopies and their interpretations as moves to movies, *J. Knot Theory Ramif.* 2 (1993) 251-284

- [14] Chmutov S., Polyak M.: Elementary combinatorics of the HOMFLYPT polynomial, *Int. Math. Res. Notes* 3 (2010) 480-495
- [15] Costantino F., Guéritaud F., van der Veen R. : On the volume conjecture for polyhedra, [arXiv: 1403.2347](#)
- [16] Dunfield N., Garoufalidis S. : Incompressibility criteria for spun-normal surfaces. *Trans. Amer. Math. Soc.* 364 (2012) 61096137.
- [17] Duzhin S., Karev M.: Detecting the orientation of string links by finite type invariants, *Functional Analysis and its Appl.* 41 (2007) 208-216
- [18] Fathi A., Laudenbach F., Poenaru V.: *Travaux de Thurston sur les surfaces*, *Asterisque* 66-67, SMF Paris (1979)
- [19] Fiedler T. : Gauss Diagram Invariants for Knots and Links, *Mathematics and Its Applications* 532 , Kluwer Academic Publishers (2001)
- [20] Fiedler T. : Isotopy invariants for closed braids and almost closed braids via loops in stratified spaces, [arXiv: math.GT/0606443](#) (48 pp)
- [21] Fiedler T. : The Jones and Alexander polynomials for singular links, *J. Knot Theory Ramif.* 19 (2010) 859-866
- [22] Fiedler T. : Knot polynomials via one parameter knot theory, [arXiv: math/0612115 v2](#) (95 pp)
- [23] Fiedler T. : Quantum one-cocycles for knots, [arXiv: 1304.0970 v2](#) (177 pp)
- [24] Fiedler T. : Singularization of knots and closed braids, [arXiv: 1405.5562 v2](#) (165 pp)
- [25] Fiedler T., Kurlin V. : A one-parameter approach to knot theory, *J. Math. Soc. Japan* 62 (2010) 167-211
- [26] Fox R. : Rolling, *Bull.Amer. Math. Soc.* 72 (1966) 162-164

- [27] Fuji H., Gukov S., Sulkowski P., (appendix by Awata H.) : Volume conjecture: Refined and Categorified, *Adv. Theor. Math. Phys.* 16 (2012) 1669-1777
- [28] Futer D., Kalfagianni E., Purcell J.: Guts of surfaces and the colored Jones polynomial, *Lecture Notes in Math.* (Springer) 2069 (2013)
- [29] Futer D., Kalfagianni E., Purcell J.: Jones polynomials, volume and essential knot surfaces: a survey, *Knots in Poland III*, Banach Center Publ. 100 (2014) 51-77
- [30] Futer D., Kalfagianni E., Purcell J.: Quasifuchsian state surfaces, *Trans. Amer. Math. Soc.* 366 (2014) 4323-4343
- [31] Garside F. : The braid group and other groups, *Quart. J. Math. Oxf. II Ser.* 20 (1969) 235-254
- [32] Garoufalidis S. : The Jones slopes of a knot. *Quantum Topol.* 2 (2011) 4369.
- [33] Garoufalidis T. : Quantum knot invariants, *arXiv*: 1201.3314
- [34] Garoufalidis T. van der Veen R. : Quadratic integer programming and the slope conjecture, *arXiv*: 1405.5088
- [35] Gramain A.: Sur le groupe fondamental de l'espace des noeuds, *Ann. Inst. Fourier* 27 (1977) 29-44
- [36] Goussarov M., Polyak M., Viro O.: Finite type invariants of classical and virtual knots, *Topology* 39 (2000) 1045-1068
- [37] Hatcher A. : A proof of the Smale Conjecture, *Ann. of Math.* 117 (1983) 553-607
- [38] Hatcher A. : Topological moduli spaces of knots, *arXiv*: math.GT/9909095
- [39] Hatcher A., McCullough D.: Finiteness of classifying spaces of relative diffeomorphism groups of 3-manifolds, *Geometry & Topology* 1 (1997) 91-109

- [40] Johansson K. : Homotopy equivalences of 3-manifolds with boundary, Lecture Notes in Math. 761, Springer Berlin (1979)
- [41] Jones V.: Hecke algebra representations of braid groups and link polynomials, Ann. of Math. 126 (1987) 335-388
- [42] Kashaev R.: The hyperbolic volume of knots from the quantum dilogarithm, Lett. Math. Phys. 39 (1997) 269-275
- [43] Kashaev R., Korepanov I., Sergeev S.: Functional tetrahedron equation, Theoret. and Math. Phys. 117 (1998) 1402-1413
- [44] Kauffman L. : Knots and Physics, World Scientific, Singapore (1991)
- [45] Kauffman L. : Virtual knot theory, European J. Comb. 20 (1999) 663-690
- [46] Kauffman L., Vogel P.: Link polynomials and a graphical calculus, J. Knot Theory Ramif. 1 (1992) 59-104
- [47] Ko K.H., Los J., Song W.T.: Entropy of braids, J. Knot Theory Ramif. 11 (2002) 647-666
- [48] Kolev B.: Entropie topologique et représentation de Burau, C.R. Acad. Sci. Paris Sér. I Math. 309 (1989) 835-838
- [49] Kolev B.: Dynamique topologique en dimension 2. Orbites périodiques et entropie topologique. Thèse de doctorat de l'Université de Nice (1991)
- [50] Kontsevich M.: Vassiliev's knot invariants, Adv. in Sov. Math. 16 (1993) 137-150
- [51] Thang T. Q. Le : The colored Jones polynomial and the A-polynomial for knots, Adv. Math. 207 (2006) 782-804
- [52] Mortier A.: Finite-type 1-cocycles of knots given by Polyak-Viro formulas, arXiv: 1403.3418 (to appear in J. Knot Theory Ramif.)



- [53] Mortier A.: Combinatorial cohomology of the space of long knots, arXiv: 1408.5318 (to appear in *Algebr. Geom. Topol.*)
- [54] Morton H.R.: Infinitely many fibred knots having the same Alexander polynomial, *Topology* 17 (1978) 101-104
- [55] Murakami H., Murakami J.: The colored Jones polynomials and the simplicial volume of a knot, *Acta Math.* 186 (2001) 85-104
- [56] Polyak M., Viro O.: Gauss diagram formulas for Vassiliev invariants, *Internat. Math. Res. Notes* 11 (1994) 445-453
- [57] Polyak M., Viro O.: On the Casson knot invariant, *J. Knot Theory Ramif.* 10 (2001) 711-738
- [58] Przytycki J.: Skein modules of 3-manifolds, *Bull. Polish Acad. Sci. Math.* 39 (1991) 91-100
- [59] Reshetikhin N., Turaev V. : Invariants of 3-manifolds via link polynomials and quantum groups, *Invent. Math.* 103 (1991) 547-597
- [60] Sakai K.: An integral expression of the first non-trivial one-cocycle of the space of long knots in  $\mathbb{R}^3$ , *Pacific J. Math.* 250 (2011) 407-419
- [61] Thurston W.: *The Geometry and Topology of Three-Manifolds*, <http://www.msri.org/publications/books/gt3m/>
- [62] Turchin V. : Computation of the first non-trivial 1-cocycle in the space of long knots, (Russian) *Mat. Zametki* 80 (2006), no. 1, 105-114; translation in *Math. Notes* 80 (2006), no. 1-2, 101-108.
- [63] Turaev V. : The Yang-Baxter equation and invariants of links, *Invent. Math.* 92 (1988) 527-553
- [64] Turaev V.: The Conway and Kauffman modules of a solid torus, *J. Soviet. Math.* 52 (1990) 2799-2805

- [65] Vassiliev V. : Cohomology of knot spaces // in: Theory of Singularities and its Applications, Advances in Soviet. Math. 1 (1990) 23-69
- [66] Vassiliev V. : Combinatorial formulas of cohomology of knot spaces, Moscow Math. Journal 1 (2001) 91-123
- [67] Volic I.: On the cohomology of spaces of links and braids via configuration space integrals, arXiv: 1002.2467, Sarajevo J. Math. 6 (2010) 241-263
- [68] Witten E.: Quantum field theory and the Jones polynomial, Comm. Math. Phys. 121 (1989) 351-399

Institute de Mathématiques de Toulouse  
 Université Paul Sabatier  
 118, route de Narbonne  
 31062 Toulouse Cedex 09, France  
 fiedler@math.univ-toulouse.fr